

# CHALMERS



## **Design of a tidal power park and a wave power park with a techno-economical approach**

A study of subsea components, optimisation of the collection grids and an investigation of the transmission with the opportunity to share the cable with a wind park

*Master of Science Thesis*

MIKAEL BITOWT

MALIN JOHANSSON

Department of Energy and Environment  
*Division of Electric Power Engineering*  
CHALMERS UNIVERSITY OF TECHNOLOGY  
Göteborg, Sweden, 2013



# Design of a tidal power park and a wave power park with a techno-economical approach

A study of subsea components, optimisation of the collection grids and an investigation of the transmission with the opportunity to share the cable with a wind park

Mikael Bitowt  
Malin Johansson

Department of Energy and Environment  
*Division of Electric Power Engineering*  
CHALMERS UNIVERSITY OF TECHNOLOGY  
Göteborg, Sweden, 2013

# Design of a tidal power park and a wave power park with a technological approach

A study of subsea components, optimisation of the collection grids and an investigation of the transmission with the opportunity to share the cable with a wind park

Mikael Bitowt, Malin Johansson

© MIKAEL BITOWT, MALIN JOHANSSON, 2013, all rights reserved

Division of Electric Power Engineering  
Department of Energy and Environment  
Chalmers University of Technology  
SE-412 96 Göteborg  
Telephone +46(0)31-772 1000

Printed by TeknologTryck  
Göteborg, Sweden 2013

# Abstract

This report focuses on the infrastructure of a cost efficient subsea collection grid for a tidal power park and a wave power park, 50 MW and 2.5 MW, respectively. A study has been made on subsea components, some operating today and other under development, for an offshore collection grid. Also the possibility to connect the tidal park to an offshore wind farm has been investigated. The cable dimensioning of the collection grid is based on the cost of cables and lost revenue from the power loss. AC and DC collection grids at the voltages between 0.69-14 kV and with radial and star infrastructure, respectively, have been investigated. A DC system will always be cheaper than an AC system (as long as the generator can excite high enough voltage for the collection grid) since a converter is required independent of the voltage type. However, there are no manufacturers today that offer DC cables for the considered voltage range.

One of the most expensive and weakest points of a system are the connectors. Therefore the star connection is preferable over the radial pattern, due to the lower number of connectors. The preferred collection grid, for both the tidal and the wave case, is a DC grid in star connection. The cost of the cables for these systems are approximated to be 7 424 kkr at 9.3 kV and 249 kkr at 1.4 kV, respectively. However, if it is not possible to order DC cables at this low voltage or they become too expensive, an AC system should be used instead. The preferred AC system is then a star connection at 6.6 kV and 3.3 kV, tidal and wave, respectively. The cable losses for the selected systems reaches a maximum of 0.4% when considering a whole system. All the components required for these applications will need to be special designed for its purpose and will therefore be expensive.

For the transmission from the park to the grid, three options have been studied: transmission at collection grid voltage, transmission with higher voltage using a transformer and sharing transmission cables with a large wind power park (in this study Gwynt y Môr). The most cost effective option for distances between 1.8 km to 19.3 km is to use an own cable at 66 kV<sub>AC</sub> with a cross-sectional area of 500 mm<sup>2</sup>. At distances longer than 19.3 km the most cost effective solution is to share the transmission cables at 132 kV<sub>AC</sub> and 500 mm<sup>2</sup> with Gwynt y Môr, when accounting for 3 % rental cost of using Gwynt y Môr's components. If it would be possible to increase the cross-sectional area of the Gwynt y Môr's transmission cables from 500 mm<sup>2</sup> to 630 mm<sup>2</sup>, this transmission would become the most cost effective solution at distances longer than 4.6 km (when using a rental share of 3 %). The reason for this result is that the cost of losses are lower and there is no cost in lost revenue for the 630 mm<sup>2</sup> cables, due to that they are over dimensioned.

**Keywords:** tidal power, wave power, wind power, subsea components, subsea collection grid, cable share, transmission, cost effective, techno-economical

# Acknowledgement

We are very grateful for all support which has contributed to this master thesis. Firstly, we want to express our gratitude to the supervisor Pinar Tokat and the examiner Torbjörn Thiringer who have been of great help during the whole work. Throughout the division of electric power engineering Jörgen Blennow, Ola Carlson, Peiyuan Chen, Stanislaw Gubanski, Robert Karlsson, Tuan Le Anh, Stefan Lundberg and Per Norberg have always been available and friendly answering our many questions. We owe a great deal of gratitude to Björn Andersson for his work as an opponent and for all great comments about the report. Further we want to thank Ylva Sörqvist and Martin Johnsson at Minesto as well as Niklas Almgren at Göteborg Energi for their great support and interesting discussions during the process. Extra thanks to Ylva Sörqvist for reading and commenting on the report. We also want to acknowledge support from Björn Sonerud at Nexans for his commitment in answering all our questions. Roland Wida at ABB, Darren Taylor at NKT cables, Truls Normann at Aker solutions and Jan Gren at Ericsson have all been of great help with technical questions during the work and we are full of thankfulness to them. The power flow analysis have been a large part in this project and we are very thankful to Hadi Saadat who have provided us with MATLAB code for the analysis. We want to thank British Oceanographic Data Centre (BODC) for the wind data and the support to find it, Elbyggnadsrationaliseringen (EBR) for their energy cost information and International Electrotechnical Commission (IEC) for their in-depth knowledge about the rise of temperature in cables. We are also grateful to all the companies involved that have been friendly to let us use their pictures in our thesis. At last we want to thank David Eriksson, Olle Nordqvist and Johan Wolgers for interesting discussions throughout the project.

*Mikael Bitowt and Malin Johansson*

# Contents

<b>1</b>	<b>Introduction</b>	<b>1</b>
1.1	Problem description . . . . .	1
1.2	Purpose . . . . .	2
1.3	Scope . . . . .	2
1.4	Method . . . . .	3
<b>2</b>	<b>Background theory</b>	<b>4</b>
2.1	Origin of tide . . . . .	4
2.2	Origin of wave and its correlation to wind . . . . .	5
2.3	How to generate power from tides and waves . . . . .	6
2.3.1	Deep Green - construction, specifications and generation . . . . .	8
2.3.2	Seabased - construction, specifications and generation . . . . .	9
2.4	Designing a subsea collection grid . . . . .	10
2.4.1	Knowledge from wind power parks . . . . .	11
2.4.2	AC or DC system . . . . .	12
2.4.3	Regular array connections . . . . .	12
2.5	Cable construction and theoretical loss calculations . . . . .	13
2.5.1	Equivalent circuit - pi-model . . . . .	14
2.5.2	Simple resistive cable loss calculation . . . . .	14
2.5.3	Calculation of cable operating temperature . . . . .	15
2.6	Power flow analysis . . . . .	16
<b>3</b>	<b>Subsea components</b>	<b>18</b>
3.1	Subsea transformers . . . . .	18
3.1.1	ABB subsea transformer . . . . .	19
3.1.2	Siemens subsea transformer . . . . .	20
3.2	Subsea switchgears . . . . .	21
3.2.1	Siemens subsea switchgear . . . . .	21
3.2.2	VetcoGray subsea switchgear . . . . .	22
3.2.3	Schneider Electric subsea switchgear . . . . .	22
3.3	Connector systems . . . . .	23
3.3.1	Siemens connector system . . . . .	25
3.3.2	VetcoGray connector system . . . . .	25
3.4	Seabased AB - marine substation . . . . .	25
<b>4</b>	<b>Connection of a Deep Green park</b>	<b>29</b>
4.1	Main structure . . . . .	29
4.2	Network connections preferred . . . . .	29
4.3	Full-scale system . . . . .	31
<b>5</b>	<b>Optimising cables for the tidal collection grid</b>	<b>33</b>
5.1	Voltage levels . . . . .	33
5.2	Systems' conditions . . . . .	33
5.3	Conductor and cable cost . . . . .	34
5.4	Tidal stream data . . . . .	35
5.5	Resistance corresponding to the operation temperature . . . . .	36
5.6	Cable area optimisation . . . . .	37

5.6.1	First approach - only conductor cost and losses corresponding to the resistance at 20°C . . . . .	38
5.6.2	Second approach - including resistance corresponding to the operation temperature . . . . .	39
5.6.3	Third approach - including reactive power by using Newton-Raphson . . . . .	44
5.7	Comparison of the collection grids . . . . .	47
<b>6</b>	<b>Connection of a Seabased wave power park</b>	<b>49</b>
6.1	Seabased collection grid structure . . . . .	49
6.2	Collection grid patterns used in the wave power case . . . . .	50
<b>7</b>	<b>Optimising cables for the wave collection grid</b>	<b>51</b>
7.1	Voltage levels . . . . .	51
7.2	Systems' conditions . . . . .	51
7.3	Conductor and cable cost . . . . .	52
7.4	Wave data . . . . .	52
7.5	Resistance corresponding to the operation temperature . . . . .	53
7.6	Cable area optimisation . . . . .	53
7.6.1	First approach - only conductor cost and losses corresponding to the resistance at 20°C . . . . .	53
7.6.2	Second approach - including resistance corresponding to the operation temperature . . . . .	54
7.6.3	Third approach - including reactive power by using Newton-Raphson . . . . .	54
7.7	Comparison of the collection grids . . . . .	56
<b>8</b>	<b>Connection of the tidal park to the grid</b>	<b>58</b>
8.1	Tidal and wind data . . . . .	58
8.2	Transmission at collection grid voltage . . . . .	60
8.3	Transmission at high voltage . . . . .	61
8.3.1	Costs of cables . . . . .	61
8.3.2	Results . . . . .	62
8.4	Combining the tidal park with an offshore wind farm . . . . .	63
8.4.1	Minimum power factor to transmit the total installed power . . . . .	64
8.4.2	Transmission cost when sharing cable with a wind power park . . . . .	66
8.4.3	The cost of sharing four 630 mm <sup>2</sup> transmission cables with a wind power park . . . . .	70
8.5	The most cost effective transmission option . . . . .	72
<b>9</b>	<b>Discussion and conclusion</b>	<b>74</b>
9.1	Subsea Components . . . . .	74
9.2	Collection grid . . . . .	74
9.3	Transmission to shore . . . . .	76
<b>10</b>	<b>Future work</b>	<b>78</b>
	<b>Appendix A Description of IEC 60287</b>	<b>85</b>

<b>Appendix B</b>	<b>An example of a Newton-Raphson power flow analysis</b>	<b>89</b>
<b>Appendix C</b>	<b>Enlargement of the 25 Deep Green star circuit</b>	<b>94</b>
<b>Appendix D</b>	<b>Cable data sheets</b>	<b>95</b>
<b>Appendix E</b>	<b>Calculation of cable temperature using IEC 60287</b>	<b>101</b>

**List of Figures**

2.1	Rise of tides . . . . .	4
2.2	Correlation between wave and wind . . . . .	6
2.3	Principle of how to convert potential tidal energy to electricity. . . . .	7
2.4	Three different tidal power techniques . . . . .	7
2.5	Principle of oscillating waves in an air column . . . . .	8
2.6	Three different wave power techniques . . . . .	8
2.7	Construction of Deep Green . . . . .	9
2.8	Power curve for Deep Green . . . . .	9
2.9	Construction of Seabased . . . . .	10
2.10	Measured power output for Seabased . . . . .	10
2.11	Three main structures to connect a collection grid. . . . .	13
2.12	The cross section of a one phase cable . . . . .	13
2.13	Pi-equivalent of one phase of a cable . . . . .	14
3.1	ABB subsea transformer . . . . .	20
3.2	Components in Schneider Electric subsea switchgear . . . . .	23
3.3	Schneider Electric subsea switchgear . . . . .	23
3.4	Drymate connection . . . . .	24
3.5	Wetmate connection . . . . .	24
3.6	Seabased marine substation . . . . .	26
3.7	One phase electrical scheme inside Seabased substation . . . . .	26
3.8	Seabased substation’s inner structure of the newer version . . . . .	28
4.1	Main structure of 25 Deep Green generating units. . . . .	29
4.2	Selected radial structure for 25 Deep Green generating units. . . . .	30
4.3	Selected star structure for 25 Deep Green generating units. . . . .	31
4.4	Selected radial structure for 100 Deep Green generating units. . . . .	32
4.5	Selected star structure for 100 Deep Green generating units. . . . .	32
5.1	Comparison of conductor cost and submarine cable cost . . . . .	35
5.2	Rayleigh distribution of tidal stream . . . . .	36
5.3	Cable temperature as a function of the current . . . . .	37
5.4	A first approach optimisation of the cable size . . . . .	39
5.5	Optimisation of the cables for the DC system . . . . .	42
5.6	Optimised cable cost at different voltages and powers. . . . .	43
5.7	Optimisation of the cables for the AC system . . . . .	45
5.8	Power loss as a function of the generated active power . . . . .	46
5.9	Reactive power as a function of the generated active power . . . . .	46

6.1	Example of a connection structure for Seabased park . . . . .	49
6.2	Selected structures for 100 Seabased generating units. . . . .	50
7.1	Comparison of conductor cost and submarine cable cost . . . . .	52
7.2	Optimisation of the cables for the DC system . . . . .	54
7.3	Optimisation of the cables for the AC system . . . . .	55
8.1	Wind data measured in Irish sea. . . . .	58
8.2	Tidal data measured in Irish sea. . . . .	59
8.3	Mean power output per day . . . . .	60
8.4	Cable costs at high voltage . . . . .	62
8.5	Graphical cost comparison . . . . .	63
8.6	Minimum allowed power factor . . . . .	65
8.7	Transmission cost comparison . . . . .	72
A.1	Geometric factor to calculate $T_2$ . . . . .	88
B.1	System used in Newton-Raphson example . . . . .	89
C.1	Enlargement of the 25 Deep Green star circuit . . . . .	94
D.1	Specifications for a 10 kV submarine cable from Nexans . . . . .	95
D.2	Power curve for Siemens SWT-3.6-107 used in Gwynt y Môr . . . . .	96
D.3	Isolation thickness for different voltages from Caledonian . . . . .	96
D.4	Specifications for a 3 kV submarine cable from Caledonian . . . . .	97
D.5	Specifications for a 6.6 kV submarine cable from Caledonian . . . . .	98
D.6	High voltage cable from ABB . . . . .	99
D.7	Ericsson cable, 1 kV . . . . .	100
D.8	Inductance and capacitance for Ericsson cable 1 kV . . . . .	100

## List of Tables

3.1	Parameters for ABB subsea transformer . . . . .	19
3.2	Parameters for Siemens subsea transformer. . . . .	21
3.3	Parameters for Siemens subsea circuit breaker . . . . .	22
3.4	Parameters for VetcoGray subsea switchgear. . . . .	22
3.5	Parameters for Seabased subsea substation. . . . .	27
4.1	Comparison of specification of the radial and the star connections. . . . .	30
5.1	Cable specifications for the systems under study . . . . .	34
5.2	Results from the first approach cable optimisation . . . . .	40
5.3	Conductor temperature when simplifying the temperature equation . . . . .	41
5.4	Conductor resistance when simplifying the temperature equation . . . . .	41
5.5	The DC system's optimised cable sizes . . . . .	42
5.6	The cost of the cables and losses for the DC systems . . . . .	44
5.7	The AC system's optimised cable sizes. . . . .	45
5.8	The power factor, cost of the cables and losses for the AC systems . . . . .	47
7.1	Cable specifications for the systems under study . . . . .	51
7.2	Results from the first approach cable optimisation . . . . .	53
7.3	The DC system's optimised cable sizes . . . . .	54
7.4	The cost of the cables and losses for the DC systems . . . . .	55
7.5	The AC system's optimised cable sizes. . . . .	56
7.6	The power factor, cost of the cables and losses for the AC systems . . . . .	56
8.1	Costs of cable and losses for 9.3 kV <sub>DC</sub> and 6.6 kV <sub>AC</sub> . . . . .	61
8.2	Results for high voltage transmission . . . . .	63

8.3	Minimum power factor . . . . .	65
8.4	Minimum power factor for wind power . . . . .	66
8.5	Specifications for one cable for a wind/tidal park. . . . .	67
8.6	Specifications for one cable for a wind park. . . . .	67
8.7	Direct costs for 132 kV transmission with Gwynt y Môr . . . . .	68
8.8	Rental costs for 132 kV transmission with Gwynt y Môr . . . . .	69
8.9	Summary of costs for 132 kV transmission . . . . .	70
8.10	Electrical results for 630 mm <sup>2</sup> transmission cable from a wind/tidal park	71
8.11	Comparison of transmission costs at 132 kV, 630 mm <sup>2</sup> and 500 mm <sup>2</sup> . .	71
8.12	Summary of the results of transmission cable calculations . . . . .	72
B.1	Known and estimated parameters for the Newton-Raphson example . .	92
E.1	Summary of all parameters used for the temperature calculation. . . . .	105

# 1 Introduction

Global temperature is rising due to human emissions, where transportation and coal power plants are important contributors [1]. The demand of electricity increases throughout the world as the standard of living are increasing and the global population grows. To meet the future demands the electricity production and consumption must be more efficient as well as new technologies to produce electricity must be invented. This increases the understanding that the future electricity generation should be based on renewable energy sources in order to decrease the emissions.

The EU has set an aim that 20% of their total energy production should be based on renewable sources before 2020 in order to reduce the emissions [2]. For the electricity production, one drawback of many renewable sources is that the produced electricity varies in time, depending on the weather. To get the ability to control when the power from weather dependent renewable sources should be delivered to the grid, a cost efficient energy storage would be needed. Today the alternatives to store large amount of electric energy are very limited but the development is going forward. Another way to get a more stable power production is to use a variety of renewable energy sources. Typical renewable energy sources which are commercial today are for example wind, solar and biomass. By adding other sources to the grid, such as wave and tidal energy, the combined power output from the renewables could be more stable in time [3]. The potential of these renewable energy sources is great, only in Great Britain the potential for tidal electricity generation is predicted to be 95 TWh/yr from tidal stream devices and 69 TWh/yr from wave power [4].

Tidal and wave energy are newly developed technologies with unsolved issues. Many companies have developed the generating unit but there are still many questions of how to design a cost-efficient subsea collection grid. Usual on-land techniques are not directly applicable to a subsea environment since the surrounding water and the pressure at deep waters introduce new technical challenges and costs which have to be taken under consideration.

## 1.1 Problem description

The project is performed for the two companies Minesto and Göteborg Energi. Minesto develops a tidal power device which is called Deep Green. It is specially designed to work at tidal stream velocities of 0.5 - 2.5 m/s. Deep Green is under development and the size of each device used in this project is 500 kW and will occupy an area of 40 000 m<sup>2</sup>. The case that will be investigated is a Deep Green park including 100 devices with a total installed power of 50 MW and an area of 4 km<sup>2</sup>. Minesto's interest in this study is to find out how to design the subsea collection grid for a Deep Green power plant. As well as to investigate the possibilities to connect it to the adjacent 576 MW offshore wind power park Gwynt y Môr in North Wales in order to share platforms, transformers and cables.

Göteborg Energi is a local energy distributor which focuses in a more sustainable energy production. Göteborg Energi has a ongoing project for an offshore wind farm outside of Falkenberg which is going through the permission process at the moment. The possibilities to connect a wave power plant to the wind park is considered and it is of great interest to learn about the opportunities and difficulties with offshore subsea components for a wave power park. As an inspiration for the wave power park the project studies Seabased wave power device. The Seabased solution consists of buoys which generate power by the height difference of the waves. Each buoy needs an area of 1000 m<sup>2</sup> and has an installed power of 25 kW. The case studied consists of 100 buoys with a total installed power of 2.5 MW and an occupied area of 0.1 km<sup>2</sup>.

The major task to solve is how the subsea collection grid should be designed in the most cost efficient way. To get a better understanding for the technical possibilities to design a subsea collection grid a study of subsea components will be conducted. This includes AC- or DC-system, cables, converters, breakers, coupling units and transformers. With a better understanding of available subsea components the infrastructure of the collection grid will be investigated. During the whole project the infrastructure should be chosen and designed with respect to: cost, maintenance, losses and suitability to the subsea conditions. It is of interest to investigate if the power difference between the cases will lead to different collection grid solutions or not.

When the best infrastructure has been selected the cost of the collection grid as well as the cost of the total losses for the system will be calculated. The most cost-effective transmission option will also be calculated both sharing the transmission cable together with the wind park and using an own cable.

The project is divided into four parts: firstly a summary of subsea components in service and under development are presented, secondly the collection grid for the tidal power park is investigated, thirdly the transmission options are studied and fourthly the collection grid for the wave power park is investigated.

## **1.2 Purpose**

The aim is to design two cost efficient offshore collection grids accounting for cost, losses and maintenance. The collection grids are designed for a tidal power park consisting of 100 Deep Green devices of 500 kW each and a wave power park consisting of 100 buoys, 25 kW each. A study of subsea components needs to be performed to be able to use realistic components in the subsea collection grid. Finally, the opportunity to connect the tidal park to an offshore wind farm will be analysed.

## **1.3 Scope**

In order to conduct the study within the time limit of the project some physical phenomena and some practical applications will be neglected. The mechanical forces that act on the submarine cables and components as well as the magnetic field that is created in the system will not be studied. Marine biological fouling growing on the components

and the impact by the collection grid on the environment are also outside the scope of this project. The generating units and their converters will not be investigated in detail, only the power output from each unit will be considered to be able to construct the subsea distribution network. Therefore will only steady state behaviour be studied. Electrical safety of the system have only been considered where needed to be able to design the collection grid. Also the outer border of this study ends by the shore and the main grid will be simulated as an infinite bus. The study does not include any power quality inspection or other restrictions from the grid owner.

In the case of the tidal generator the space for electrical components is limited which has been considered for generators and converters but not investigated in detail. The park is designed for the installed power in the park and no park effects have been taking into account. Data for the wind, wave and tidal speed for the specific sites of the study have not been found, instead measurements from sites nearby have been used together with statistical knowledge. When calculating costs, only costs from losses and relevant components are included, costs for construction and maintenance is not included. Costs of components have been approximated with educated assumptions or calculated from known material used for the component.

## 1.4 Method

Information about subsea components (cables, transformers, power electronics, coupling units and breakers) and their cost is gathered by searching online and by contacting companies and organisations in the area of interest; ABB, Minesto, Nexans, NKT cables, Ocean energy center, RWE npower renewables, Siemens, VetcoGray, Aker Solutions and Ericsson.

There are some differences between the two parks, but the major goal is the same and therefore the method used for finding the most cost effective collection grid is similar. The first step is to compare different collection infrastructures in order to choose the most cost efficient one. Furthermore, a simplified collection grid with only one tidal/wave power device and cable will be theoretically studied and optimised. The next step is to expand and optimise a whole collection grid when considering: losses, cost and maintenance (as few components as possible). If AC is concerned the optimisation is made by using the mathematical Newton Raphson method in the software MATLAB.

An effort is made to find the data of wind, tidal and wave speed for the different sites which should be used to calculate the generated power from each device with respect to time. The specific information required are:

- Wind speed versus time from the Irish sea
- Tidal stream speed versus time from the Irish sea
- Power curve of the tidal/wave devices
- Cable data from the wind power farm Gwynt y Môr

## 2 Background theory

This chapter gives an overview of how the natural phenomena in the oceans such as tides and waves can be used to generate electricity. The focus will be on the two power plants under study, Deep Green and Seabased. Furthermore, the components of a collection grid and requirements when designing one will be described, as well as a deeper understanding for a cable construction and the theoretical model. Finally, different power flow analysis methods will be described with the focus on Newton-Raphson, which is the one used later in this project.

### 2.1 Origin of tide

The tide in the oceans mainly rises from the force of the gravity and from the centrifugal force between the earth, the moon and the sun [5]. As can be seen in Fig.2.1, the gravitation force and the centrifugal force are counteracting each other. The gravitational force is dependent on the mass and the distance between the three bodies while the centrifugal force is dependent on the elliptical movement between the bodies. The resulting force is combined by the moon force and the sun force, where the moon contribution is almost twice as big due to the distance to the earth [6]. The tides are also influenced by landmasses, the topography of the seabed and the rotation of the earth. Due to the landmasses that reflect the tidal waves, the depth which inflicts on the tidal waves size and the earth rotation that modifies the shape, the tides will occur differently around the world.

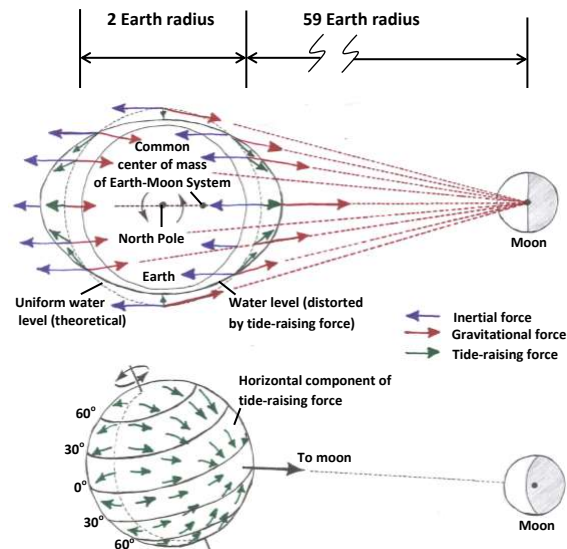


Figure 2.1: Forces on the earth that contributes to the rise of tide.

The tide occurs periodically in relation to the rotational speed of the earth and the moon. Since the earth makes one revolution every 24 hours one high-tide and one low-tide will occur during one day which corresponds to the sun's impact on the tide. The moon orbits the earth in 24 hours and 50 minutes (since the moon moves in the same

direction as the earth rotates around its axis) which will also give rise to a high-tide and a low-tide. This results in four tide changes during a day where the two strongest is caused by the moon [7]. Twice a month, during full moon and new moon, the sun, the earth and the moon are in a line in a way that the forces from the sun and the moon add up to each other. This results in the strongest tide, which is called spring-tide. On the other hand, the tide is at its minimum during half moon as the forces counteracts each other, this is called neap-tide.

The biggest difference between low-tide and high-tide is measured in North America with the result of 12.9 m, but at some places the tide is not even noticeable [5]. The streams caused by the tide are not strong out in the large oceans. In straits or close to the coast however, the streams can be strong enough to be used to generate electricity.

## **2.2 Origin of wave and its correlation to wind**

Waves consist of a complex pattern from different sources where the main contributor is the wind. The minor contributors consist of tidal streams, earthquakes and Coriolis force (from rotation of the earth) [8]. The wind is created from temperature differences around the earth which force the air to move, both from the poles to the equator and from lower to higher atmosphere. When the wind is blowing at the seas, small water ripples first appear that grow into waves as long as the wind speed is greater than the wave speed. However, since the wind is changing in time in both speed and direction, the waves will have a complicated relation to the wind. There are plenty of methods and equations to explain this behaviour which will not be covered here, but can be found in [8]. In Fig.2.2 a simplified model (which does not take the wind direction into account) shows the correlations between the wave height and the wind's speed and duration.

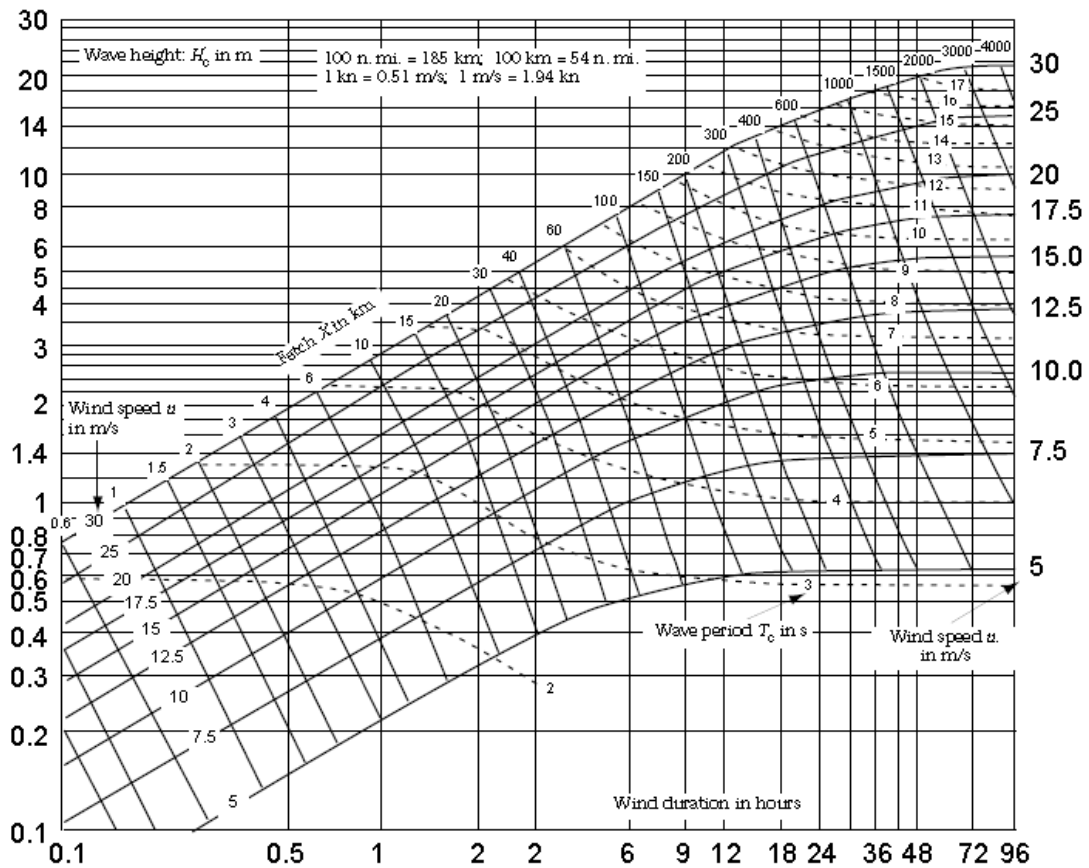


Figure 2.2: The correlation between wave height and the wind's speed and duration [8].

A wave can be described from its period and height, where normally a wave does not exceed 10 m in height and 15 seconds in period. The world's largest wave was recorded in 1933 in the North Pacific with a height of 33 m [8]. When the waves are travelling in a certain speed and direction out at the deep seas, the water particles are almost static. However, when the waves approach the shore the kinetic energy in the wave will be converted to potential energy which forces the wave to slow down and grow in height. During the travelling of a wave the energy loss is therefore rather small and even when the wave hits the shore a lot of the energy will be reflected back to the sea [8]. The power density of a one meter high and wide wave that strikes the shore is about 10 kW [9] and the wave energy potential throughout the world is about 15 000 TWh [10].

### 2.3 How to generate power from tides and waves

Today there exist plenty of different techniques that can be used to produce electricity out of waves and tidal streams. Still the market is at its birth and the different power devices are under development and yet no technique has been industry-leading.

There are two main principles to convert tidal energy to electricity; either by using the kinetic energy from the streams or by using the potential energy from the height difference. A schematic picture, shown in Fig.2.3, explains the principle of how the potential energy can be converted to electricity by using a turbine and force the water to flow this way. However, the majority of the devices on the market today uses kinetic energy, contributed from both tidal and regular streams in the sea [11]. In Fig.2.4 some different technologies that are under development today are shown; SeaGen, OpenHydro and Deep Green. The SeaGen has the same working principle as a regular wind turbine and the rotor blades can be moved along the pillar out of the water for easy maintenance. The OpenHydro is placed at the bottom of the sea with the open centre turbine in the middle. The Deep Green consist of a kite construction which is connected to the bottom and driven in a specific pattern. Minesto’s Deep Green product has the advantages to be light weighted and work at rather low stream speeds compared to the other techniques. Therefore Deep Green is suited to fit at more sites where also the maintenance is easier to perform. Deep Green will be further explained and discussed in Section 2.3.1.

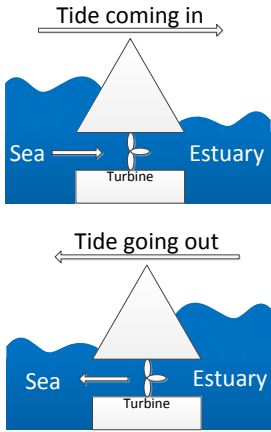
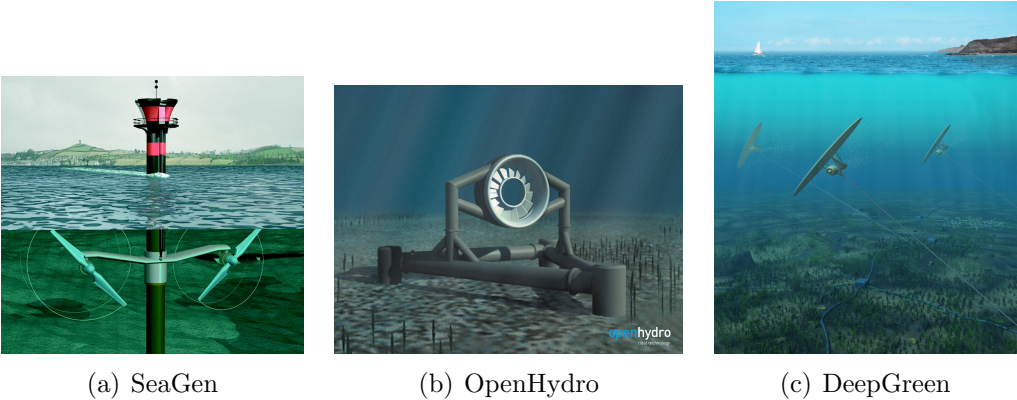


Figure 2.3: Principle of how to convert potential tidal energy to electricity.



(a) SeaGen (b) OpenHydro (c) DeepGreen

Figure 2.4: Three different tidal power techniques [12–14].

When using waves for electricity production there are three main methods; use the height difference from the waves, trap the waves in a fixed reservoir or use the oscilla-

tions of the waves next to the shore. The last method is shown in Fig.2.5, where the waves press the air in and out of an air column to drive a turbine that can produce electricity in both directions. In Fig.2.6 some different wave power technologies are shown; Pelamis, Wave Dragon and Sea Based. The Pelamis consists of tube sections which are hydraulic connected and will compress air when it moves on the waves which will be converted into electricity in a hydraulic generator. The Pelamis was the first wave power plant that delivered electricity to the grid. The Wave Dragon uses the reservoir technique to produce electricity where a regular hydro power generation is used after the waves get trapped in the reservoir, as shown in Fig.6(b). Seabased is a buoy construction with a floating buoy which follows the waves up and down and is connected to a generator at the bottom. Seabased will be further explained and discussed in Section 2.3.2.

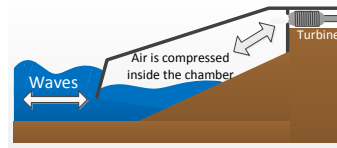


Figure 2.5: Principle of how oscillating waves and an air column can be used to produce electricity.

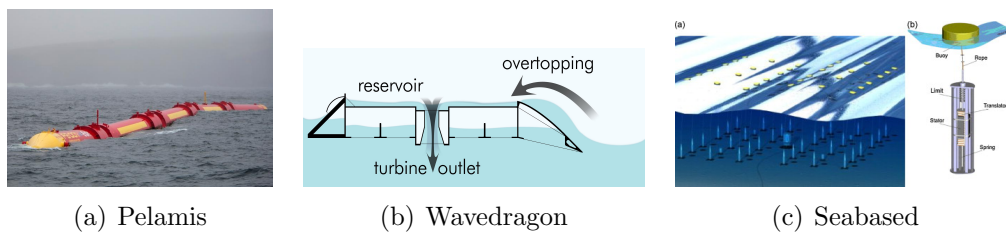


Figure 2.6: Three different wave power techniques [15–17].

### 2.3.1 Deep Green - construction, specifications and generation

As described in Section 2.3 Deep Green consists of a kite construction, as shown in Fig.2.7, and uses the tidal and regular streams to produce electricity. The turbine connected to the nacelle is the heart of Deep Green and is held up by a wing and connected to the bottom by a tether. When the stream passes through the turbine it starts to rotate and generates electricity, which is transferred through a sea cable down to the bottom and further to the shore. The tether length can be between 85-120 m and the tip to surface between 12-16 m, which results in a possible sweep area of 2000 m<sup>2</sup>. Since Deep Green is adapted for rather low streams, 0.5-2.5 m/s, the kite is programmed to follow a specific pattern to gather as much streams as possible and therefore still gets a high power output for rather low streams. The Deep Green, rated for 500 kW, has a 12 m wide and 2.6 m deep wing span and the total weight is about seven tons. Compared to other tidal power plants Deep Green is both small and light weighted and has also the advantage to work at low stream speeds. The power curve for a rated Deep Green of 500 kW is shown in Fig.2.8.

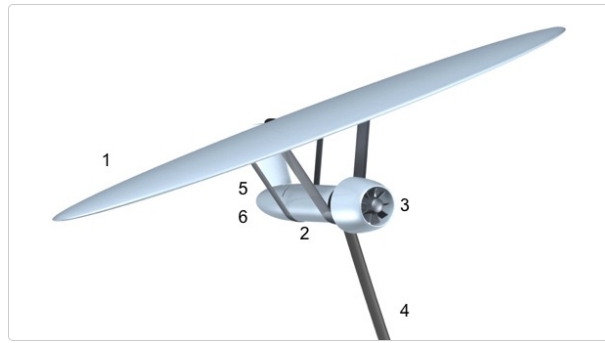


Figure 2.7: Construction of Deep Green: 1) wing, 2) nacelle, 3) turbine, 4) tether, 5) rudder, 6) rear cone.

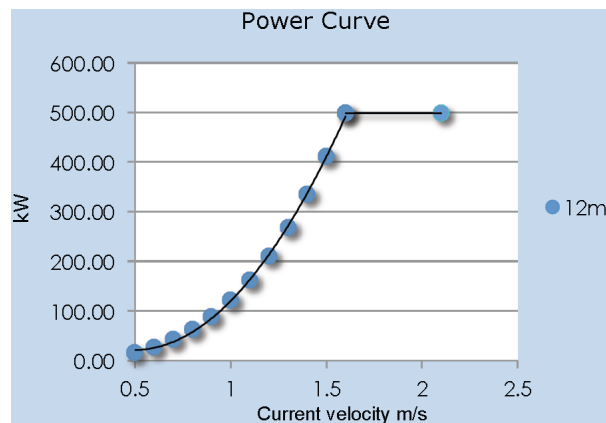


Figure 2.8: The power curve for Deep Green with a rated power of 500 kW [18].

### 2.3.2 Seabased - construction, specifications and generation

Seabased has a buoy solution with a permanent magnet linear generator, as can be seen in Fig.2.9. The buoy is connected with a rope to the translator of the generator. When the buoy follows the waves up and down the translator, which is equipped with strong permanent magnets, will move inside the generator and produce alternating electricity which will be transferred by submarine cables to shore. Each buoy has a rated power of 25 kW and can be placed at depths between 25-200 m. The buoy is six meters in diameter and the generator reaches a height of ten meters. This gives the possibility to place 1000 buoys in 1 km<sup>2</sup>, which is the same as a need of 1000 m<sup>2</sup> per buoy. The predicted operating time of a Seabased park is at least 20 years and afterwards all components involved will be recycled. According to seabased the generator is designed to last for 20 years without any maintenance at a depth of 50 meters [19]. Seabased has also developed an underwater substation equipped with a filter to adjust the power quality and a transformer to increase the voltage for long transmissions. The generated power at different wave heights for a Seabased generator (8 kW) at different non-linear loads is seen in Fig.2.10.

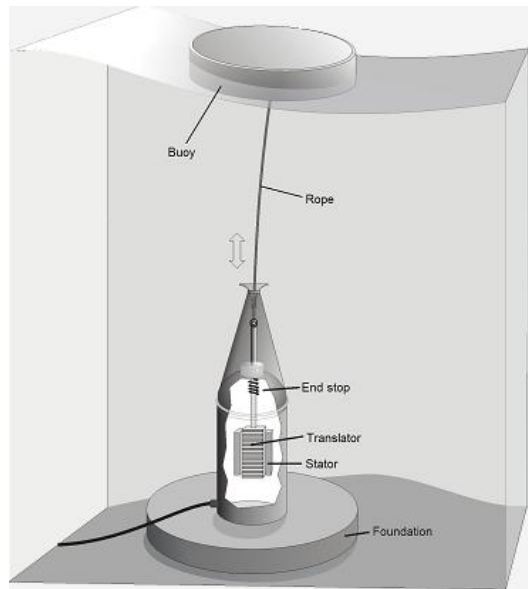


Figure 2.9: Construction of Seabased [20].

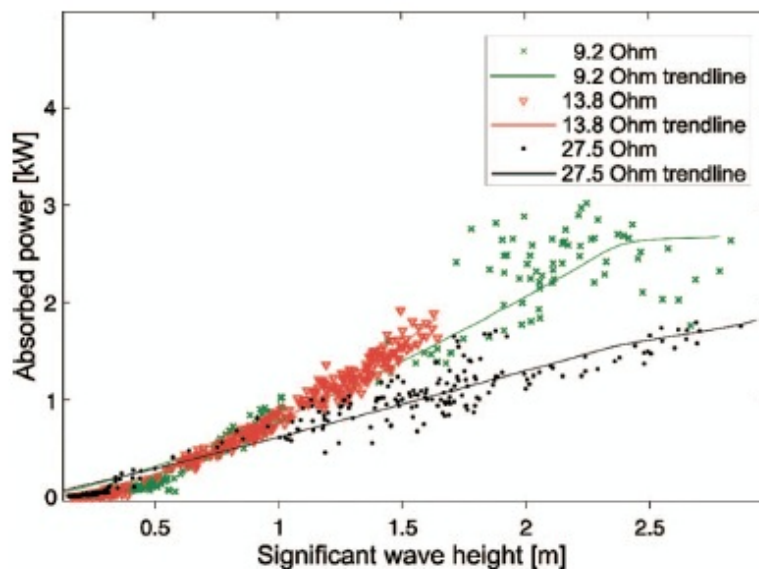


Figure 2.10: Generated power at different wave heights for a Seabased generator (8 kW) at different non-linear loads [36].

## 2.4 Designing a subsea collection grid

The main structure when designing a collection grid offshore is the same as for onshore, with the only difference that the offshore collection grid needs to withstand a harsher environment. However, one advantage with placing components in the sea is that the cooling will be more efficient. It is also very important when designing an offshore grid to minimise the maintenance of the grid, since it is usually more complicated and expensive to maintain components deep under the sea.

A collection grid consists of the following parts:

- **generators** which produce electricity
- **converters** which ensure the power quality
- **coupling units** which connect several generators
- **transformers** which increase the voltage in order to lower the transfer losses
- **breakers** which open the circuit when a fault occur
- **disconnectors** which can open the circuit during, for example, maintenance
- **cables** which connect all mentioned parts above

When designing a collection grid all parts will be dimensioned for the maximum power that the system can deliver. Though, during most of the time the system will only deliver a fraction of the maximum power, which implies that the full capacity is not utilised during most of its operation time. For example, wind power deliver only about 40% of its installed power in average.

#### 2.4.1 Knowledge from wind power parks

The most established offshore power generation technology today is offshore wind power parks. Knowledge from how these parks are constructed can only partially be used for wave and tidal parks, since there are some major differences between the technologies. For a wind park, the generator at the top of the tower is usually of low voltage type (around 400-700 V) and is transformed to a higher voltage (around 30-36 kV) at the bottom of the tower. Here, the generator, the converter and the transformer are all kept inside the protective tower and therefore the components can be regular components designed for onshore conditions. The next step for a wind power park is to transform the voltage to about 132 kV which can be done on a platform offshore. If the park is smaller than 100 MW or at a distance of 10 km or less from the shore it is usually preferred to place the transformer at the shore. A common earth for a grid normally used and offshore wind power solves this by using the concrete steel as ground in each wind tower.

When it comes to wave and tidal power parks, the generator, converter and transformer are usually placed under water and will therefore need to be designed to withstand this environment. However, regular land based components could be used (with only some extra weather protection) if either a floating or a stationary platform were used offshore. A large transformer platform should be valid for wave and tidal power parks under the same circumstances as for the wind power park. Furthermore, submarine cables and coupling units should have the same construction independently of the generation technology. However the voltage and power may differ between the different parks and therefore the cable dimensions will differ as well. The grounding for the Seabased device can be done in the same way as for the wind power since it includes a foundation. For the Deep Green case the grounding can easiest be solved by using either a metal net or a metal skewer at the sea bottom, which is connected to the nacelle of the kite.

### 2.4.2 AC or DC system

Usually an AC generator is used to produce electricity from the turbine. Since the environmental friendly power sources studied here are somewhat irregular and not controllable, an AC/DC/AC converter is used to ensure the power quality delivered to the grid. This converter can be divided into two converters, one AC/DC and one DC/AC, and therefore be placed apart; one at the generator and one close to the grid connection, in order to create a DC system.

There are advantages and disadvantages with AC and DC systems respectively, which will make them more or less suitable for different parks. The advantages when using DC is that only two conductors are needed and that the cable will be overall smaller compared to an AC cable. This gives a low cable cost and low cable losses, since only the resistance contributes to the losses. However, the converter is expensive and its cost increases rapidly with the converter size. If an increase in voltage is requested, as it normally is at high powers, a DC/DC converter can be used for transformation. This will increase the cost of the DC system dramatically. Because of the high installation cost and low losses, DC systems are usually used for long distances and high power applications. AC systems are instead used for shorter distances and lower power applications since transformers are much less expensive than to converters. On the other hand, the drawbacks with AC systems are that the cables need to be dimensioned for the peak current (which differs with a square root of two from the average current) and there are more losses due to the reactive power.

### 2.4.3 Regular array connections

There are three well known main structures for how to connect generation units in an array; radial feeding, loop feeding and star feeding. The connection principles for these are shown in Fig.2.11, where the circles are generator units, the square is a transformer and the lines are cables.

The radial connection is the most simple pattern, where the generation units are connected in rows. One drawback with this structure is that if a fault occurs close to the transformer the whole row will be disconnected. Also if the dimension of all cables are perfectly designed for each distance, there will be several different cables in the system. Alternatively, fewer cables can be used, but the drawback will be over-dimensioned cables for parts of the distances.

The loop connection has the advantage to disconnect a section with a fault and redirect the power flow of the intact generators by closing the disconnecter. This however implies that the cables need to be over-dimensioned during normal operation to be able to carry more power during a fault. A loop construction does not only result in longer, thicker and more expensive cables, but also added disconnectors. That is why this connection is mostly used for systems where faults occur relatively often and/or when the reliability demand is high.

The star connection has a more complicated pattern compared to radial and loop connection. The advantage here is that fewer generators are connected together which results in decreased cable dimensions and fewer generator units are disconnected when a fault occurs. This connection does not require as many different cables to fit the power and distances within the system.

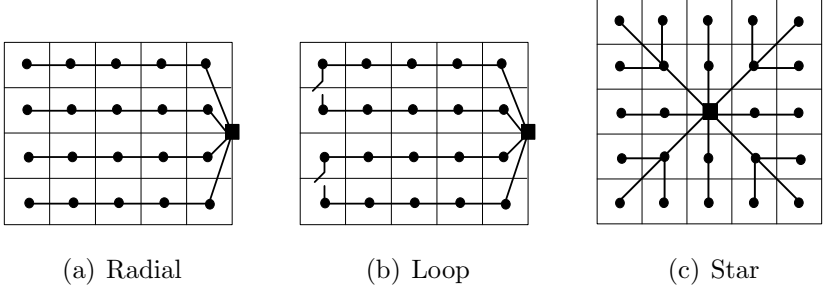


Figure 2.11: Three main structures to connect a collection grid.

## 2.5 Cable construction and theoretical loss calculations

A simple construction of a cable consists of a conductor, screen, insulation, binder, sheath and finish, as can be seen from the cross section of a one phase cable in Fig.2.12. The conductor is normally made of aluminium or copper, which are materials with good conduction properties for a rather low cost compared to silver and gold which have a better conductivity. When constructing submarine cables, copper conductors are preferred since they are less corrodible compared to aluminium. The screen, insulation, binder, sheath and finish protects the conductor from external impact and force the power to stay in the conductor. The sheath is usually grounded for safety reason which creates a large voltage drop over the insulation that it needs to withstand. Furthermore, the insulation needs to be made of a material that is insensitive to ageing as well as heat from the conductors. When considering a three phase cable, all three conductors are usually placed in the same cable, but spaced apart with conductor screen and insulation.

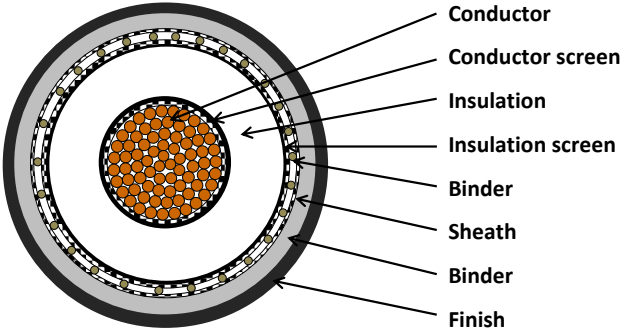


Figure 2.12: The cross section of a one phase copper cable.

### 2.5.1 Equivalent circuit - pi-model

The electrical specification of a cable can be theoretically described by a pi-equivalent, shown in Fig.2.13, where  $Z$  and  $Y$  is explained by

$$Z = R + jX = R + j\omega L \quad (2.1)$$

$$Y = G + jB = G + j\omega C \quad (2.2)$$

This model describes the electrical properties corresponding to one phase, where the parameters usually are referred to as per kilometre. The impedance,  $Z$ , in series consists of the resistance,  $R$ , from the conductor and the inductance,  $L$ , from both the conductor itself and the contribution from the other two phases. The admittance,  $Y$ , in parallel consists of the conductance,  $G$ , between both the conductors and the conductor and the sheath, and the capacitance,  $C$ , which also is created between both the conductors and the conductor and the sheath. The conductance is usually rather low due to good insulation and can therefore be neglected.

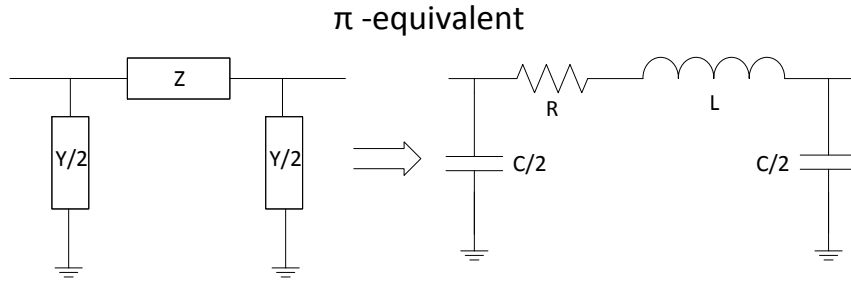


Figure 2.13: Pi-equivalent of one phase of a cable where the parameters usually are given in per kilometre. To the left the lumped parameters are shown as an impedance and two admittances. To the right all the corresponding electrical components is shown.

### 2.5.2 Simple resistive cable loss calculation

From the pi-equivalent representation, described in Section 2.5.1, only the resistance contributes to the active losses. In a DC cable this is the only losses that occur, but for an AC cable the power transferred consists of both active and reactive power, where the latter is not desired. The reactive power is created by the inductance and the capacitance in the cable and will occupy part of the conductor and therefore force the active power to use less area which is the same as increasing the resistive losses.

The minimum conductor area needed for a specific current can be calculated using

$$P_{tot} = 3U_{ph}I\cos\theta = \sqrt{3}U_{LL}I\cos\theta \quad (2.3)$$

$$\text{if } \cos\theta = 1 \implies I = \frac{P_{tot}}{\sqrt{3}U_{LL}} \quad [A] \quad (2.4)$$

$$A = \frac{I}{J} = \frac{I}{2} \quad [mm^2] \quad (2.5)$$

Equation (2.3) can be simplified by setting the power factor to 1 which implies that only active power is involved. With the simplification in (2.3) the active current can be calculated as in (2.4). The current density,  $J$ , is set to 2 A/mm<sup>2</sup>, which is regularly used for long run conditions to avoid heating problems.

When the minimum area have been found from (2.5), the resistance per meter can be calculated by

$$R_{20} = \frac{\rho_{20}}{A} = \frac{1.68 * 10^{-8}}{A} \quad [\Omega/m] \quad (2.6)$$

The resistivity,  $\rho$ , for copper is 1.68e-8  $\Omega m$  at 20°C. The conductor however can be much warmer than this during operation and therefore the corresponding resistance for the operation temperature,  $T$ , can be calculated by

$$R_T = R_{20} \frac{T + 273}{20 + 273} = R_{20} \frac{T + 273}{20 + 273} \quad [\Omega/m] \quad (2.7)$$

When the resistance per meter is found for the conductor it can be multiplied by its length to get the total resistance for this distance. The active power loss for three phases can then be calculated by

$$P_{loss} = 3R_T I^2 \quad [W] \quad (2.8)$$

### 2.5.3 Calculation of cable operating temperature

As mentioned in Section 2.5.2, the temperature in the cable affects the corresponding resistance and therefore the losses in the cable. How high temperature the cable reaches depends on the current flowing in the cable, the size of the cable and the thermal conductivity of the surrounding material. The International Electrotechnical Commission (IEC) is an organisation that sets standards for all electrotechnology. In IEC-60287 [21], which is a commonly used standard document and is referred to in a majority of cable specifications, there is a description of how to calculate the conductor temperature by

$$\Delta\theta = (I^2 R + \frac{1}{2} W_d) T_1 + [I^2 R(1 + \lambda_1) + W_d] n T_2 + [I^2 R(1 + \lambda_1 + \lambda_2) + W_d] n (T_3 + T_4) \quad (2.9)$$

where  $\Delta\theta$  is the temperature difference between the conductor and the ambient environment,  $I$  is the current in the conductor,  $R$  is the resistance corresponding to the maximum temperature of the conductor,  $W_d$  is the dielectric losses,  $T_{1-4}$  is the thermal resistances between different parts of the cable,  $\lambda_{1-2}$  is loss ratios and  $n$  is the number of conductors in the cable. For a more specific description of the different parameters and how to calculate them, see appendix A.

## 2.6 Power flow analysis

Power flow analysis is a very important tool and is used, among other things, during the planning of system expansions, stability studies and to decide the most cost-effective operation mode in an existing system. The power flow analysis is performed during steady-state and there are four variables which should be calculated and these are; the voltage magnitude and phase angle at all buses, as well as the active and reactive power flow in the system. At each bus two of these variables are known and two are unknown. In a power flow analysis the system is modelled with three types of buses; load bus, slack bus and generator bus.

- **Load bus**

This bus is connected to a load with known active and reactive power and can also be called PQ-bus. Nodes which only has transmission lines and/or a transformer connected to it are also set to a load bus.

- **Generator bus**

At the generator bus the active power and the voltage magnitude are known and can also be called PU-bus. It is important to keep the voltage magnitude and the power at these buses constant.

- **Slack bus**

The slack bus is either a generator bus or the main grid, when a whole system or when a part of the grid is investigated respectively. The slack bus is also known as a  $U\theta$ -bus where the voltage magnitude and the voltage angle at the slack bus are usually put to one p.u and zero degrees and kept constant. There is only one slack bus in each system which is used as a reference. The slack bus is used to take care of the variations of power demand in the system. The generator at the slack bus have to be of high rating to be able to produce the extra power that can be needed if another generator in the system is disconnected.

The power flow analysis can be solved by using different mathematical approaches, where three common examples are: Gauss-Seidel, Newton-Raphson and fast decoupled power flow solution. There are some different drawbacks and advantages with these methods which are described below.

- **Gauss-Seidel** is a simple and reliable method which is suited for smaller systems since the computational time increases rapidly with the system's size. It has a slow convergence rate and problems in convergence may occur when the system is stressed.
- **Newton-Raphson** is more complicated but still fast since the computation time increases linearly with system size. It has also a very good convergence rate and is well adapted for large systems where high accurate solutions are required. However, problems may occur when initial values of the voltage are substantially different from the true values.

- **Fast decoupled power flow solution** is a fast method with good accuracy and is not very sensitive to initial values. The method requires a high X/R ratio and small angles in the system since the solution is based on some simplifications.

In this project the Newton-Raphson method has been used to solve the power flow analysis. The fundamental theory of the Newton-Raphson algorithm is to determine the solutions of a non-linear function. The process is basically an iterative process where the unknown variables get a first estimation and then the iterative process continues until the error in the known parameters are zero or close enough. A more detailed description of the Newton-Raphson power flow analysis together with an example is shown in appendix B.

### 3 Subsea components

When a power system is built offshore today the sensitive components, such as transformers and circuit breakers, are usually positioned on dry land or on a platform out at the sea. The only components which are submerged under the water are the cables. During recent years there has been an increasing rate of interest to place these sensitive components under water as well. With a growing interest of sustainable electric power the area of business in tidal and wave power are rapidly increasing and their need for subsea components are crucial. However, the major driving force of the development of subsea components comes from the oil and gas industry which wants to pump oil and gas fields in very deep oceans and also has the money to invest in this development.

This chapter will present subsea transformers, switchgears and connectors, some are used in the oil and gas industry today and some of the components are under development. The big producers of components for subsea environment are ABB, Siemens, VetcoGray and Schneider Electric. The information about subsea components are based on information from the producers [22–38]. There are no theoretical differences between subsea components compared to land based components [39]. The main challenges with subsea components are to design a construction which can withstand the high pressure from the surrounding water and to isolate the components from the water. Another problem is the extremely limited availability of the components under deep water. To be able to carry out repair or maintenance work the components have to be retrieved from the water. This problem is partly solved by using components with high reliability and to minimise the amount of components under water [22, 23]. According to Truls Normann [39] from Aker Solutions the reliability is usually increased by delivering  $N+1$  components to a system. If a component needs maintenance or is out of service the repair time can become up to several months. The costs for having one spare component in store compare to the loss of income from oil production for several months is low. One benefit with the subsea placement of components is the efficient cooling with natural convection to the water. This also increases the reliability since failures in the cooling system is no longer a risk. In some cases it can also be cheaper to submerge the components under water compared to build a platform [37, p. 6].

#### 3.1 Subsea transformers

Subsea transformers are mainly based on a traditional oil filled transformer, with no special difference with the active parts of the transformer [24, 25]. The major difference between a subsea transformer and a traditional transformer is the design of the protective tank which have to withstand the pressure and to protect the inner parts from the water. The transformer tanks are usually constructed of two shells to protect the electrical parts from water [26, 27, 29]. But for transformers with ratings higher than 6 MVA, a single shell is used because the natural cooling in a double shell is not sufficient for higher transformer ratings [24]. The tanks are oil filled, which gives support to the external pressure. A pressure compensator system is also installed which main assignment is to counterbalance the volume variations in the oil which are dependent on the operation of the transformer. The internal pressure of the transformer

tank is kept close to the surrounding pressure [24, 26, 29]. The pressure compensator and all penetrations through the tank will always have two barriers independent of the number of shells. The oil also works as an insulator and a cooling medium and if the oil would get in contact with water it would lose its isolating properties already at water contents of 30-40 ppm [24]. In [24, 26] the assembly of a transformer from ABB is described. The procedure is performed in vacuum and the tank with the active parts are filled with a vacuum treated oil in order to eliminate all potential gas cavities.

### 3.1.1 ABB subsea transformer

ABB started their research on subsea components in 1984 and delivered their first subsea transformer 1998. This transformer was rated at 1.6 MVA 11 kV/1kV and has been in operation since 1999 at a depth of 500 m [26]. ABB has since then delivered 20 subsea transformers working with high reliability, safely and with no maintenance needed [26]. Today they are developing their largest subsea transformer so far to the Ormen Lange project, the specifications are presented in Table 3.1.

Table 3.1: Parameters for ABB's subsea transformer to the Ormen Lange project.

Water depth	1000 m
Rated power	70 MVA
Design primary voltage (ph-ph)	120 kV
Design secondary voltage (ph-ph)	22 kV
Rated currents	337/919 A
Impedance	9 %
Housing	Single shell & double barrier

The construction of ABBs pressure compensators consist of an inner barrier made of corrugated thin stainless steel plates and an outer barrier made of nitrile rubber. Four compensator can be seen mounted on the transformer in Fig.3.1. The upper end of the compensator is fixed to the transformer and the lower end can move up and down to vary the volume of the compensation. The pressure compensator is connected to the lower part of the transformer tank as a safety procedure. If a water leakage would occur somewhere in the tank the water would gather at the bottom of the tank since water have a higher density than oil. The compensator would then stop working and remain at its neutral position independently of the volume variations. A camera is used to monitor the movement of the compensator with respect to the neutral point which is carefully marked [24]. This process is dependent on a time constant which is affected by the leakage size, loading condition, temperature and sea current conditions.



Figure 3.1: ABB transformer with three pressure compensators in the back and one in the front [26].

### 3.1.2 Siemens subsea transformer

Siemens first subsea transformer was delivered to their client Petrobras as early as 1998 [28, 30]. It is an oil filled transformer designed for a depth of 1000 m and is rated 750 kVA with a transformation from 10.5 kV to 3.5 kV. The development of the transformer was divided into three stages where the first stage was to establish the electrical characteristics. The second phase started with testing standard transformer materials overpressure tolerance. Based on the results a scaled-down transformer was constructed and tested. In the third phase the full-scale subsea transformer was constructed and tested. More detailed information about the development of the transformer is available at [28, p. 3].

In 2010 Siemens presented their latest development, a step-down transformer which can be placed at a depth up to 3050 m [29, 30]. An illustrative picture of a cross-sectional transformer is shown in [29]. The picture shows a double shell construction of the tank and a double barrier pressure compensator connected to the lowest part of the transformer similar to the ABB's construction in Section 3.1.1. The specification for the step-down transformer are presented in Table 3.2.

Table 3.2: Parameters for Siemens subsea transformer.

Water depth	3050 m
Total length - width height	4500 x 2400 x 2840
Total weight	23 000 kg , fluid 9 600 kg
Design primary voltage (ph-ph)	72 kV to 22 kV
Design secondary voltage (ph-ph)	6.6 kV
Design life	30 years
Operational frequency range	33 to 66 Hz
Winding configuration	Delta – high resistance ground
Seawater temperature	4 °C
Design temperature range	-5 °C to 40 °C (storage and transport)
Cooling type	Natural circulation
Housing	Double shell design

## 3.2 Subsea switchgears

The switchgear has multiple functions where the most important one is protection using circuit breakers. It is also equipped with disconnectors and works like a power distribution unit.

### 3.2.1 Siemens subsea switchgear

The subsea switchgear from Siemens consists of four standard vacuum breakers insulated with SF<sub>6</sub> which are installed inside two pressure resistant capsules at 1.5 bar [29]. The circuit breakers are then mounted on a fluid filled busbar which is equipped with a pressure compensator, current- and voltage transformers and a control system, an illustration of a circuit breaker from Siemens can be viewed [29]. It also works like a distribution unit with four independent outputs with a circuit breaker connected to each output, which increases the reliability of the system. It is possible to increase the system by adding a fifth output on the switchgear used to connect a second module. The specifications are presented in Table 3.3.

Table 3.3: Parameters for Siemens subsea switchgear.

Water depth	3050m (10,000 ft)
Design primary voltage (ph-ph and ph-gnd)	36 kV
Number of outputs	4
Max power per outputs	10 MW
Design life	30 years
Operational frequency range	33 to 66 Hz
Grounding configuration	Low resistance ground at topside
Seawater temperature	4°C
Design temperature range	-5°C to 40°C storage and handling
Short circuit current (max.)	15 kA rms

### 3.2.2 VetcoGray subsea switchgear

The VetcoGray switchgear uses standard switches and electrical components proven with "extensive in-field experience" and that has "maintenance free vacuum circuit breakers with magnetic actuators" which contribute to high reliability [31]. The switchgear is equipped with a control system and multiple switches which enables multiple controllable outputs. The specifications for VetcoGrays switchgear are presented in Table 3.4.

Table 3.4: Parameters for VetcoGray subsea switchgear.

Water depth	2000 m
Rated voltage (ph-ph and ph-gnd)	24 kV
Rated current	1800 A
Overall dimensions (3-switch version)	Approx. 5.5 x 2.5 x 3.5 meters
Total weight (3 switch version)	Approx. 35 tons

### 3.2.3 Schneider Electric subsea switchgear

Schneider Electric has developed a subsea switchgear used to supply variable frequency drives and control systems [32]. They have constructed a cylindrical tank equipped with two identical busbars and each busbar consists of two transformers (22 kV to low voltage), two high voltage circuit breakers, low voltage protection and a control system. The tank and one busbar are shown in Fig.3.2. One design criteria was to ensure that the electrical system should be able to operate faultlessly and without any maintenance for at least five years. The reliability is ensured mainly by using standard electrical components which has been proven in service for many years [32, p. 4]. Also the choices of material is important to improve the reliability For example, standard steel was chosen over stainless steel as material to support structures for the components.

The reason was that standard steel reduces the coupling between components emitting electromagnetic fields and electronic components which can take damage.

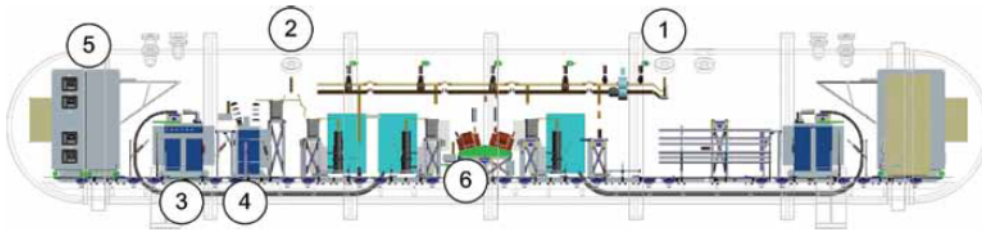
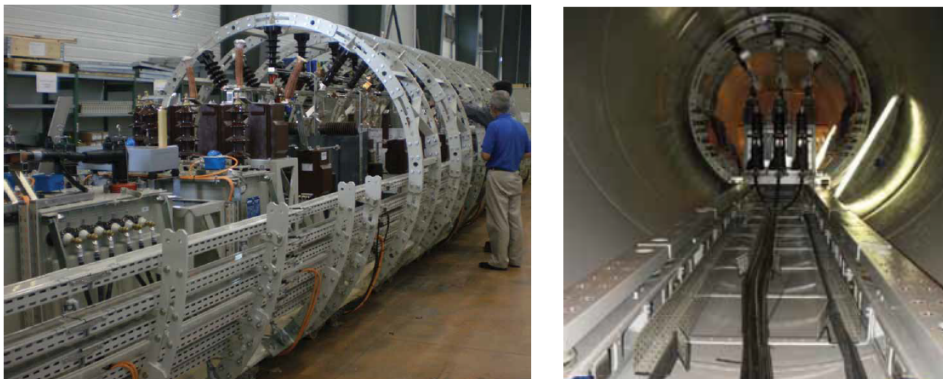


Figure 3.2: The component layout of the Schneider Electric switchgear for busbar 1 [32]. 1) Penetrator for incoming 22 kV cable. 2) Penetrator for outgoing 22 kV cable to variable frequency drives. 3) Transformer 2. 4) Transformer 1. 5) Low voltage power, protection and control cubicles. 6) Voltage transformers.

The cylindrical tank has an exterior diameter of 2.8 m and a length of around 17 m. The tank is designed to withstand the pressure at the depth of 1000 m which corresponds to about 100 bar and with a life-span of at least 30 years. The construction is shown in Fig.3.3 and Schneider Electric installed the switchgear at the depth of 1000 m in 2011.



(a) A pre-assembly of the complete subsea switchgear system for testing. (b) Beginning to install components inside the cylindrical tank.

Figure 3.3: Schneider Electric subsea switchgear [32].

### 3.3 Connector systems

The connector systems consist of a connector, mounted on the cable, and a penetrator, mounted on the component, and are considered to be the weakest point in a system [23, p. 13]. There are two types of connectors, the drymate and the wetmate connector. The drymates are connected above the sea level and then the component is lowered down to the seabed together with the cable, see Fig.3.4. The wetmates are constructed to be able to interconnect the cable and the component at the seabed, see Fig.3.5.

The drymate is considered to be the safest choice and has also the advantage to withstand very high power ratings compared to the wetmate. The drymate alternative is also much cheaper compared to the wetmate. However, there are several drawbacks with the drymate connector which have to be taken into consideration when comparing the costs [40];

- as can be seen in Fig.3.4 the cables need to be longer to be able to retrieve the components which brings an additional cost of cables.
- the extra length of cables needed when retrieving the component cannot be fixed to the seabed and can therefore be moved by strong currents.
- the cables add an additional weight and make a retrieval of the component more difficult and expensive.

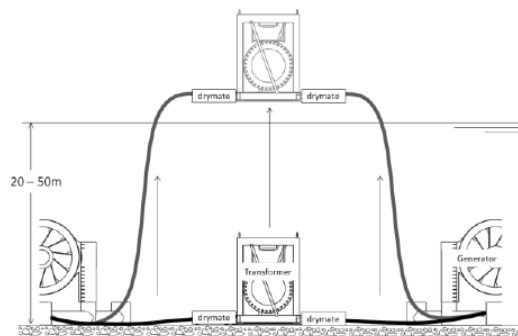


Figure 3.4: Drymate connection [40].

The wetmate connectors have their biggest advantage in very deep seas since there is no need of extra long cables when wetmates are used. Therefore are wetmate connectors often used in oil and gas subsea distribution systems. But still the HV wetmate connections and penetrations are very expensive and is usually the factor which makes the subsea components much more costly compared to land based components [39]. Even though the wetmate connector has a more advanced construction the risk of failure is still relatively high [40]. Since there is a high demand of wetmate connectors from the oil and gas industry, as well as the tidal and wave power business, their development is rapid with increasing reliability and higher power ratings.

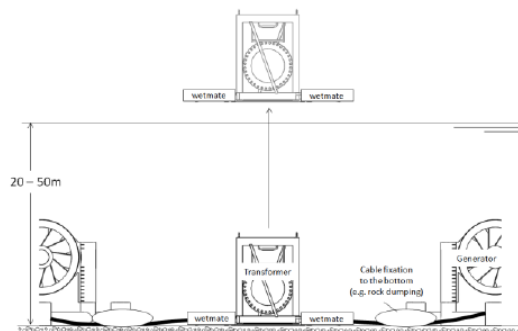


Figure 3.5: Wetmate connection [40].

### **3.3.1 Siemens connector system**

Siemens has a series of wetmate connectors at a voltage range from 2 kV to 10 kV, called SpecTRON [33], and a 60 kV wetmate connector under development. Siemens used SpecTRON 5 wetmate connectors when they installed their first subsea high power system for Petrobras to power a submersible pump, the transformer used in this project is presented in Section 3.1.2. Since then Siemens claim that the SpecTRON 5 system is seen as the industry standard installed at 28 different locations all over the world. The SpecTRON connector system is constructed for a maintenance free design life of at least 25 years. The working principle of the SpecTRON system is illustrated in [33].

The 10 kV connector system, SpecTRON 10, is a one phase connector which results in three SpecTRON 10 connectors per cable. The maximum current is limited by the penetrator and varies between 330 - 520 A depending on the ambient temperature and supply frequency. The design life of SpecTRON 10 is 30 years and it can be submerged to 3000 m. The force needed to connect and disconnect a SpecTRON 10 is 2000 N.

### **3.3.2 VetcoGray connector system**

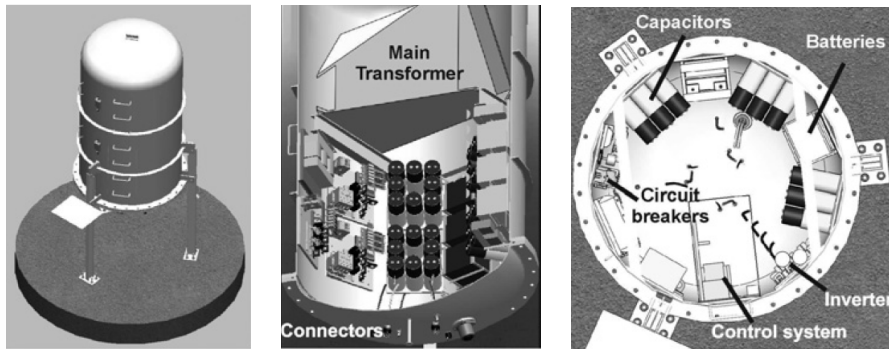
VetcoGray developed the worlds first 145 kV drymate penetrator which is attached at ABB transformer in the Ormen Lange project [24]. The penetrator is based on VetcoGray's standard 36 kV cable termination. All electrical parts are isolated from the water with two housings filled with an ester based oil and each housing has their own compensator system. Halfway inside the inner housing a conducting pin is placed and it is surrounded by an electric cable termination and epoxy container. The pin is connected to the transformer via the bushing. An illustration of the VetcoGray drymate connector can be seen in [24].

VetcoGray also delivers a wetmate connector system called MECON with a voltage range between 7.2 - 36 kV [34]. The construction consist of a double barrier system and with two electrical insulation layers. The first electrical insulation layer is made of a solid material and the second is a di-electric fluid [35]. It has a design life of 25 years, a maximum depth of 2500 m and the connection principle is shown in [27].

## **3.4 Seabased AB - marine substation**

Seabased AB has developed and patented a wave power converter and its associated electrical system. All the electrical components, except the generator, is placed in a substation. The advantages of using a subsea substation is that the components are shielded from the harsh environment at the sea level, the surrounding water enables efficient cooling and the completely sealed substation enables a pollution free environment. One disadvantage is the need of retrieving the substation for maintenance. To ensure a continued operation of the system during maintenance of a substation Seabased plans to replace the substation with a new one and perform the maintenance in a controlled environment onshore [38, p. 4394].

So far a substation made for testing has been constructed with a volume of 3 m<sup>3</sup> and a diameter of 1250 mm. It is designed to handle an internal pressure of 3 bar but the substation is pressurised at 2.5 bar with nitrogen in order to reduce the risk of leakage [37, p. 5-6]. To protect components from leaking water a vertical orientation was chosen and all cables are connected at the bottom of the substation. A water detection system was also developed with four sensors at different heights to measure the potential water level in the substation [36, p. 65]. When choosing components it is important to make sure they can withstand the pressure inside the substation. The components are mounted on the inner wall of the substation in order to achieve an efficient cooling. The electrical design inside the substation consists of a filter, transformer, breakers and a control system which can be seen in Fig.3.6 and Fig.3.7 which illustrates the electrical scheme for one phase [37].



(a) The design of the substation. (b) A visualisation of the substation from the side with the transformer positioned on the top and the connectors in the bottom. (c) Components shown from the top of the substation.

Figure 3.6: Seabased marine substation [37].

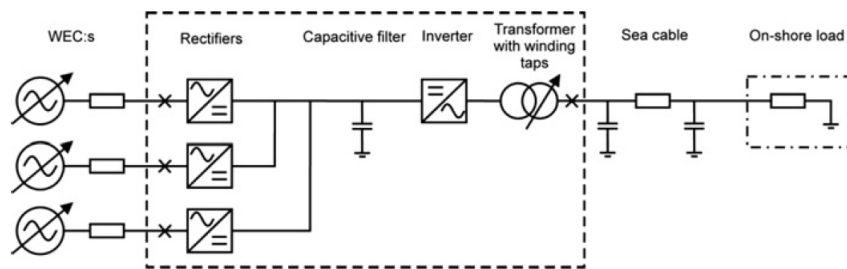


Figure 3.7: One phase electrical scheme inside Seabased substation [37].

Since the wave generators are producing a voltage and current with varying frequency and amplitude, the voltage needs to be rectified before the wave power plants are connected together in parallel. To ensure high reliability and efficiency a passive rectifier was chosen over an active one. An active rectifier is good to use for individual damping for each generator, but it was dismissed because of the need for individual driver circuit and semiconductors. The extra components will increase the cost and the system

will become more complex which will decrease the reliability of the system, especially in the future when a park can consist of up to a thousand generators [37, 38]. After the rectifier a capacitor is used to smoothen out the DC-voltage even more. When choosing a capacitor the pressure in the substation was a critical parameter and an aluminium electrolytic capacitor was chosen [37, p. 6]. The next step is to invert the DC-voltage to an AC-voltage This is achieved with a IGBT based inverter which is used to control the power output of the inverter. This on the other hand controls the DC-voltage level and by that controlling the loading to the generators. The last step is to increase the AC-voltage before the transmission to the grid on shore. This is done with a tap-changing transformer and the voltage is kept constant at 1000 V, the transformer ratios are presented in Table 3.5 together with the specifications for the substation [37, p. 5].

Table 3.5: Parameters for Seabased subsea substation.

Substation power	96 kVA
Maximum water depth for present design	30 m
Vessel volume	3 m <sup>3</sup>
Concrete foundation weight	5 tonne
Substation output voltage	1 kV
Max. DC voltage	500 V
DC-link capacitance (DC+ to DC-)	0.24 F
Transformer winding ratios [V]	1000/250, 180, 125,100, 80
Tap changing mechanism	Circuit breakers (off-load)

As can be seen in Fig.3.6 the substation is also equipped with a control system. The control system is powered by three parallel power supply systems based on 24 V batteries which are charged from the substation AC output through a transformer and a standard battery charger. There are no fuses in the power supply system because its very complicated to replace them under water [36, p. 57]. The diodes and resistors used in the power system are constructed to withstand a short circuit. A second safety procedure is to power all critical control systems with all three 24 V systems.

The control system in the substation is divided into three controllers; the first controller is used for the safety and relays, the second controls the inverter and the rectifiers and a third controller is installed for the measuring systems used during the developing stage. The safety and relay controller is used to control the breakers, the tap changer at the transformer and the power supply to other systems. The breakers are positioned at all the inputs and the output of the substation which can be seen in Fig.3.7. The control of the power supplies to other systems makes it possible to manually reset the system. The controller was first programmed to trig on a pre-defined current value in the neutral conductor. This works fine for a three phase generator connected to a symmetrical load. But it did not work when the wave generator was connected to a non linear load since the current in the neutral gets much higher. Instead the controller triggers on a critical temperature inside the inverter and the rectifiers [36, p. 59]. Directly after a generator is disconnected, a delta connected dump load in form of an electric water

heater at  $12 \Omega$  is connected to the generator in order to stop the generator [37, p. 5]. The second controller is used to control the inverter in the substation. This controller measure the voltages and currents at the DC side, the output of the IGBT and the transformer output which is then used to control the switching of the IGBTs [36, p. 60].

In the future, Seabased is planning to construct parks with up to a thousand generators and this requires a larger substation. The generators are supposed to have a power rating of approximately 25 kW for the Swedish west coast. At better locations, for example at the Norwegian coast, generators with a power rating up to 100 kW are possible [38, p. 1]. Seabased Industry AB started to construct a substation for the Norwegian conditions in 2009 [38, p. 3]. The substation is constructed for 40 to 50 wave generators and has a volume of  $5 \text{ m}^3$ . In order to make future serial production more efficient, the layout of the components has been changed. All components are now mounted on an inner structure and heat sensitive components will have heat sinks which are pressed against the inner wall of the substation which is shown in Fig.3.8. The substation presented so far is a low voltage substation which should be sufficient for smaller parks close to the shore. For bigger parks Seabased is planning to develop a second substation to interconnect several low voltage substations and then if necessary transmit the power to the grid with a medium voltage level.

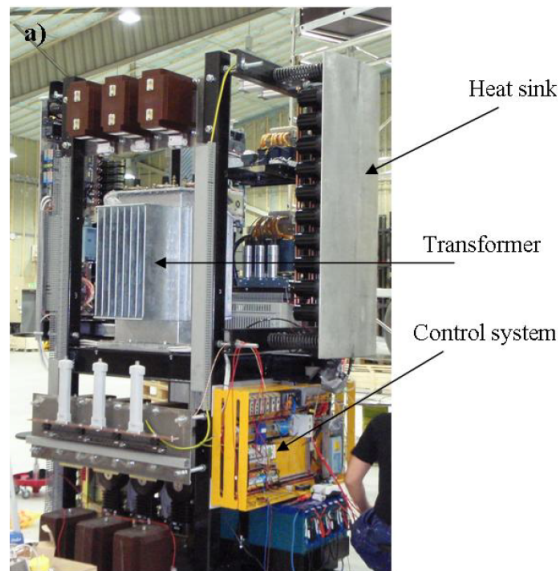


Figure 3.8: Seabased substation's inner structure of the newer version [38].

## 4 Connection of a Deep Green park

This chapter includes the main structure of the Deep Green tidal park and the two best solutions for how to connect the park. The system is simplified to a fourth of the final park at a first stage and then expanded to the full 100 kites system. This simplification is done for two reasons; the connection pattern is easier to construct and also a smaller park may be the alternative to build at a first stage in reality.

### 4.1 Main structure

In Section 2.3.1 it was stated that the tether length could be between 85-120 m. From now on the length of the tether is set to 100 m for simplicity. The main structure for 25 kites, each represented by a black dot, can be seen in Fig.4.1, where each kite takes up a square with the side of 200 m, i.e. two tether lengths.

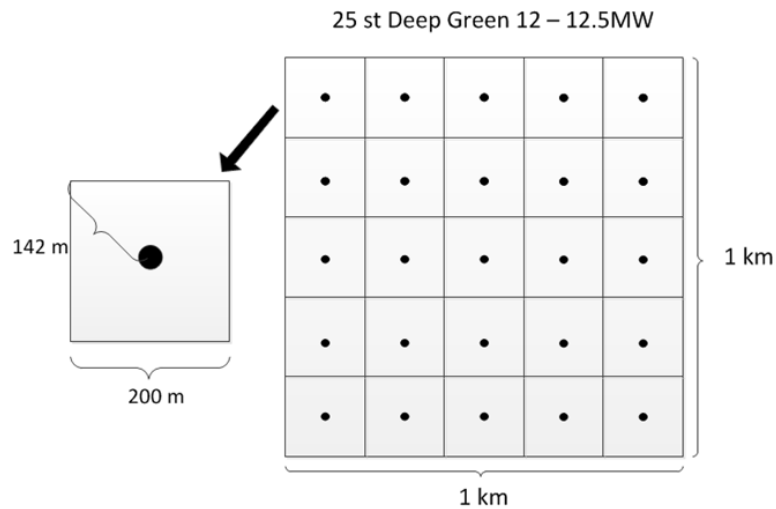


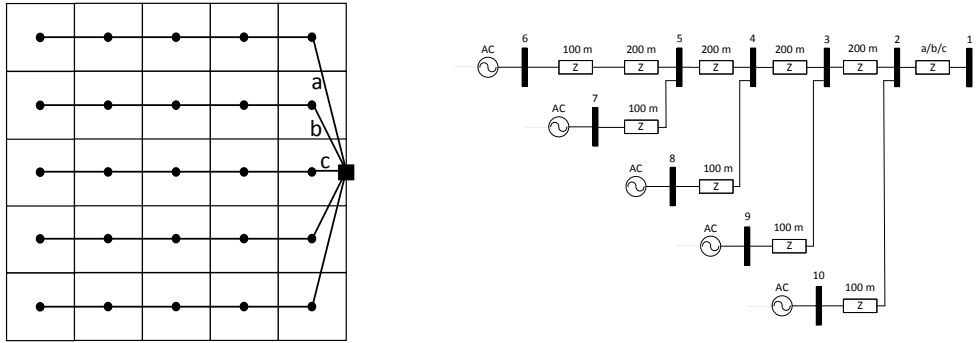
Figure 4.1: Main structure of 25 Deep Green generating units.

### 4.2 Network connections preferred

With this main structure set there are numerous of ways to connect these kites together. As was described in Section 2.4.3 there are three regularly used connection pattern: radial-, loop- and star connection, where loop connection was not investigated in this case due to its high expense. Left are the radial and star pattern, however, for both of these two connection patterns, there are several different opportunities of how to connect the system. To be able to find the best connecting pattern, different connections were tested and compared with respect to:

- total cable length
- the amount of different cable sizes needed to perfectly match the transmitted power
- total number of connector units
- number of different connector units that is needed

After the comparison, two different patterns, one within the radial and one within the star connection were found to be preferable. These structures can be seen in Fig.4.2 and Fig.4.3, respectively. The radial system have the advantage to have the shortest total cable length and a very simple pattern. The drawbacks with this structure is the high number of connectors which reaches 66 and that five different cable types are needed to perfectly fit each distance. The star connection on the other hand only needs 34 connectors and two different cables. The total cable length though is longer than for the radial connection and the pattern is perhaps somewhat more complicated. In Table 4.1 a summary of the radial- and star connection specification are listed.



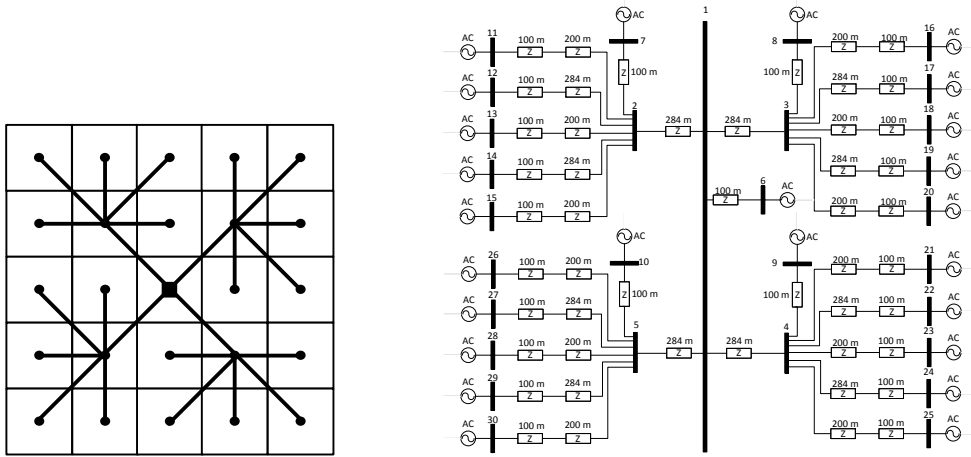
(a) Selected radial connection. The black dots are representing the generating units and a/b/c stands for the different length of the cable.

(b) Corresponding circuit for one branch in the radial connection, i.e. five kites.

Figure 4.2: Selected radial structure for 25 Deep Green generating units.

Table 4.1: Comparison of specification of the radial and the star connections.

	Radial	Star
Total cable length [m]	7872	8308
Number of cable types	5	2
Number of connectors	66	34
Number of connector types	2	2



(a) Selected star connection. The black dots are representing the generating units, including one in the middle and at each connection point.

(b) Corresponding circuit for the star connection. A larger copy is to be find in appendix C.

Figure 4.3: Selected star structure for 25 Deep Green generating units.

### 4.3 Full-scale system

To construct a full-scale system from four small-scale systems of 25 kites each, again different opportunities of how to connect them enables. The best solution is now depending on if transformers are needed, and if so, where to place them. Since transformers are rather expensive components, especially offshore due to the extra cost of either a platform or a subsea transformer, it is decided to keep the number of transformers low. Therefore, the whole connection grid will be collected to one single point where a transformer can be placed and used by the whole park. If no transformer is needed offshore, the systems of 25 kites can be used by themselves, i.e. the cable from each park will be connected directly to a transformer on land.

When it was decided that the whole park should be connected to one point the options of how to connect the parks decreased dramatically. For the radial system, the 25 kites park will be slightly rearranged by directly connecting each radial to the center of the 100 kites park, as is shown in Fig.2(a). The star connection needs a more dramatic rearrangement from the 25 kites park. Otherwise the power from the kites closest to the centre of the 100 kites park would have to be transferred back and forth which contribute to more losses. The solution was to connect the three kite groups (of six kites each) at the edges of the park to the fourth group closest to the middle and then connect all 25 kites to the connection point in the centre of the 100 kites park, as can be seen in Fig.2(b).

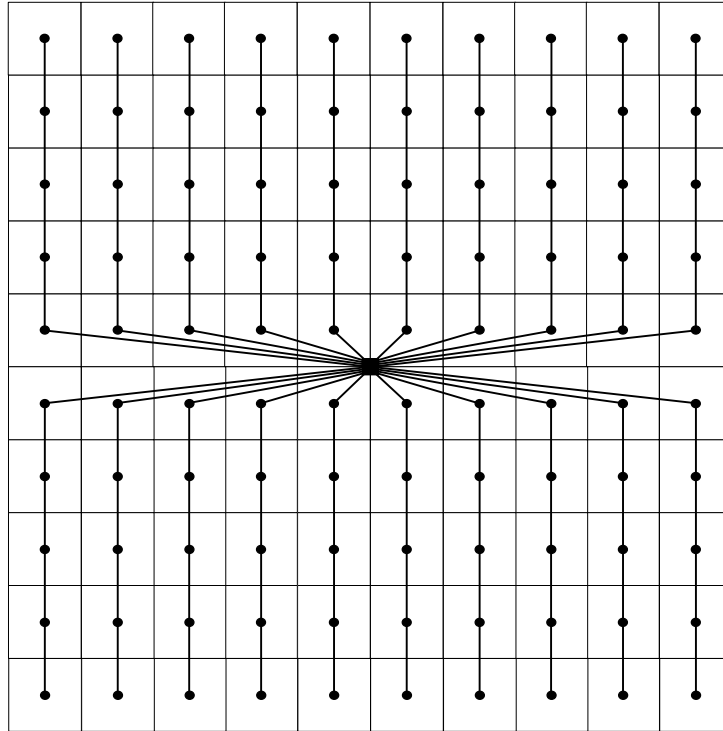


Figure 4.4: Selected radial structure for 100 Deep Green generating units.

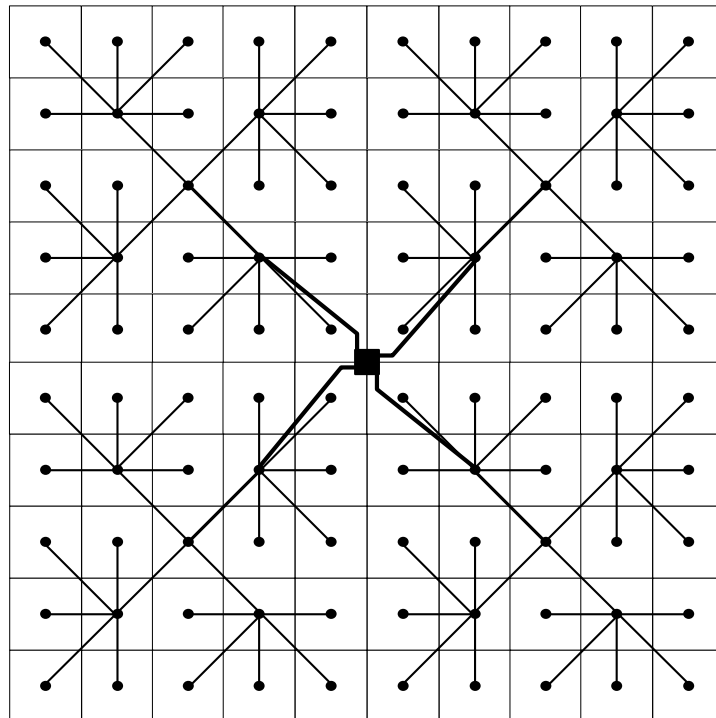


Figure 4.5: Selected star structure for 100 Deep Green generating units.

## 5 Optimising cables for the tidal collection grid

This chapter includes the optimisation of all cables in each system under study as well as the cost determination and final result. The first five sections treat the start conditions; voltage level, system design, cable cost, tidal data and resistance corresponding to the operation temperature. Then the cable optimisation is done in three steps where the final results for the DC system is represented in the second part and the AC system in the third part. The final section includes a discussion, comparison and selection between the systems.

### 5.1 Voltage levels

Four different AC voltage levels have been considered for the collection grid; 690 V, 3.3 kV, 6.6 kV and 10 kV. The DC voltage, after the rectification, will be (at least) as high as the peak value of the AC voltage; 980 V, 4.7 kV, 9.3 kV and 14.1 kV. The selection of 690 V is based on that wind power commonly uses generators at this voltage level. The higher voltage steps are selected because they are standard levels for generators and cables. Furthermore, according to Roland Wida at ABB, there is no big difference in either size, weight or cost between these voltage levels for the generator [41]. This statement seems reasonable since the power of the generator will be the same independent of the voltage level. The only difference between the generators will be the thickness of the wires as well as the number of turns, while the total amount of copper will be the same. However, other components like converters and transformers may be more expensive with increased voltage. Therefore, all four voltage levels will be compared at a first stage.

### 5.2 Systems' conditions

To be able to choose the most cost efficient cables, some basic knowledge for the different cable distances need to be known. Firstly, to minimise the complexity of the systems, the number of cable types need to be kept low. This is not a problem for the star system, which only needs two optimised cable types. However, for the radial system there are five different power levels and to reduce the complexity only three different cables will be used. This will result in that two of the cable distances, the one carrying two kites and four kites, respectively, will be over dimensioned. In Table 5.1 the fundamentals for each cable distance and for each system are presented.

Table 5.1: Cable specifications at four different voltage levels, AC (line-to-line rms) and DC, for radial and star connection, respectively. Where the maximum length represents the longest cable distance in the specific system.

	Radial connection			Star connection		
	1	3	5	1	6	25
Number of kites	1	3	5	1	6	25
Power [kW]	500	1500	2500	500	3000	12 500
Maximum length [m]	300	200	412	384	284	710
Current @ 0.69 kV <sub>AC</sub> [A/conductor]	418	1255	2092	418	2510	10459
Current @ 3.3 kV <sub>AC</sub> [A/conductor]	87	262	437	87	525	2187
Current @ 6.6 kV <sub>AC</sub> [A/conductor]	44	131	219	44	262	1093
Current @ 10 kV <sub>AC</sub> [A/conductor]	29	87	144	29	173	722
Current @ 0.98 kV <sub>DC</sub> [A/conductor]	256	769	1281	256	1537	6405
Current @ 4.7 kV <sub>DC</sub> [A/conductor]	54	161	268	54	321	1339
Current @ 9.3 kV <sub>DC</sub> [A/conductor]	27	80	134	27	161	670
Current @ 14.1 kV <sub>DC</sub> [A/conductor]	18	53	88	18	106	442

### 5.3 Conductor and cable cost

The cost of submarine cables is not easy to find among the companies in the cable business industry. Nevertheless EBR (Elbyggnadsrationaliseringen), which is an organisation in the Swedish energy sector, has compiled cost information from the energy business. Among the cost information there are four submarine cables at two different voltage levels. The conductor sizes are in the range of 35-240 mm<sup>2</sup> for 10 kV and 20 kV, respectively. These costs together with their linearisation is shown in Fig.5.1.

At a first stage only the copper cost of the cable is accounted for. This since the linearisation of the total cable cost might not be credible for very large cables. According to Björn Sonerud at Nexans the copper cost of a cable is a good indicator of how expensive the total cable will get [42]. This statement can also be proved by comparing the copper cost of the conductors with the submarine cable costs from EBR [43]. However, it should be noticed that the copper price varies in time. It is not uncommon that the price changes 20-30% in one year, and from 2009 to 2013 the copper price has doubled.

Figure 5.1 shows that the cable cost is almost parallel to the copper cost and therefore is a good indicator of the cable cost. In Fig.5.1, also an estimated cable cost are shown for 3.3 kV and 6.6 kV, respectively. The linearisation in Fig.5.1 stops at 500 mm<sup>2</sup>

because of uncertainties in the costs for larger cables. If there is need for larger cables than  $500 \text{ mm}^2$ , parallel cables at smaller sizes have been used instead. These cable costs are calculated by comparing the difference between the cable cost and the conductor cost for the four known cable costs at 10 kV. The cost difference is then assumed to be proportional to the insulation thickness, which is the parameter that changes the most between the different voltage levels. The cost for the insulation per mm is then calculated and applied for the insulation level for 3.3 kV and 6.6 kV, respectively. Insulation details for each voltage level is to be found in appendix D.

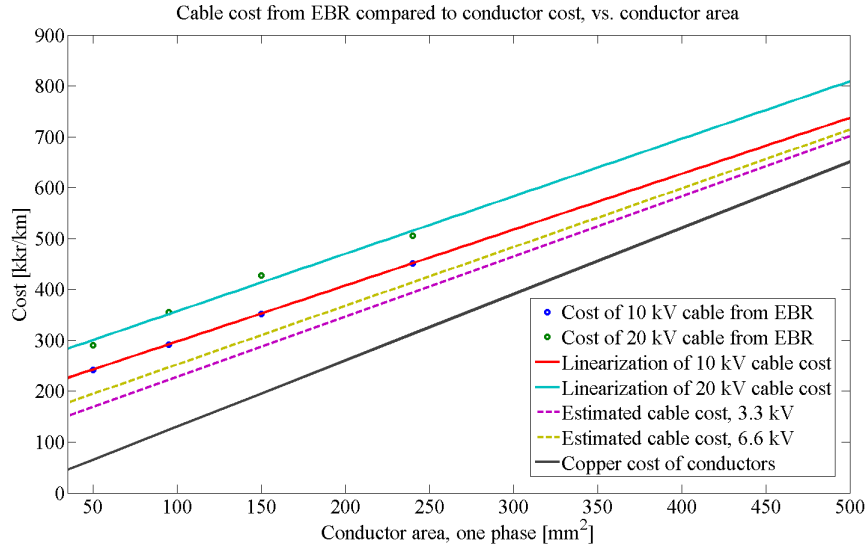


Figure 5.1: Comparison of copper conductor costs with the total cost of a submarine cable from EBR at 10 kV [43].

## 5.4 Tidal stream data

The power production from the Deep Green depends on the tidal stream according to the power curve shown in Fig.2.8. The tidal stream data being used was measured by Minesto AB at a beneficial site in the Irish Sea during 2012, with a time interval of 10 minutes. The stream data can be modelled by a Rayleigh distribution with the scale factor of 0.9045, as can be seen in Fig.5.2. The mean stream speed for this site is 1.14 m/s, which corresponds to a power production of 182 kW. The capacity factor,  $K$ , is then calculated to 36 % by dividing the mean power production with the maximum power production of 500 kW.

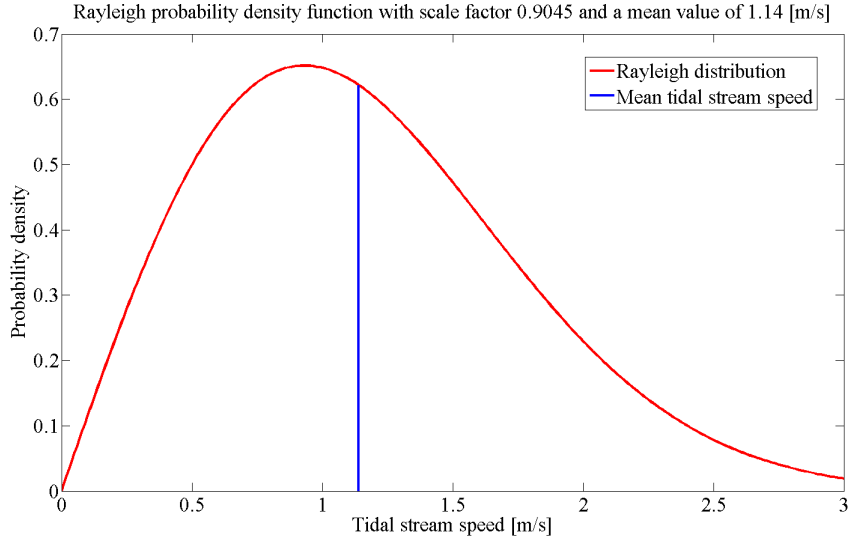


Figure 5.2: Rayleigh distribution of tidal stream measured during 2012 in the Irish Sea.

## 5.5 Resistance corresponding to the operation temperature

In order to calculate the correct active losses, the resistance requires to be calculated for the corresponding operation temperature. Since the resistance at a given temperature is known from the data sheet or calculated by (2.6), a new resistance corresponding to another temperature can be calculated by using (2.7). For 10 kV there exist submarine cables having sizes between 35-240 mm<sup>2</sup> from Nexans, with data sheets that include the corresponding resistance at 90 °C, AC and 20 °C, DC. The insulation for the submarine cables consists of XLPE which withstands a maximum temperature of 90 °C.

The complicated part is to calculate the new temperature. The temperature of the cable depends on several things; the current in the cable, the cable size, the surrounding temperature and the thermal resistivity of the different materials involved. To be able to calculate a more precise resistance, (2.9) is used. However, this equation requires a detailed knowledge of the cable construction (including both dimensions and material properties), which is normally not even included in the cable data sheets.

Therefore, to be able to use this equation for cables with less information, some simplification can be made. To ensure that the simplifications can be made without a major change in the result, a well documented 10 kV submarine cable from Nexans have been used for comparison. The temperature as a function of the current have been calculated for the 10 kV cable of two different sizes, 50 and 240 mm<sup>2</sup>. Both with using (2.9) and by neglecting  $T_2$ ,  $T_3$ ,  $\lambda_1$  and  $\lambda_2$  in (2.9), i.e. by

$$\Delta\theta = T - T_a = (I^2R + \frac{1}{2}W_d)T_1 + W_d n T_4 \quad (5.1)$$

where  $T$  is the temperature in the conductor and  $T_a$  is the ambient temperature set to 20°C. The results of this comparison is shown in Fig.5.3 and the calculations can be

found in appendix E. As can be observed from Fig.5.3 there is a major difference in the temperature at high currents, especially for the smaller cable. However, in a worst case scenario, when the simplified temperature model reaches 90 °C for the 50 mm<sup>2</sup>, the difference in the resistance is only 7 %. Therefore are these simplifications only applicable for operations at low temperatures depending on how low errors that can be acceptable.

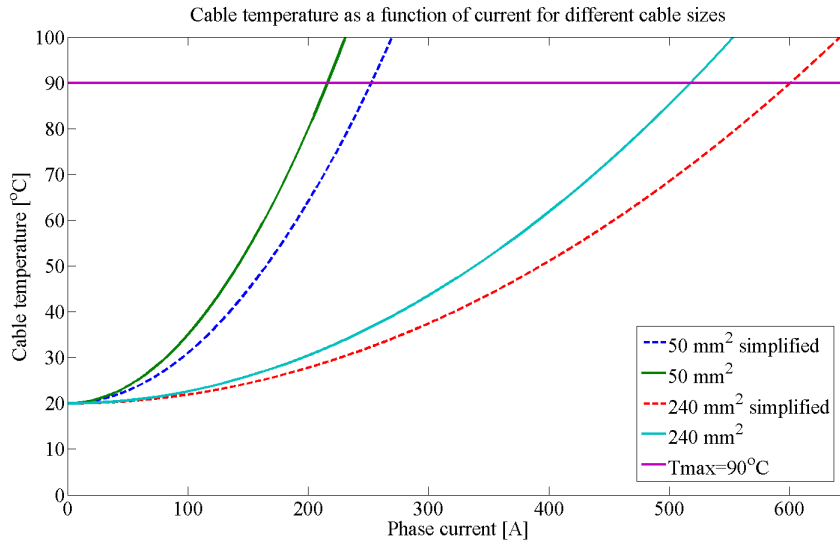


Figure 5.3: Cable temperature as a function of the current in two different cables, with and without simplifications of the temperature equation.

## 5.6 Cable area optimisation

In order to choose the most cost efficient cable the lost revenue from the power loss will be compared to the cable cost. To get a first approximation of which cable to choose, only the resistive losses at 20°C and the conductor cost will be included. The next step is to recalculate the resistance for the corresponding operation temperature and including the total cable cost. This will give a good approximation of the DC-cable sizes, but for the AC-cables also the reactive power will affect the results. Therefore a power flow analysis is done to calculate the losses for the AC-cables.

Throughout this section an AC cable will be referred to as a three phase cable and a DC cable to a two conductor cable with the same voltage level at opposite polarities. For simplicity, when comparing conductor sizes, the DC cable in this section will be recalculated to an equivalent three phase AC cable. The recalculation is done by holding the total copper volume constant for each case and divide it by the number of conductors of interest.

### 5.6.1 First approach - only conductor cost and losses corresponding to the resistance at 20°C

To calculate the copper cost, the area and the length of each cable need to be known in order to get the total copper volume. Then, by adding the density and the price of copper, the conductor cost can be calculated by

$$C_{conductor} = Al\rho_{copper}C_{copper} \quad [kr] \quad (5.2)$$

where  $A$  is the conductor area,  $l$  is the length of the cable,  $\rho_{copper}$  is the density of copper and  $C_{copper}$  the copper price (value used is 48 428 SEK/ton, 2013-02-08). Observe, when calculating the total conductor cost for three phase AC cables the value from (5.2) will be multiplied by three and similarly multiplied by two for the DC cable. By choosing different conductor areas and various lengths of the cables the conductor cost can be modelled as a function of its area.

The losses is calculated by (2.6) and (2.8), where the resistance at this first stage is calculated for 20°C. To calculate the cost of the losses some assumptions have been made:

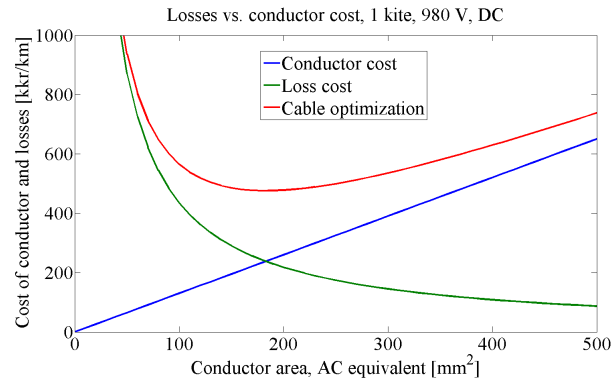
- the accounted lifetime is set to 20 years
- the power loss is calculated as a worst case where the current corresponding to the maximum power production is considered together with the capacity factor of 36 %
- the sale price of electricity is an average value set to 47 öre/kWh [44,45], where the assumption have been made that the electricity price will follow the inflation

The total loss cost can then be calculated by

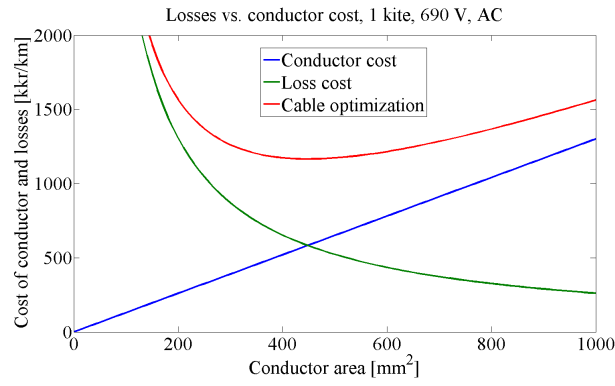
$$C_{loss} = P_{loss,max}C_{el}T_Y LK \quad (5.3)$$

where  $P_{loss,max}$  is the power loss at the maximum power production and with resistance at 20°C,  $C_{el}$  is the electricity sale price,  $T_Y$  is the hours of a year,  $L$  is the lifetime in years and  $K$  is the capacity factor for Deep Green.

In order to select the preferred conductor area, firstly the minimum area is calculated by using the maximum allowed current density of 2 A/mm<sup>2</sup> in (2.5). Then the area is increased in steps and the loss cost is compared to the conductor cost to find the optimum cable size. As an example of the cable optimisation procedure, the results for one kite in the radial system at 980 V<sub>DC</sub> and at 690 V<sub>AC</sub> are shown in Fig.5.4. From this first approach it can be seen that the most cost efficient cable to select for this distance is of an approximate conductor area of 180 mm<sup>2</sup> and 450 mm<sup>2</sup>, DC and AC, respectively. The same procedure is used for all the different cables in Table 5.1 and the final results is shown in Table 5.2.



(a) DC system. The conductor area is recalculated to one phase in a three phase AC-cable for easier comparison.



(b) AC system

Figure 5.4: Cost of active losses and conductors for a cable in the radial system carrying one kite at  $980 V_{DC}$  and  $690 V_{AC}$ , respectively.

When studying the results in Table 5.2 some important conclusions can be made. For all cases, the optimum conductor area results in over dimensioned cables in order to become cost efficient. At low voltages of 980/690 V the cable sizes are extremely large and there are no manufactures of cables of these sizes. The alternative is to place many smaller cables in parallel which is expensive, heavy and the losses will increase due to the relatively low voltage. Therefore the voltage at 980/690 V will not be further studied in this report. It can also be noticed from Table 5.2 that the DC cables are cheaper per meter compared to the AC cables, as was stated in Section 2.4.2.

### 5.6.2 Second approach - including resistance corresponding to the operation temperature

In order to select an even better cable size for the different distances, the resistance need to be calculated for the corresponding operation temperature. Fortunately, the calculated temperature for the cables at 10 kV in Table 5.2, for 1 kite ( $50 \text{ mm}^2$ ) and 6 kites ( $240 \text{ mm}^2$ ), respectively, became rather low as can be seen in Table 5.3. This is expected, since the cables selected at the first approach already indicates that the cables should be over dimensioned to be cost efficient.

Table 5.2: Most cost efficient conductor area per phase, at a first approach, for radial and star connection, respectively. Observe that the conductor area for DC is recalculated to an equivalent one phase AC area for easier comparison.

	DC		AC	
	Conductor area (AC-equivalent) [mm <sup>2</sup> ]	Cost of two conductors and losses [kkR/km]	Conductor area [mm <sup>2</sup> ]	Cost of three conductors and losses [kkR/km]
<b>Voltage [kV]</b>	<b>0.98</b>		<b>0.69</b>	
1 kite	180	476	450	1 166
3 kites	550	1 428	1340	3 499
5 kites	910	2 381	2240	5 831
6 kites	1100	2 857	2690	6 997
25 kites	4570	11 903	11 200	29 155
<b>Voltage [kV]</b>	<b>4.7</b>		<b>3.3</b>	
1 kite	40	100	90	244
3 kites	110	299	280	732
5 kites	190	498	470	1 219
6 kites	230	597	560	1 463
25 kites	960	2 489	2340	6 096
<b>Voltage [kV]</b>	<b>9.3</b>		<b>6.6</b>	
1 kite	20	50	50	122
3 kites	60	149	140	366
5 kites	100	249	230	610
6 kites	110	299	280	732
25 kites	480	1 244	1170	3 048
<b>Voltage [kV]</b>	<b>14.1</b>		<b>10</b>	
1 kite	10	34	30	81
3 kites	40	99	90	242
5 kites	60	164	150	403
6 kites	80	197	190	483
25 kites	320	821	770	2 012

Table 5.3: Comparison of conductor temperature when simplifying the temperature equation.

	True temperature [°C]	Simplified temperature [°C]
50 mm <sup>2</sup> , 1 kite	21.18	20.86
240 mm <sup>2</sup> , 6 kites	27.73	25.74

In Table 5.4 the corresponding resistances for the temperature is calculated by (2.7), and from here it can be seen that the temperature difference does not influence the resistance that much. The largest impact (for the cable and corresponding power considered) is for the 240 mm<sup>2</sup> cable, which corresponds to a 0.7 % difference in the resistance. Therefore, as long as the temperature in the cable is kept low (which will be the case for the cables here since they are over dimensioned), the simplified temperature model can be used without any big change in the resistance and therefore the result.

Table 5.4: Comparison of conductor resistance when simplifying the temperature equation.

	True resistance [Ω/km]	Simplified resistance [Ω/km]
50 mm <sup>2</sup> , 1 kite	0.3971	0.3967
240 mm <sup>2</sup> , 6 kites	0.0828	0.0823

In order to calculate the optimised cable sizes for the DC system, all needed information is now given. Since no cost information for DC cables have been possible to find, the cables are recalculated to correspond to an AC equivalent cable and the cost for it will be taken from Fig.5.1. To select the correct cable cost, the DC voltage is divided by two since there are two conductors with opposite polarities in the DC cable where the voltage drop over the conductors correspond to the total voltage of 4.7 kV<sub>DC</sub>, 9.3 kV<sub>DC</sub> and 14.1 kV<sub>DC</sub>, respectively. Therefore, the AC voltages to investigate are 2.4 kV<sub>AC</sub>, 4.7 kV<sub>AC</sub> and 7 kV<sub>AC</sub>, respectively, and since there is no insulation information at these voltage levels the voltages are rounded to the closest higher value; 3 kV<sub>AC</sub>, 6.6 kV<sub>AC</sub> and 10 kV<sub>AC</sub>, respectively. All conductor area options are included in the study, since no standard DC cable sizes have been found in the study, and the resistances are therefore calculated from (2.6) and (2.7).

Furthermore, the losses in the system were simplified in the first approach by using the resistance at 20°C, the capacity factor K and the losses corresponding to the maximum power. By instead using the power corresponding to the Rayleigh distribution, in Fig.2.8 and in Fig.5.2, and the new resistance calculated by (2.9), with  $\omega$  set to zero (see appendix A), the losses will be more correctly calculated. Therefore, (5.3) will be rearranged to

$$C_{loss} = P_{loss}C_{el}T_Y L \quad (5.4)$$

where  $P_{loss}$  is the power loss calculated from the Rayleigh distribution and with resis-

tance corresponding to the operation temperature. The results from the cable optimisation are shown in Fig.5.5 and in Table 5.5. For the cable carrying 25 kites at 4.7 kV (shown in Fig.5(d)) the cable size is larger than 500 mm<sup>2</sup> and is therefore recalculated as two parallel 500 mm<sup>2</sup> cables (see Section 5.3 for more information about the limitation at 500 mm<sup>2</sup>).

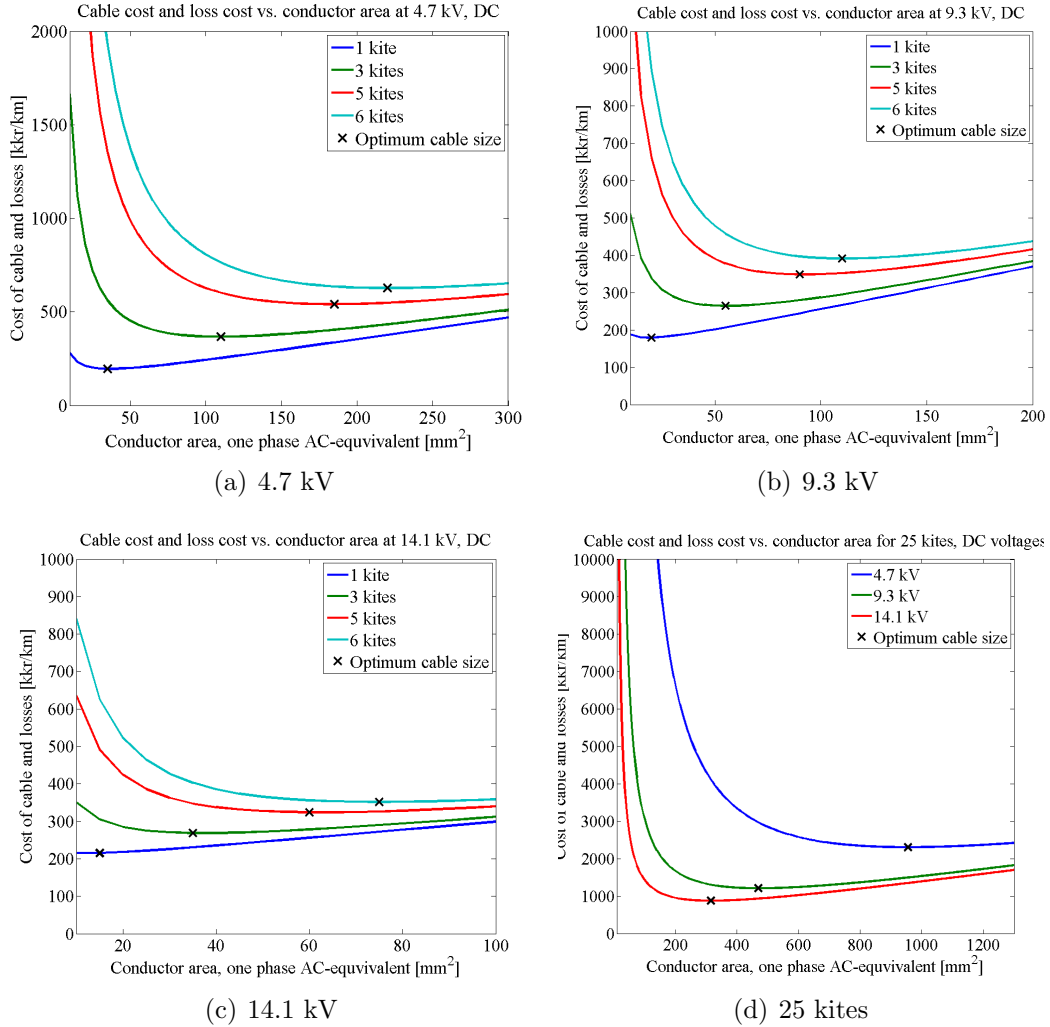


Figure 5.5: Optimisation of the cables for the DC system, cost as a function of the AC equivalent conductor area; a)-c) cables carrying 1-6 kites' power at different voltages, d) cables carrying 25 kites' power at different voltages.

Table 5.5: The DC system's optimised cable sizes as an AC equivalent as well as the recalculated area for the DC conductor.

	Area per conductor AC/DC [mm <sup>2</sup> ]				
	1 kite	3 kites	5 kites	6 kites	25 kites
4.7 kV	35/53	110/165	185/278	220/330	955/1433
9.3 kV	20/30	55/83	90/135	110/165	475/713
14.1 kV	15/23	35/53	60/90	75/113	315/473

When the cable optimisation is completed, the total cost of the cables and losses for the system can be calculated. In Table 5.6 the final results for the DC systems are shown. It should be observed that, unexpectedly, the cable cost and therefore also the total cost for the 9.3 kV systems are the lowest. One reason for this could be that the DC cable cost is an approximation based on the insulation thickness at AC voltage levels as close as possible to the DC voltage. Further, when optimising the cables, the area differences (at the power below 25 kites) between the voltage levels does not compensate for the cost differences, as can be seen in Fig.5.6.

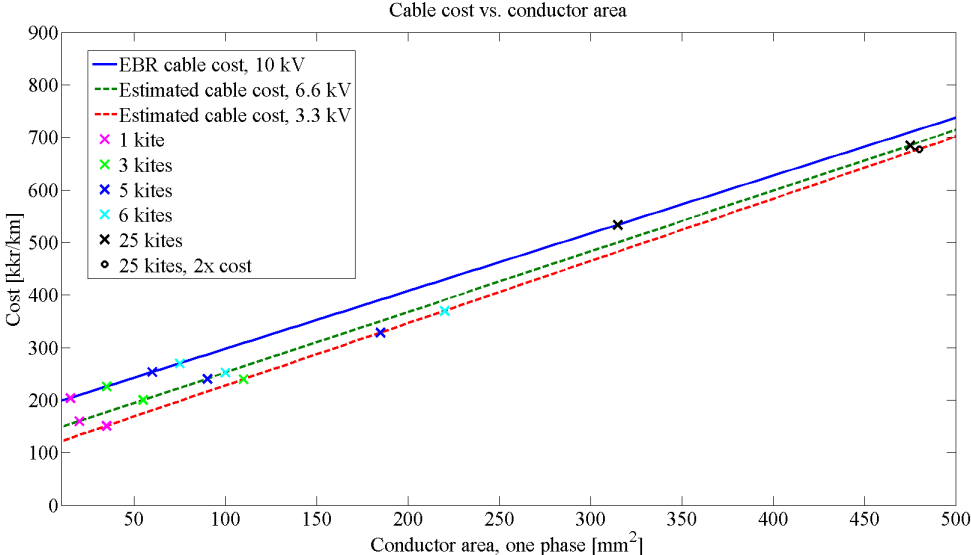


Figure 5.6: Optimised cable cost at different voltages and powers for a DC system. This benefits the voltage at 6.6 kV.

However, since the voltage levels for DC did not match the AC cables' voltage levels that well the cable cost leads to this result. From Table 5.6 it can be noticed that the cheapest 25 kites system is the star connection at 9.3 kV and the cheapest 100 kites system is the radial connection at 9.3 kV. The losses in the cables reach 0.16% when considering the whole collection grid.

Table 5.6: The cost of the cables and losses for the DC systems in radial and star pattern at different voltages.

	Cable cost [kkkr]	Loss cost [kkkr]	Total cost [kkkr]
<b>Radial</b>			
4.7 kV, 25 kites	1 785	918	2 703
9.3 kV, 25 kites	1 529	455	1 984
14.1 kV, 25 kites	1 765	295	2 060
4.7 kV, 100 kites	8 727	4 702	13 429
9.3 kV, 100 kites	7 281	2 343	9 624
14.1 kV, 100 kites	8 285	1 524	9 809
<b>Star</b>			
4.7 kV, 25 kites	1 501	614	2 115
9.3 kV, 25 kites	1 445	286	1 731
14.1 kV, 25 kites	1 768	176	1 944
4.7 kV, 100 kites	9 103	5 201	14 304
9.3 kV, 100 kites	7 424	2 493	9 917
14.1 kV, 100 kites	8 279	1 587	9 866

### 5.6.3 Third approach - including reactive power by using Newton-Raphson

In order to select an even better cable size for the AC cable, the reactive power needs to be included since it occupies the cable and contributes to the active power losses. Both the inductance and the capacitance in the cable contributes to the reactive power, and their value per kilometre is given in the cable data sheets from Nexans and Calendonian, see appendix D. At 10 kV, the cable from Nexans is used while for the lower voltage levels the cables from Calendonian are used. By using the given inductance and capacitance, as well as the recalculated resistance for the operation temperature, a power flow analysis for each cable is done in MATLAB. The program used is a Newton-Raphson analysis, created by Hadi Saadat for MATLAB [46], with added input data for the systems under study.

The active losses are calculated by (5.4) and the cable cost is taken from Fig.5.1. When considering the AC system, only the cables available on the market is investigated when optimising the cable sizes. The results from the power flow analysis together with the cable cost are shown in Fig.5.7 and Table 5.7. Where the cables exceed 500 mm<sup>2</sup>, a number of parallel cables are instead used with the largest area already used in the system. The reason for choosing the largest cable size already used is to keep the number of different cables sizes down.

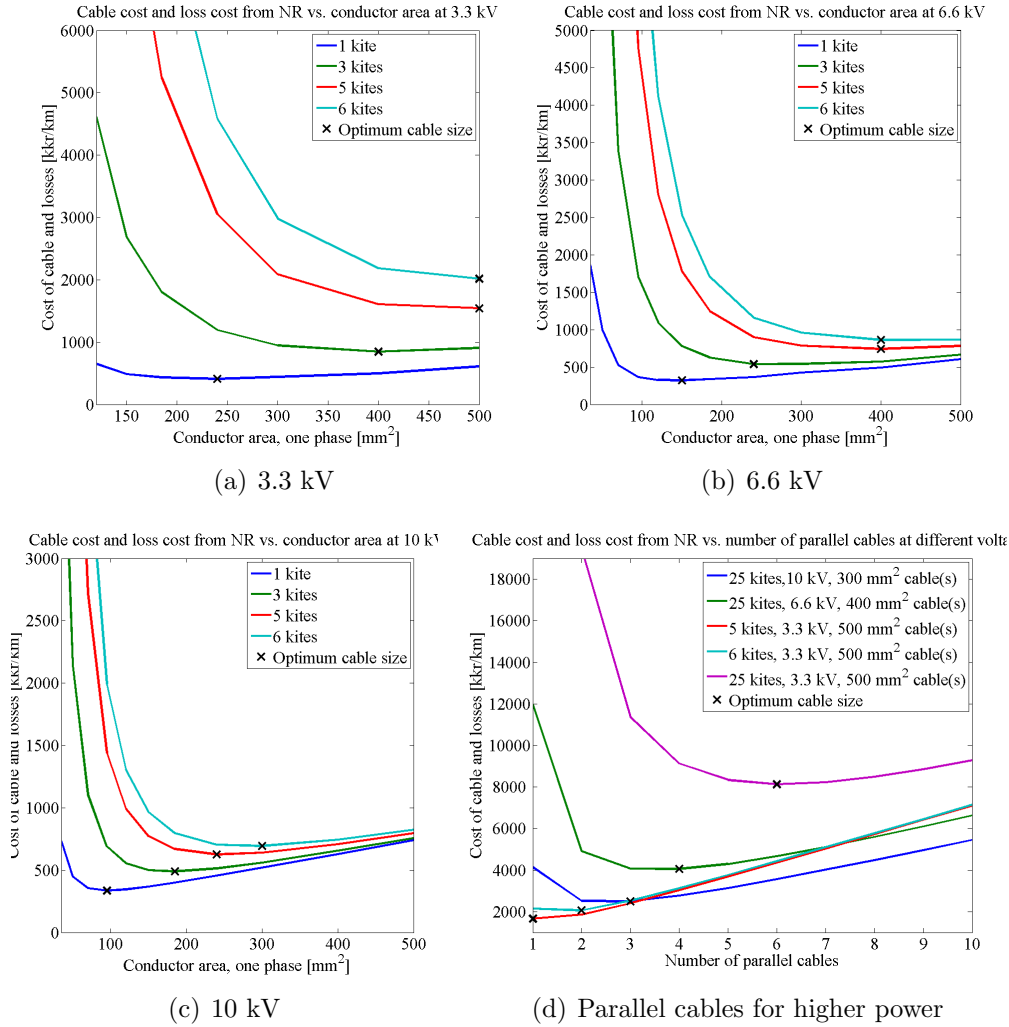


Figure 5.7: Optimisation of cables at different power levels and voltages; (a)-(c) cable cost and loss cost as a function of conductor area for cables carrying 1-6 kite's power, (d) cable cost and loss cost as a function of number of parallel cables for cables carrying 25 kite's power.

Table 5.7: The AC system's optimised cable sizes.

Area per conductor [mm <sup>2</sup> ]	1 kite	3 kites	5 kites	6 kites	25 kites
3.3 kV	240	400	500	2x500	6x500
6.6 kV	150	240	400	400	4x400
10 kV	95	185	300	300	3x300

When comparing the AC results with the DC results, it may seem unreasonable that the 6.6 kV cable cost in the AC case is not that favourable as it was for the DC case. This is due to the larger difference in the optimised conductor area between the different voltages in the AC case compared to the DC case. In Fig.5.1 it can be noticed that for small differences in the conductor area, for different voltage levels, the cable cost is

more expensive for higher voltages. On the other hand, for larger differences between the optimised conductor area, the cable cost can be lower for the higher voltages.

The power loss, as well as the reactive power, can be modelled as a function of the generated power. The relationship, when using the cables optimised for 6.6 kV, are shown in Fig.5.8 and Fig.5.9, respectively. The active power loss in percent has a linear relationship to the generated power while the reactive power, as a fraction of the generated power, has a more complicated relation to the generated power.

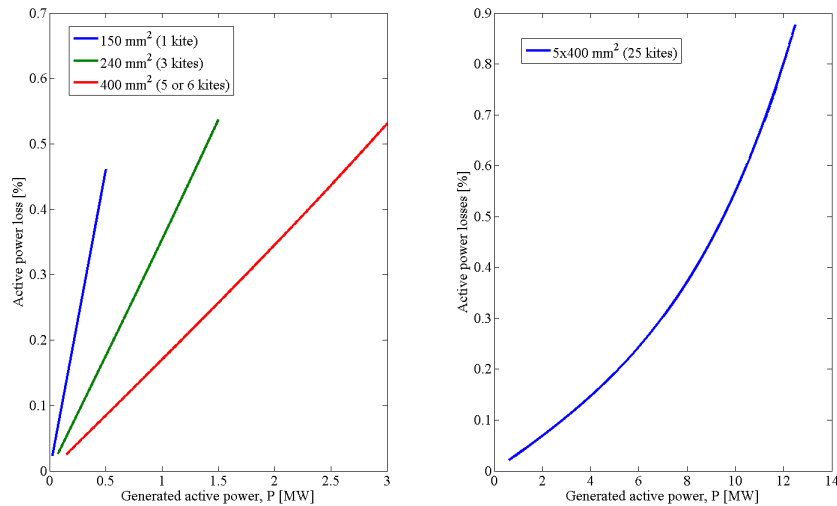


Figure 5.8: The power loss in percent of the generated power as a function of the generated power for different cable sizes at 6.6 kV.

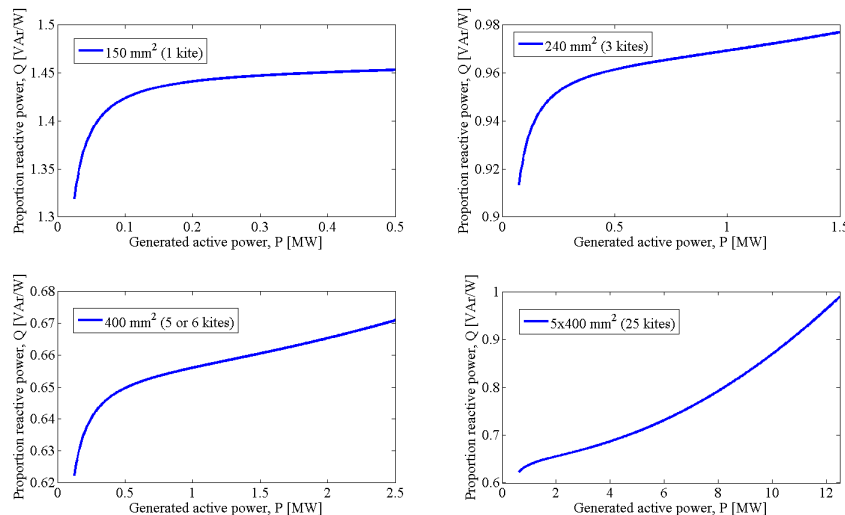


Figure 5.9: The reactive power per generated active power as a function of the generated active power for different cable sizes at 6.6 kV.

The final results for all the AC systems under study are shown in Table 5.8. It can be noticed that the cheapest 25 kites system is the star connection at 10 kV and the

cheapest 100 kites system is the star connection at 10 kV. The power factor is over all larger for the radial system compared to the star system. This is an advantage for the radial system since the compensation of the reactive power can be smaller and less expensive.

Table 5.8: The power factor, cost of the cables and losses for the AC systems in radial and star pattern at different voltages.

	Power factor, average	Cable cost [kkkr]	Loss cost [kkkr]	Total cost [kkkr]
<b>Radial</b>				
3.3 kV, 25 kites	0.82	4 205	2 799	7 004
6.6 kV, 25 kites	0.81	3 330	942	4 272
10 kV, 25 kites	0.84	3 028	485	3 513
3.3 kV, 100 kites	0.83	20 209	15 792	36 001
6.6 kV, 100 kites	0.80	16 212	5 181	21 393
10 kV, 100 kites	0.85	14 613	2 408	17 021
<b>Star</b>				
3.3 kV, 25 kites	0.80	4 414	1 346	5 760
6.6 kV, 25 kites	0.77	2 901	758	3 659
10 kV, 25 kites	0.80	2 679	392	3 071
3.3 kV, 100 kites	0.82	28 007	13 416	41 423
6.6 kV, 100 kites	0.80	17 718	6 383	24 101
10 kV, 100 kites	0.84	14 534	3 491	18 025

## 5.7 Comparison of the collection grids

This chapter has focused on the cost related to the cables and its corresponding losses of the different systems. However, there are several more components that need to be added to the system to complete it. To be able to make a fair comparison between the systems, the components required can be divided into two categories; the components needed independently of the selected system and the components which will change dependently on the system selected. The first category includes the generators, disconnectors, possibly used transformer and cable used from the park to the grid. These components are independent of which system to choose and is there for not accounted for.

However, when concerning the converter, the connector units and the reactive power compensation, the differences between the systems are important. It should also be mentioned that components and their costs are overall hard to find and most components need to be specially made for each case since standard components are rare.

The size and cost of the converter will depend on the voltage level selected. A higher voltage will increase both the size and the cost of the converter. One major conclusion that can be made after discussions with the industry is that there are no manufactures today of converters at 10 kV for 500 kW. Wida at ABB states that the cost of a

converter at 3.3 kV or 6 kV for 500 kW is the same and about 1 400 kkr [41]. For the DC system only the rectifier is needed inside the kite and the inverter can be placed in the end of the system. The inverter will for certain be needed to be much larger to be able to handle the whole park's power, but will also be cheaper than a number of smaller inverters.

An other difference between the systems are the number of connector units. As was stated in Section 3.3, the connectors are one of the weakest points in the system. The connectors are also an expensive part in a sub sea collection grid, especially if wetmate connectors are chosen. When comparing the radial and star connection patterns in Table 4.1, the star connection is preferable due to the low number of connectors.

The results in this chapter show that the DC systems are cheaper than the AC systems which is expected when only considering the cables. Normally the distances in a collection grid need to be long in order to be preferable for a DC system, where the converters usually are the major cost. However, since a converter is required independently of the voltage type to ensure the power quality, the AC system will be more expensive than the DC system. In addition, the AC system has the reactive power to compensate as well, which can make the system even more expensive.

When combining all the statements above the final selection will be to choose a 9.3 kV DC system in star connection. The reasons for this are that only the rectifier is needed in the kite, no reactive power needs to be compensated for, the converter cost will not increase from 3.3 kV to 6 kV, but the losses will decrease. The only drawback with this system is that there are no known manufactures of subsea DC cables at this low voltage. Therefore, if the DC cables will become much more expensive than the AC cables due to special order, the AC system at 6.6 kV (with cable losses of 0.4%) in star connection is to prefer.

## 6 Connection of a Seabased wave power park

This chapter presents how Seabased have designed their collection grid. The Seabased collection grid is very limited due to the fact that the rectifier is positioned in the switchgear. To be able to make a good comparison with the tidal park collection grids some assumptions has to be made which are also presented in this chapter.

### 6.1 Seabased collection grid structure

A Seabased wave power park consists of permanent magnet linear generators and sub-sea substations, see Section 2.3.2 and 3.4 respectively for more information. Since Seabased has chosen not to equip each generator with a rectifier and a filter it is not possible to directly connect multiple generators together, as for example in a radial system. An example of a possible star connected system is illustrated in Fig.6.1 where each generator is connected directly to a substation. In the substation the connection is done according to Fig.3.7, where each generator is connected to a rectifier before interconnected, filtered, inverted and then transformed to a higher voltage. The substation is either connected directly to shore, or at larger parks multiple substations are interconnected and transformed to a high voltage in a bigger subsea substation and then connected to shore. Each generator has a power output of 25 kW and occupies a square with each side equal to 32 m. Fig.6.1 gives an illustration of how a large Seabased park can be connected according to Seabased [50].

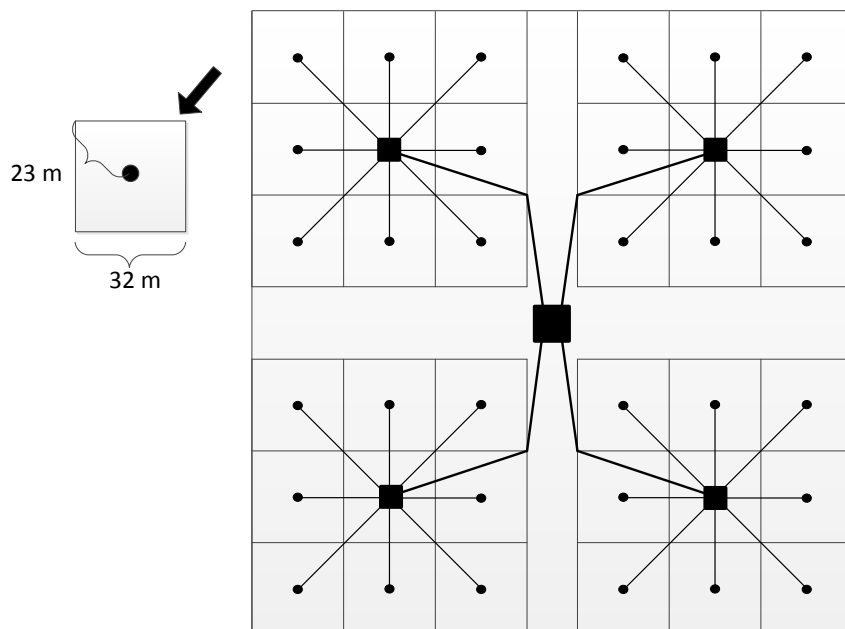


Figure 6.1: Example of a connection structure for Seabased park. The circles represents generators, a square represent a subsea substation and the thin and thick lines represent low voltage cables and medium voltage cables respectively.

## 6.2 Collection grid patterns used in the wave power case

The study of Seabased will be made with the same amount of generators and the same structures of collection grid as for Minestos tidal power park. The study is performed in this way in order to be able to recognise any differences and similarities between a collection grid based on Minestos tidal power generator DG-12 and a collection grid based on Seabased wave power generator. For more information about the structures see Section 4.3. Since Seabased design prevent direct interconnection of generators, which is used in the tidal structures, the assumption is made that each generator capsule is equipped with a filter and converter so a perfect sinus can be assumed. The structures used for calculations in the Seabased case are shown in Fig.6.2.

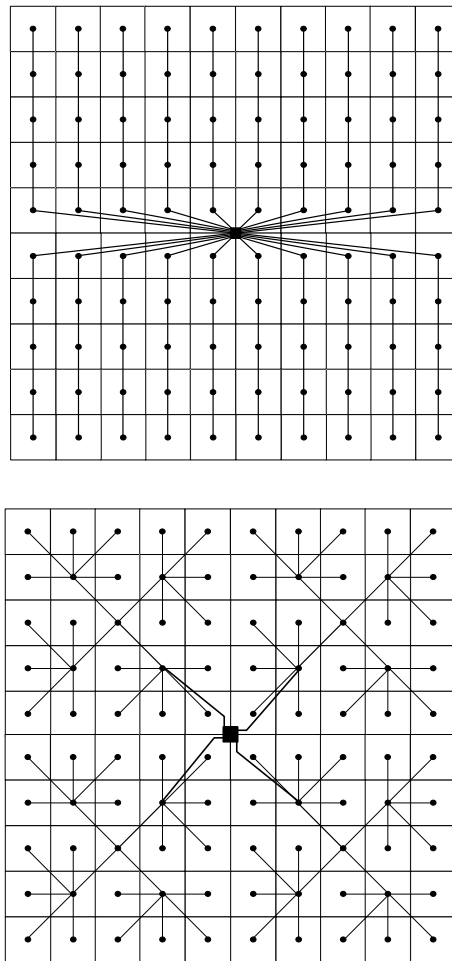


Figure 6.2: Selected structures for 100 Seabased generating units.

## 7 Optimising cables for the wave collection grid

This chapter includes the cable optimisation for two wave power systems with 100 buoys each, star and radial connection, respectively. The procedure is the same as for the tidal cable optimisation and with changes only in the parameters used. First the conditions for the Seabased system are presented, then the three cable optimisation approaches are done and finally the results are discussed.

### 7.1 Voltage levels

The output voltage from the generator is assumed to be  $1000 V_{RMS,AC}$ . The DC voltage after the rectification will be (at least) as high as the peak value of the AC voltage, i.e.  $1414 V_{DC}$ . This is based on that the maximum voltage output of the Seabased substation is 1000 V, see Section 3.4. The opportunity to use  $3.3 kV_{RMS,AC}$  and  $4.7 kV_{DC}$  is also investigated in order to be able to compare the results with the ones from the tidal park.

### 7.2 Systems' conditions

The conditions for the wave power park is shown in Fig.7.1. It is the same structure as for the tidal park, but with the differences in voltage, power and distances.

Table 7.1: Cable specifications at two different voltage levels, AC (line-to-line rms) and DC, for radial and star connection, respectively.

	Radial connection			Star connection		
Number of buoys	1	3	5	1	6	25
Power [kW]	25	75	125	25	150	625
Maximum length [m]	32	32	145	45	45	113
Current @ $1 kV_{AC}$ [A/conductor]	14	43	72	14	87	361
Current @ $3.3 kV_{AC}$ [A/conductor]	4	13	22	4	26	109
Current @ $1.4 kV_{DC}$ [A/conductor]	9	27	45	9	54	223
Current @ $4.7 kV_{DC}$ [A/conductor]	3	8	13	3	16	66

### 7.3 Conductor and cable cost

When using  $3.3 \text{ kV}_{RMS,AC}$  and  $4.7 \text{ kV}_{DC}$ , the cable cost will be used in the same way as was described in Section 5.3 and in Section 5.6.2, respectively. For the lower voltage of  $1 \text{ kV}_{RMS,AC}$  and  $1.4 \text{ kV}_{DC}$  another solution is required. Ericsson provides cables at  $1 \text{ kV}_{RMS,AC}$  which are made of aluminium and tolerates to be placed in water, see appendix D for detailed specifications. EBR only has the costs for cables at 400 V, which at least follows the aluminium cost well, as is shown in Fig.7.1. Therefore, the cost of the 400 V cable will be used for the  $1 \text{ kV}_{RMS,AC}$  case as well as for the  $1.4 \text{ kV}_{DC}$  case when the conductor area have been recalculated.

It can also be noted from Fig.7.1 that the cost difference between aluminium and copper is large. Copper on the other hand has better conductivity than aluminium, which will lead to lower losses. The final comparison between the voltage levels will therefore not be that reliable. However, the comparison between the tidal and wave system at  $3.3 \text{ kV}_{RMS,AC}$  and  $4.7 \text{ kV}_{DC}$  is still valid.

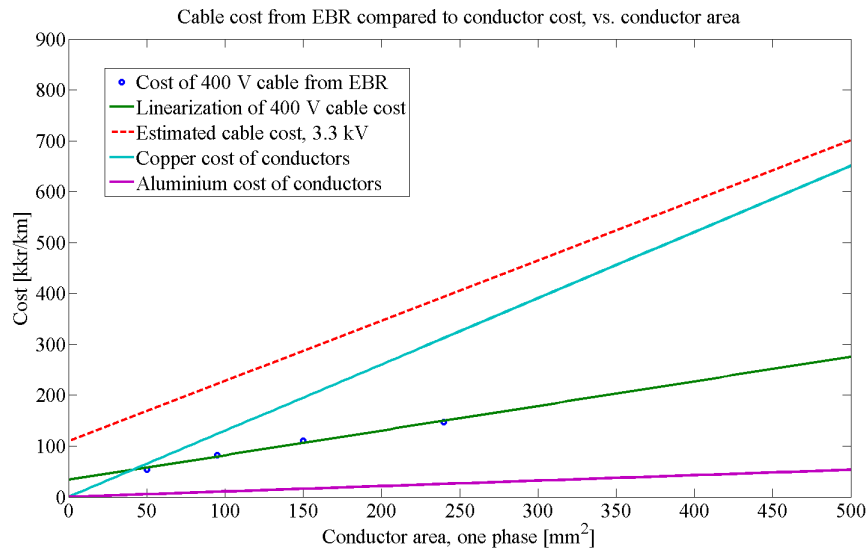


Figure 7.1: Comparison of the cable cost from EBR at 400 V and the aluminium cost, as well as the estimated 3.3 kV cable cost and the copper conductor cost [43].

### 7.4 Wave data

It has not been possible to find the wave data for the specific site of interest outside of Falkenberg. The opportunity to use available wave data outside of the Norwegian coast have been considered, but is decided to not be used. This is mainly due to two reasons; the data will most likely differ a lot from the site of interest and even if real data were used the power curve for Seabased needs to be more specific than the one in Fig.2.10. Therefore, the capacity factor will be used for all the approaches in the same way as in Section 5.6.1, which is set to  $K=0.36$ , the same as for the tidal generation.

## 7.5 Resistance corresponding to the operation temperature

The resistance corresponding to the operation temperature is calculated in the same way as in Section 5.5.

## 7.6 Cable area optimisation

The cable optimisation is done in the same way as for the tidal case. By doing the optimisation in three steps the final result for the DC case is found in the second approach and for the AC case in the third approach.

### 7.6.1 First approach - only conductor cost and losses corresponding to the resistance at 20°C

The first approach is done in the same way and with the same assumptions as for the tidal case in Section 5.6.1. Equation (5.2) is used for 3.3 kV while for 1 kV the copper specifications is replaced by aluminium specifications where the aluminium price used is 13 168 SEK/ton, 2013-04-24. The results from the first approach are found in Fig.7.2.

Table 7.2: Most cost efficient conductor area according to the first approach, for radial and star connection, respectively. Observe that the conductor area for DC is recalculated to an equivalent one phase AC area for easier comparison. The conductor material is aluminium for 1 kV and copper for 3.3 kV.

	DC		AC	
	Conductor area (AC-equivalent) [mm <sup>2</sup> ]	Cost of two conductors and losses [kkR/km]	Conductor area [mm <sup>2</sup> ]	Cost of three conductors and losses [kkR/km]
<b>Voltage [kV]</b>	<b>1.4</b>		<b>1</b>	
1 buoy	30	6	70	14
3 buoys	85	18	205	43
5 buoys	140	30	340	72
6 buoys	165	35	405	87
25 buoys	690	148	1 695	362
<b>Voltage [kV]</b>	<b>4.7</b>		<b>3.3</b>	
1 buoy	5	7	5	12
3 buoys	5	15	15	37
5 buoys	10	25	25	61
6 buoys	10	30	30	73
25 buoys	50	125	115	304

### 7.6.2 Second approach - including resistance corresponding to the operation temperature

The second approach differs a little from the tidal case. The resistance is still recalculated to the operation conditions as well as the total cable cost is accounted for. However, there are no wave data used in this approach, instead the capacity factor is used together with the maximum power output from the generators. The cable optimisation for the DC case is found in Fig.7.2 and Table 7.3, and the resulting system costs are found in Table 7.4.

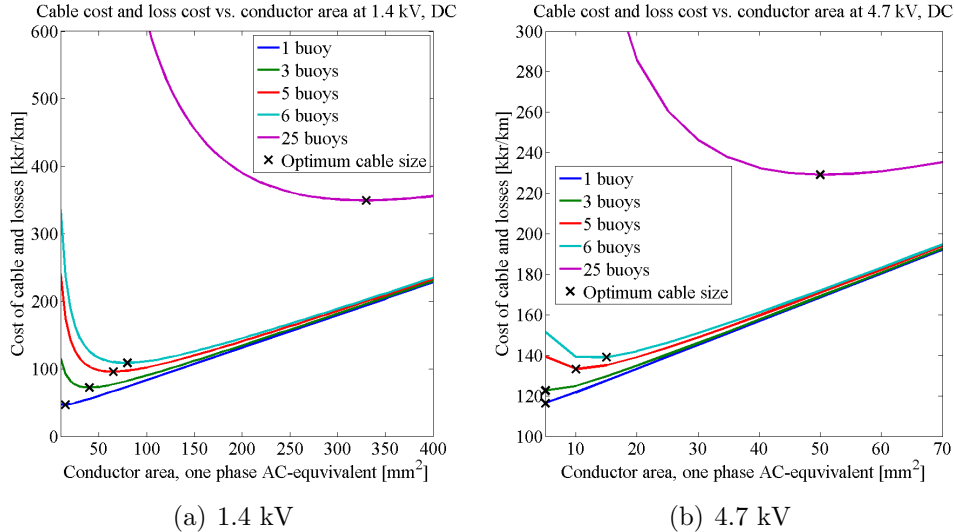


Figure 7.2: Optimisation of the cables for the DC system, cost as a function of the AC equivalent conductor area. Cables carrying 1-25 buoys' power at two different voltages.

Table 7.3: The DC system's optimised cable sizes as an AC equivalent as well as the recalculated area for the DC conductor.

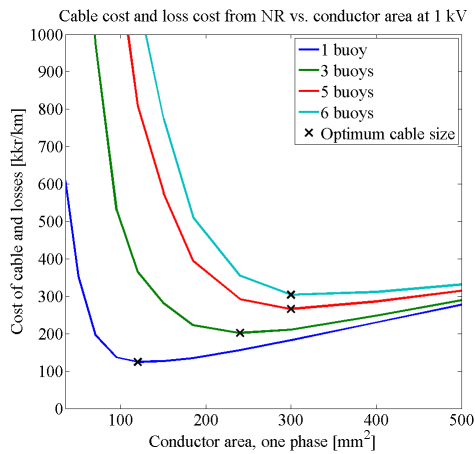
	Area per conductor AC/DC [mm <sup>2</sup> ]				
	1 buoy	3 buoys	5 buoys	6 buoys	25 buoys
1.4 kV	15/23	40/60	65/98	75/113	325/488
4.7 kV	5/8	5/8	10/15	15/23	50/75

### 7.6.3 Third approach - including reactive power by using Newton-Raphson

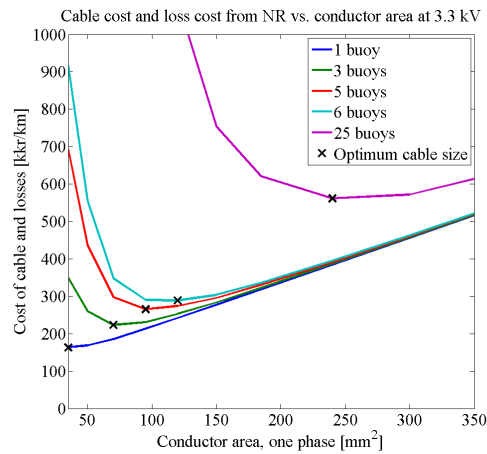
The third approach optimises the cables for the AC systems in the same way as for the tidal case in Section 5.6.3. The difference is still that instead of real wave data the capacity factor and the maximum power are used. The cable optimisation are found in Fig.7.3 and Table 7.5, and the final cost is found in Table 7.6.

Table 7.4: The cost of the cables and losses for the DC systems consisting of 100 buoys in radial and star pattern at different voltages.

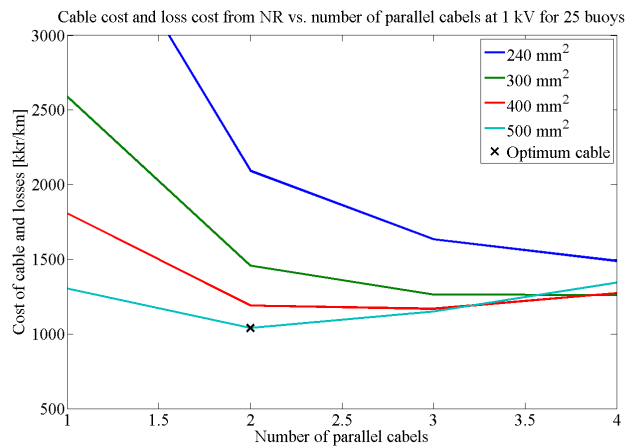
	Cable cost [kkkr]	Loss cost [kkkr]	Total cost [kkkr]
<b>Radial</b>			
1.4 kV	244	98	342
4.7 kV	499	38	537
<b>Star</b>			
1.4 kV	249	107	356
4.7 kV	488	37	525



(a) 1 kV



(b) 3.3 kV



(c) 1 kV, 25 buoys

Figure 7.3: Optimisation of cables at different power levels and voltages; (a)-(b) cable cost and loss cost as a function of conductor area for cables carrying 1-6 buoys, (c) cable cost and loss cost as a function of number of parallel cables for cables carrying 25 buoys.

Table 7.5: The AC system's optimised cable sizes.

Voltage [kV]	Area per conductor [mm <sup>2</sup> ]				
	1 buoy	3 buoys	5 buoys	6 buoys	25 buoys
1	150	240	300	400	2x500
3.3	50	70	95	120	240

Table 7.6: The power factor, cost of the cables and losses for the AC systems consisting of 100 buoys in radial and star pattern at different voltages.

	Power factor	Cable cost [kkkr]	Loss cost [kkkr]	Total cost [kkkr]
<b>Radial</b>				
1 kV	0.73	671	242	913
3.3 kV	0.39	814	161	976
<b>Star</b>				
1 kV	0.79	689	289	978
3.3 kV	0.68	769	126	895

## 7.7 Comparison of the collection grids

As mentioned in Section 7.3, it may not be fair to compare the two voltage levels studied in this chapter due to the difference in conductor material and the estimated cable costs. However, if a comparison is done anyway, there are some conclusions that can be drawn from the results. For the DC case the radial connection, low voltage is to prefer. The reason for this is the much lower cable cost due to that the conductors are made of aluminium. It can also be seen in Fig.7.4 that the loss cost on the other hand is higher for the low voltage. This is both due to the lower voltage itself, but also that the aluminium conductivity is lower than it is for copper. For the AC case the preferred system is not that easy to select, the differences in the final cost is rather small between all the systems compared. However, the cheapest system is the star connected system at the higher voltage. The reason for the small cost difference between the high and low voltage AC cables (which was not the case for the DC cables) is that the conductor sizes are increased dramatically and the cost difference is therefore less. The cable losses for the two selected systems, DC at 1.4 kV and AC at 3.3 kV, reaches 0.05% and 0.17%, respectively.

A general conclusion, same as for the tidal case, is that the connection units are expensive and a weak point of the system. Therefore, as long as the cost difference is not too large, the star system will be preferred in all cases. Furthermore, the DC system is again cheaper than the AC system since the same converters are needed independently on the system voltage type. However, still the problematic aspects of using DC is that there are no manufacturers today of DC cables for these low voltages.

The systems at 3.3 kV and 4.7 kV with 100 generating units each can be compared to the identical systems in the tidal case. In general, the wave systems are much cheaper than the tidal system, which is expected since the distances and power levels are much larger for the tidal case. However, there are a main difference in the results for both DC and AC; in the tidal case the radial system is cheaper than the star system while in the wave case the result is the opposite. One reason for this, in the AC case, could be the low power factor that occurs in the radial system, but this does not explain the whole difference. Again, the main differences are probably due to the cable cost and the large variation in the conductor areas. As mentioned earlier, the star connection pattern is to prefer due to the lower number of connection units. Over all is the power factor worse for the wave case compared to the tidal case. This indicates that reactive power compensation is required if an AC system is selected. If the compensation required is not too large the converter can control the reactive power by itself, otherwise additional compensation will be needed.

## 8 Connection of the tidal park to the grid

This chapter studies the transmission line from the tidal power park, consisting of 100 generators, to the shore. Three options will be studied and compared with respect to the cable cost and loss cost. The options which are studied are; transmission at the same voltage as in the collection grid, transmission with a higher voltage using a transformer and transmission sharing a nearby high voltage cable with a large wind power park. To have a fair comparison all the losses in the collection grid for all options will be neglected since the losses of the wind park is not available.

### 8.1 Tidal and wind data

The calculations are based on the tidal stream data shown in Fig.5.2 and wind speed data provided by British Oceanographic Data Centre [47], both from the Irish Sea. The wind data consist of 134 incoherent days of measurements between 2012-01-04 to 2012-09-28 where each day consists of a various amount of measurements. This data has been recalculated to the mean wind speed per day and is presented in Fig.8.1.

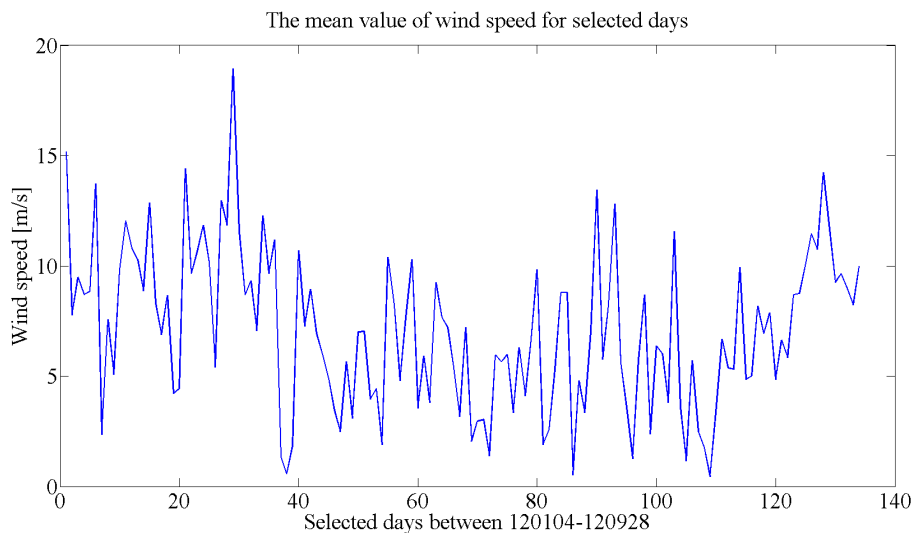


Figure 8.1: Wind data measured in Irish sea.

The wind data is not as detailed as the tidal stream data and to get a realistic power production the tidal stream data is chosen in a way that date and time are equal with the wind data. The mean value of the chosen tidal stream data per day is presented in Fig.8.2.

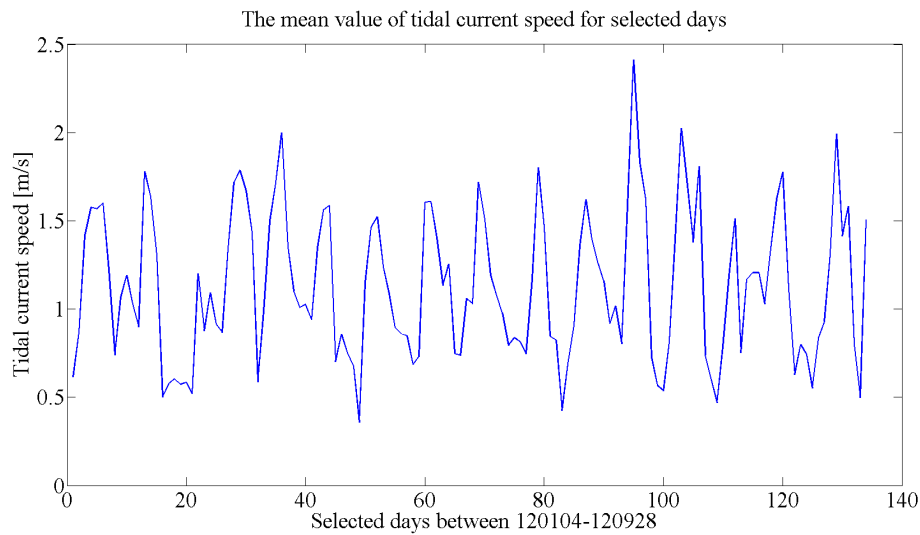
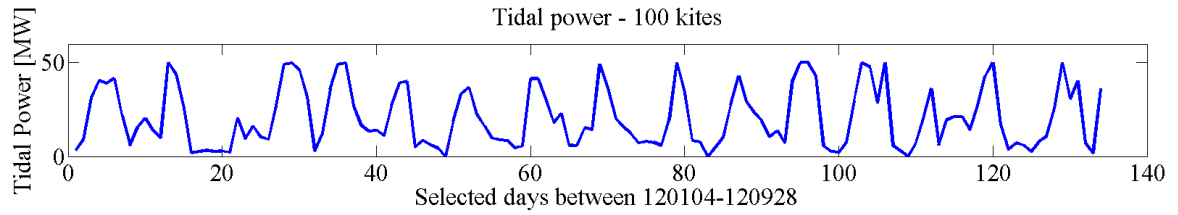


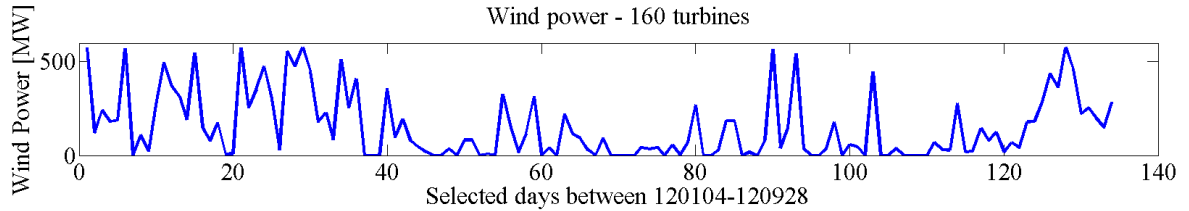
Figure 8.2: Tidal data measured in Irish sea.

The wind and tidal data are used together with their respective power curves in order to calculate the power output. The power curve for Minestos Deep Green is presented in 2.8 and the power curve for the wind power generator used in Gwynt y Môr is available in appendix D.

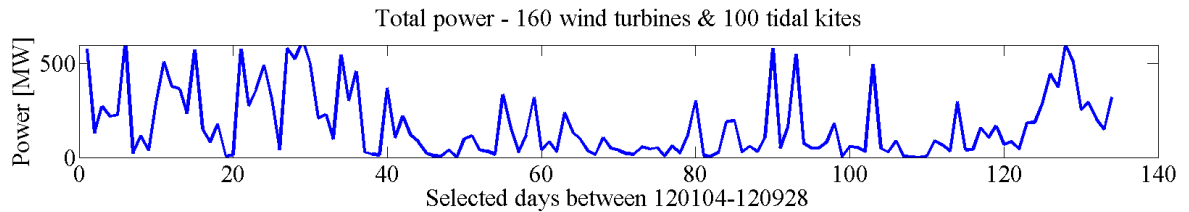
The resulting mean power output per day for the tidal and wind park, respectively, as well as together are presented in Fig.8.3. The presented power production will be used to find the most cost effective transmission cable. The calculations are performed using the temperature dependent calculation presented in Section 2.5.3 and the power flow analysis method presented in Section 2.6, i.e. the same procedure as for the calculations of the AC collection grid, see Section 5.6.3.



(a) The mean tidal power output. The data has been selected to match the wind power data.



(b) The mean wind power output.



(c) The total mean power output when combining the tidal and wind park together.

Figure 8.3: The data shows the mean power output per day for 134 incoherent days between 4th January - 28th September 2012.

## 8.2 Transmission at collection grid voltage

Using the same voltage as the collection grid is beneficial since costs for transformers and inverters out at the sea are avoided. The drawback is the large amount of cables needed to transmit the energy. In Section 5.7,  $9.3 \text{ kV}_{DC}$  or  $6.6 \text{ kV}_{AC}$  were presented to be the most optimal grids. For these grids the most optimal cables for 25 generators were calculated to one  $713 \text{ mm}^2$  and four  $400 \text{ mm}^2$  for the DC and the AC case, respectively. In the case of transmitting the power from the park to the shore there is a need of four DC cables or 16 AC cables for 100 generators. The calculations for the transmission cable will be based on the voltages and cross-sectional area selected in Section 5.7. The results of the calculations are presented in Table 8.1.

Table 8.1: Costs of cable and losses for 9.3 kV<sub>DC</sub> and 6.6 kV<sub>AC</sub>.

	9.3 kV <sub>DC</sub> 713 mm <sup>2</sup>	6.6 kV <sub>AC</sub> 400 mm <sup>2</sup>
Max. current per cable [A]	1 344 at 12.5 MW	330 at 3.77 MVA
Power factor at max. current	-	0.8244
Cable cost [kkkr/km]	679	598
Losses per cable [kkkr/km]	531	264
Total cost [kkkr/km]	4 840 (4 cables)	13 787 (16 cables)

### 8.3 Transmission at high voltage

Transmitting the power at higher voltage than the collection grid requires a transformer, and if DC is used in the collection grid an inverter has to be positioned out at the sea. The placement of these components can either be on a platform or they can be customised for subsea placement. These costs as well as the inverter cost are not taken into account in the study. The voltages of 45 kV, 66 kV and 132 kV has been chosen since at these voltages price information for cables and transformers are available in EBR [48]

#### 8.3.1 Costs of cables

All the costs used in the calculations for cables and transformers are found in the EBR-list [48]. The only prices found for cables at the voltage levels of interest are land based cables in the EBR-list, which will be used in the calculations. The main difference between land based and submarine cables is that the latter is also including armouring. In Fig.8.4 the cable costs are presented at three different voltage levels as well as linearisations based on the costs in the EBR-list. Submarine cables from ABB are used as input data for the calculations performed in this section. Available areas of the submarine cables from ABB are also shown in Fig.8.4, data sheets are available in appendix D.

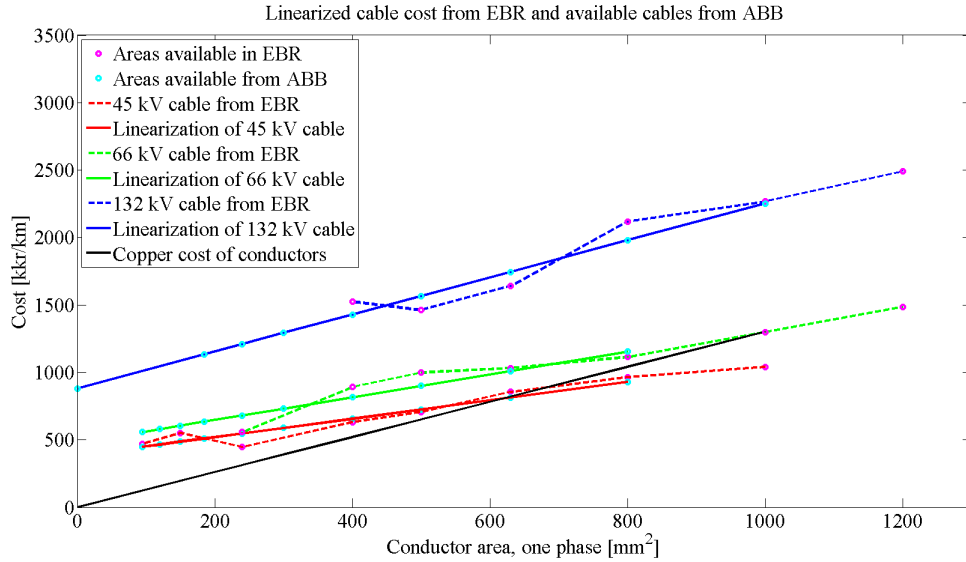


Figure 8.4: Linearised land based cable cost from EBR and available submarine cables from ABB.

As can be seen in Fig.8.4, the cable costs are not as linear as been seen for AC cables at lower voltages in Fig.5.1. Some cables in Fig.8.4 are even cheaper than the copper price. One explanation for the non-linear behaviour may be that the copper price has big variations in time. Another reason could be that cables with high turnover rate may become cheaper and also companies using a lot of copper can have reduced price.

### 8.3.2 Results

Calculations have been performed using both linearised cable cost and precise EBR costs, see Fig.8.4, to compare the results. Independent of which cable cost that were used as input for the calculations the result was the same and the preferred transmission line was at 66 kV and with 500 mm<sup>2</sup> for distances over 1.6 km. The specifications and electrical results, after completing the power flow analysis for each voltage level, are presented in Table 8.2. The electrical parameters (current, apparent power and power factor) are the results when using the maximum produced tidal power. The power flow analysis is only made on the transmission cable and with the assumption of no losses in the tidal park.

The cost calculations have been made for each voltage level and the results are presented in Fig.8.4. The costs and specifications of the transformers, found in EBR [48], are presented in Table 8.2. Unfortunately the available voltage level of the transformers in EBR did not match the precise voltage level in the selected system. The transformer cost for each voltage level is a fixed cost while the cable cost as well as the loss cost for each cross-sectional area is a variable cost. The cost for the cheapest option for each voltage level is presented in Table 8.2.

Table 8.2: Cost results and electrical parameters for each voltage level.

Voltage [kV]	45	66	132
Conductor area [mm <sup>2</sup> ]	800	500	240
Max. current [A]	567	418	223
Apparent power at max. current [MVA]	51	52.5	56
Power factor at max. current	0.9788	0.9515	0.8912
Transformer specifications [kV] [MVA]	45/10-20 63	66/10-20 63	132/10-20 63
Cable cost [kkr/km]	929	901	1 209
Loss cost [kkr/km]	467	406	239
Total variable cost [kkr/km]	1 396	1 306	1 448
Transformer (fixed cost) [kkr]	6 145	6 291	6 931

Figure 8.5 shows a presentation of the resulting costs for each voltage level. As can be seen in Fig.8.5 the cheapest option for distances up to 1.6 km is at 45 kV with a 800 mm<sup>2</sup> three phase cable. Though, as can be seen in Table 8.2 the cheapest variable cost is at 66 kV and it becomes the most optimum choice at distances longer than 1.6 km.

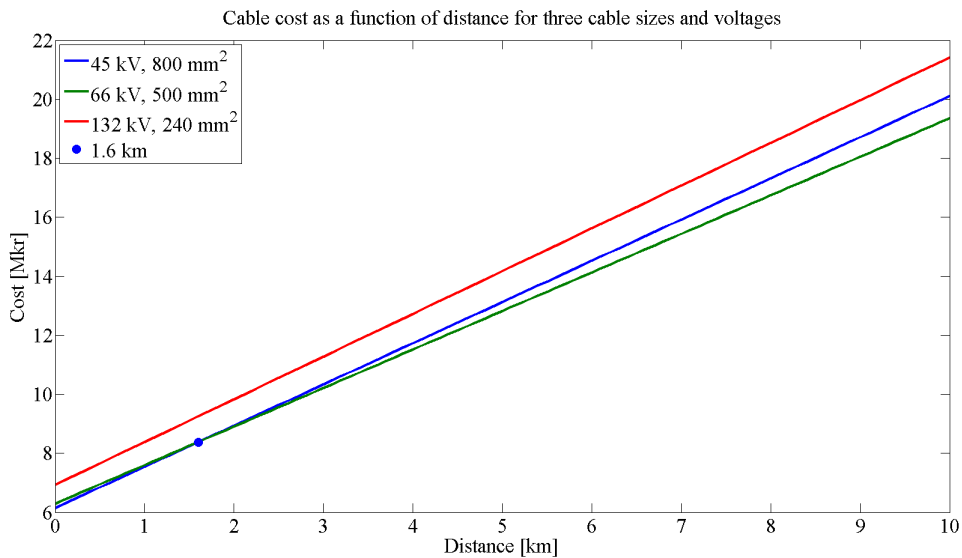


Figure 8.5: Graphical comparison between the three voltage options in Table 8.2, cost of cables, losses and transformers are taken into account.

## 8.4 Combining the tidal park with the offshore wind farm Gwynt y Môr

This section studies the possibility to connect the Deep Green tidal park with Gwynt y Môr, a wind park under construction outside of North Wales. The gain of using the same cable as Gwynt y Môr can be both environmental and economical. The

environmental contribution comes from avoiding the production of a new cable and the placement of the new cable at the sea ground. Economical benefits may arise in form of avoided or shared investment cost, but a higher cost caused from losses will appear.

Gwynt y Môr has an installed power of 576 MW and a transmission voltage at 132 kV<sub>AC</sub>. Four three-phase 500 mm<sup>2</sup> transmission cables with the length of 18 km is used from the park to the shore. The cables used in Gwynt y Môr are delivered from NKT cables. Since the data sheet from NKT cables is confidential, a similar 132 kV, 500 mm<sup>2</sup> cable from ABB will be used for calculations, see data sheet in appendix D, Fig.D. It is assumed that the rated current for the cable is 700 A which corresponds to a maximum power transmission of 640 MW for four cables. The tidal power park which should be investigated as a potential addition to the transmission line has a power output of 50 MW.

It is important to make sure that the cable is not under dimensioned compared to the maximum power output of the parks. If the cable is under dimensioned it can in worst case be damaged when the parks simultaneously have a high power production. This can be solved by limiting the power output or building a smaller park. The choice between these two options is dependent on the correlation between the peaks of the parks. The correlation between the peaks are not studied in this project, instead a study of the correlation between the mean values has been performed.

#### 8.4.1 Minimum power factor to transmit the total installed power

This section studies if the transmission cable at Gwynt y Môr can transmit the maximum power from both parks. It is no problem to transmit the power when only accounting for the active power (since the transmission cable can transmit 640 MW while the installed power is 626 MW). However, when taking the reactive power into account, the cable used will maybe be under dimensioned. The calculations are made by comparing the current at maximum power production for both parks with the maximum rated current in the transmission cable. The current transmitted from each park separately, at maximum power output, is calculated as

$$I = \frac{P/4}{\sqrt{3}UP_F} \quad [\text{A/conductor}] \quad (8.1)$$

where P is the maximum power installed at the park, 576 MW or 50 MW respectively, U is the nominal voltage, 132 kV, and P<sub>F</sub> is the power factor for the each park. Since Gwynt y Môr is connected to shore with four transmission cables, the transmitted power per cable will be a fourth of the total power production. This will be true with the assumption that the transmitted power is equally divided between the cables. The power factor is of great importance when studying the maximum power the cable can transmit. The line in Fig.8.6 represent the minimum power factor for each park which gives a transmission current equal to the maximum allowed current in each conductor (700 A) and is calculated with

$$I_m = I_c - I_w - I_t \quad [\text{A}] \quad (8.2)$$

where  $I_m$  is the marginal current per cable,  $I_c$  is the maximum rated current for each cable (700 A),  $I_w$  is the current contributed from one fourth of the maximum wind park power production and  $I_t$  is the current contributed from one fourth of the maximum tidal park power production.  $I_w$  and  $I_t$  are calculated with (8.1) for each respective power and with the power factor varying accordingly to the axes in Fig.8.6.

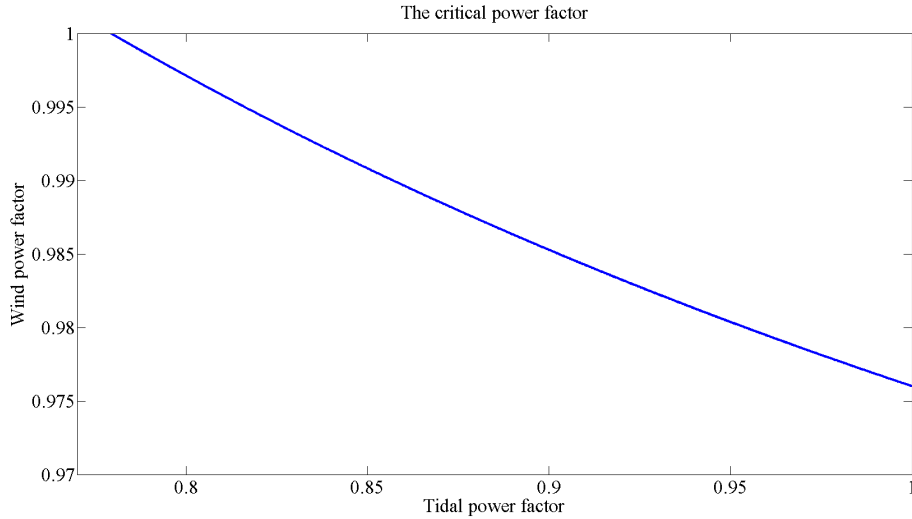


Figure 8.6: The line represent the minimum allowed power factor, i.e.  $I_m$  is equal to zero. For safe operation power factors higher than the line should be kept.

Power factors larger than the line represent a safe operation. In Table 8.3 the marginal currents are presented for some randomly selected power factors which ensures a safe operation for the transmission cables.

Table 8.3: Marginal currents for different power factors when both parks produce maximum installed power using (8.1) and (8.2).

Marginal current $I_m$ [A]	Wind		Tidal	
	$I_w$ [A]	$P_{Fw}$	$I_t$ [A]	$P_{Ft}$
15.5	629.8	1	54.7	1
3	639.4	0.985	57.6	0.95
3.1	636.2	0.99	60.7	0.9
2.7	633	0.995	64.3	0.85

The transmission cable has been designed with respect to the installed power of the wind park. To be able to compare the results in Table 8.3, the minimum power factor when only transmitting the wind power is presented in Table 8.4.

Table 8.4: Marginal currents when only the wind park is connected at maximum installed power for different power factors.

Marginal current	Wind	
$I_m$ [A]	$I_w$ [A]	$P_{Fw}$
67	633	0.995
0	700	0.9

There is quite a difference in power factors when comparing Table 8.3 and Table 8.4. In Table 8.4 it is seen that the marginal is very good for power factors close to one compared to the marginals in Table 8.3. The lowest power factor possible for the wind farm is 0.9 according to Table 8.4 while such low power factors is not possible in the combined park. However, the percentage when the power exceeds the installed wind power can be calculated by comparing the mean wind power output per day and the combined power output from both wind and tidal, see Fig.3(b) and Fig.3(c). The total power only exceeds the maximum installed wind power seven days of 134 days of data. This means that 95 % of the time the loading of the cable does not exceed the maximum power output of the wind park, even though the tidal park is connected.

#### 8.4.2 Transmission cost when sharing cable with a wind power park

Since the tidal park is a later extension to the original wind park, it is interesting to calculate the cost of the additional losses created in the transmission cable by the tidal park. The first step to calculate the additional cost of the losses, created by connecting the tidal park, is to calculate the produced currents. The current for the wind park,  $I_w$ , and the total current,  $I_{tot}$ , is calculated using (8.1) where  $P$  in this case is the the wind and tidal mean power per day shown in Fig.3(b) and Fig.3(a), respectively. The powers are divided by four since there are four cables in the transmission line. The voltage,  $U$ , is 132 kV<sub>AC</sub> as before and the power factor,  $P_F$  is assumed to be equal to one for both the wind and tidal case. The currents,  $I_w$  and  $I_{tot}$  are used to calculate the corresponding temperature dependent resistances according to Section 2.5.3 which are used as an input to the power flow analysis. With the correct resistances two power flow analysis are performed. The first is based on a fourth of the wind power, see Fig.3(b) and the second is performed on a fourth of the total power, see Fig.3(c). The power flow results for the wind/tidal power park are presented in Table. 8.5. These results can be compared to the wind power park results presented in Table. 8.6.

Table 8.5: Specifications for one cable for a wind/tidal park.

Voltage [kV]	132
Mean power loss per cable [kW/km]	8.8
Area [mm <sup>2</sup> ]	500
Max. current [A]	718 at 164 MVA
Power factor at max. current	0.9523

Table 8.6: Specifications for one cable for a wind park.

Voltage [kV]	132
Mean power loss per cable [kW/km]	7.6
Area [mm <sup>2</sup> ]	500
Max. current [A]	660 at 151 MVA
Power factor at max. current	0.9542

It is assumed that the rated current in a cable is 700 A but as can be seen in Table 8.5 the maximum current reaches 718 A. Calculations show that the current for both parks exceeds 700 A two times during 134 days (0.3 % of the total time) of data used in the calculations. The maximum current for the wind park is 660 A which is lower than the maximum rated current allowed in the cable. Using 660 A as maximum current for both parks results in a contravention seven times out of 134 days of data (5 % of total time).

The power flow analysis is performed for both the wind park and the two parks together. The result of the analysis is used to find the difference in power losses using

$$P_{diff} = P_{totloss} - P_{wloss} = 8.8 - 7.6 = 1.2 \quad [\text{kW/km}] \quad (8.3)$$

where  $P_{totloss}$  are the losses for both wind and tidal parks together, Fig.3(c), and  $P_{wloss}$  are the losses for the wind park, Fig.3(b). The cost of the additional losses for one cable is calculated by (5.3) from Section 5.6.1 using  $P_{diff}$  as power input instead. The additional losses caused by the tidal park results in a cost of 96 kkr/km per cable and a total cost of 382 kkr/km for all four transmission cables. This cost represents a minimum charge that is expected from the cable owner and can be accounted as a direct cost for the tidal park.

Since the collection grid for the tidal park is at 9.3 kV<sub>DC</sub>, an inverter as well as an additional transformer rated at 60 MVA is needed to be positioned out at the sea close to a wind park transformer. The costs for the additional transformer will be assumed to be similar to two transformer rated to 25 MVA each with a voltage ratio of 10/20 kV. The cost of these two transformers are equal to 6 768 kkr according to the EBR-list [48] and should be counted as a direct cost. The costs for the platform or adaptation for

subsea placement is neglected as well as the inverter cost since it will be needed at shore anyway.

Another direct cost which should be taken into account comes from the limited power production. The limitation is needed when the current exceeds the current rating of the cables (700 A), this is measured twice during the 134 days of data. At these two occasions the current reached 701.4 A and 718.5 A per cable which represents the mean current per day. The power which corresponds to the exceeded current is calculated by

$$P_{lost} = \sqrt{3}I_{ex}UP_F \quad [\text{W}] \quad (8.4)$$

where  $I_{ex}$  is the exceeded current, 1.4 A and 18.5 A, respectively,  $U$  is the transmission voltage of 132 kV and  $P_F$  is the power factor, 0.95. The cost of the lost revenue is calculated by

$$C_{lost} = P_{lost}C_{el}T_D L \quad [\text{kkkr}] \quad (8.5)$$

where  $C_{el}$  is the electricity cost of 0.47 kr/kWh [44,45],  $T_D$  is the amount of hours for three days,  $L$  is the lifetime of 20 years and 134 is the amount of data. The reason for using  $T_D$  as hours for three days is since the current was limited once every 134 days for each occasion which corresponds approximately to three times every year. The loss which occurs when the power production is limited to 700 A when using mean values per day equals 11 701 kkr over a period of 20 years. All the direct costs are presented in Table 8.7. To avoid overloading the transmission cables the maximum amount of tidal generators which can be installed are 68 generators.

Table 8.7: Summary of direct costs at 132 kV when sharing transmission with Gwynt y Môr.

Direct costs for tidal park		
Component	Amount and specification	Cost
Losses in cable	4x500 mm <sup>2</sup>	382 kkr/km
Transformers	2x25 MVA 10/20 kV	6 768 kkr
Cost of lost revenue	Six occasion per year	11 701 kkr

Since the tidal park uses Gwynt y Môr's transformers and transmission cables a rental cost should be taken into account. Gwynt y Môr uses four submarine transmission cables with a cross-sectional area of 500 mm<sup>2</sup> at 132 kV. A similar land based cable costs 1 461 kkr/km according to EBR [48]. Gwynt y Môr uses four transformers with the voltage ratio 33/132 kV rated at 160 MVA each [49]. The cost for Gwynt y Môr's transformers are assumed to be similar to eight 80 MVA transformers with the voltage ratio of 45/132 kV since this is the most similar transformers found in EBR [48]. The cost for these eight transformers is 70 968 kkr.

The rental cost of using Gwynt y Môr's components should be divided and one way of calculating this share is to calculate the share usage of the components. This can be done by using the mean power production per day, from Fig.3(a) and Fig.3(c), and is calculated as

$$share = 100 \cdot mean\left(\frac{P_t}{P_w + P_t}\right) \quad [\%] \quad (8.6)$$

In this case the mean share of the tidal park is 35 % of the instant production. This share is considerably high when comparing with the installed power between the wind park and tidal park. The reason for such a high percentage is that the wind park has a mean production of zero many days, which results in 100 % tidal production according to (8.6). Another way to calculate the share is to calculate the produced tidal power divided with installed maximum power.

$$share = 100 \cdot mean\left(\frac{P_t}{3.6 \cdot 160 + 0.5 \cdot 100}\right) \quad [\%] \quad (8.7)$$

This results in a share of 3 % where  $P_t$  is the mean tidal production per day, 3(a). A summary of the rental costs at the different shares is presented in Table 8.8.

Table 8.8: Summary of rental costs at 132 kV when sharing transmission with Gwynt y Môr.

Costs for Gwynt y Môr		
Component	Amount and specification	Cost
Cable (100 %)	4x500 mm <sup>2</sup>	5 844 kkr/km
Transformer (100 %)	8x80 MVA 45/132 kV	70 968 kkr
Share costs of Gwynt y Môr for tidal park		
Cable (35 %)	4x500 mm <sup>2</sup>	2 045 kkr/km
Transformer (35 %)	8x80 MVA 45/132 kV	24 839 kkr
Cable (3 %)	4x500 mm <sup>2</sup>	175 kkr/km
Transformer (3 %)	8x80 MVA 45/132 kV	2 129 kkr

All the resulting costs, specifications and the amount of each component for this section is presented in Table 8.9.

Table 8.9: Summary of transmission costs at 132 kV when sharing transformers and cables with Gwynt y Môr.

Total cost for tidal park with 35 % share		
Component	Amount and specification	Cost
Losses	4x500 mm <sup>2</sup>	382 kkr/km
Transformers	2x25 MVA 10/20 kV	6 768 kkr
Cost of lost revenue		11 701 kkr
Cable (35 % )	4x500 mm <sup>2</sup>	2 045 kkr/km
Transformer (35 %)	8x80 MVA 45/132 kV	24 839 kkr
Total		43 308 kkr
		2 427 kkr/km
Total cost for tidal park with 3 % share		
Losses	4x500 mm <sup>2</sup>	382 kkr/km
Transformers	2x25 MVA 10/20 kV	6 768 kkr
Cost of lost revenue		11 701 kkr
Cable (3 % )	4x500 mm <sup>2</sup>	175 kkr/km
Transformer (3 % )	8x80 MVA 45/132 kV	2 129 kkr
Total		20 598 kkr
		557 kkr/km

#### 8.4.3 The cost of sharing four 630 mm<sup>2</sup> transmission cables with a wind power park

If hypothetically, the park is still in the planning stage and the transmission cable is not yet selected. One option could be to over dimension the transmission cables and by that avoid overloading the cables. This section studies the costs if the transmission would consist of four 630 mm<sup>2</sup> cables for both the tidal park and Gwynt y Môr. The size of 630 mm<sup>2</sup> is the next step available after the 500 mm<sup>2</sup> cables which can be found among manufacturers and in the EBR-list. Four 630 mm<sup>2</sup> cables are able to transmit a maximum power of 806 MW when assuming the same current density as for the 500 mm<sup>2</sup> cable, 1.4 A/mm<sup>2</sup>. The installed power of both parks is 626 MW and it can be seen that there is a large marginal to the transmission cables limit. In the case of using the 500 mm<sup>2</sup> cables the maximum power limit is 640 MW. The power flow analysis made for four 630 mm<sup>2</sup> transmission cables resulted in the electrical parameters presented in Table 8.10.

Table 8.10: Electrical results for one cable when transmitting the power from a wind/tidal park.

Voltage [kV]	132
Mean power loss per cable [kW/km]	7
Area [mm <sup>2</sup> ]	630
Max. current [A]	706 at 161 MVA
Power factor at max. current	0.97

The cost for transformers are the same regardless of which cable dimension are used and can therefore be neglected when comparing the two sizes of transmission cables. When comparing the transmission losses they results in 630 kkr/km and 548 kkr/km for 500 mm<sup>2</sup> and 630 mm<sup>2</sup>, respectively. The cost of losses for 500 mm<sup>2</sup> are calculated with only the wind park connected and in the case of 630 mm<sup>2</sup> transmission both the wind and the tidal park are connected. Since the cost of losses are lower with 630 mm<sup>2</sup>, even though the installed power has increased, the tidal park should not pay for the losses.

On the other hand the tidal park have to pay for the extra cost of thicker cables. The 630 mm<sup>2</sup> cable costs 1 639 kkr/km per cable and the additional total cable cost that the tidal park should pay is 712 kkr/km for four cables. A comparison between the costs for using 500 mm<sup>2</sup> and 630 mm<sup>2</sup> transmission cables is presented in Table 8.11, all the costs except transformers are presented.

Table 8.11: Comparison of variable transmission costs at 132 kV 630 mm<sup>2</sup> and 500 mm<sup>2</sup>.

Extra cable cost [kkr/km]	4x630 mm <sup>2</sup>	712
Total cost at 18 km [kkr]		12 816
Cable and losses (35 % case) [kkr/km]	4x500 mm <sup>2</sup>	2 427
Cost of lost revenue [kkr]		11 701
Total cost at 18 km [kkr]		54 345
Cable and losses (3 % case) [kkr/km]	4x500 mm <sup>2</sup>	557
Cost of lost revenue [kkr]		11 701
Total cost at 18 km [kkr]		20 685

As can be seen in Table 8.11 it is preferable to use an over dimensioned cable. Even though the cable is more expensive, the gain from the lower losses and the fact that both parks can deliver maximum power simultaneously makes the 630 mm<sup>2</sup> transmission cable more profitable. It should be noted that the rental cost of Gwynt y Môrs transformers should be added to the cost, the cost depends on the share and is presented in Table 8.9. Since the 630 mm<sup>2</sup> transmission cables are over dimensioned it is possible to increase the amount of tidal generators to a maximum of 405 generators without exceeding the rated current of the cables. However, if the installed power of

the tidal park is changed, the solution for the most cost effective transmission cable and collection grid may also differ.

## 8.5 The most cost effective transmission option

In this chapter three different options of transmission cables have been evaluated: at collection grid voltage, at high voltage and sharing a high voltage transmission cable with a large wind park. In the calculations only costs for cables, transformers, losses and lost revenue have been taken into account. A summary of the costs is presented in Table 8.12 and a graphical presentation can be seen in Fig.8.7.

Table 8.12: Summary of the results of transmission cable calculations. The costs are presented as a present value for 20 years.

Transmission system	Cost	
9.3 kV <sub>DC</sub> , 4 cables at 713 mm <sup>2</sup>	Cable & losses	4 840 kkr/km
6.6 kV <sub>AC</sub> , 16 cables at 400 mm <sup>2</sup>	Cable & losses	13 787 kkr/km
66 kV, 1 cable at 500 mm <sup>2</sup>	Cable & losses	1 306 kkr/km
	Transformer	6 291 kkr
132 kV, 500 mm <sup>2</sup> , 35 %	variable cost	2 427 kkr/km
	fixed cost	43 308 kkr
132 kV, 500 mm <sup>2</sup> , 3 %	variable cost	557 kkr/km
	fixed cost	20 598 kkr
132 kV, 630 mm <sup>2</sup> , 35 %	variable cost	712 kkr/km
	fixed cost	31 607 kkr
132 kV, 630 mm <sup>2</sup> , 3 %	variable cost	712 kkr/km
	fixed cost	8 897 kkr

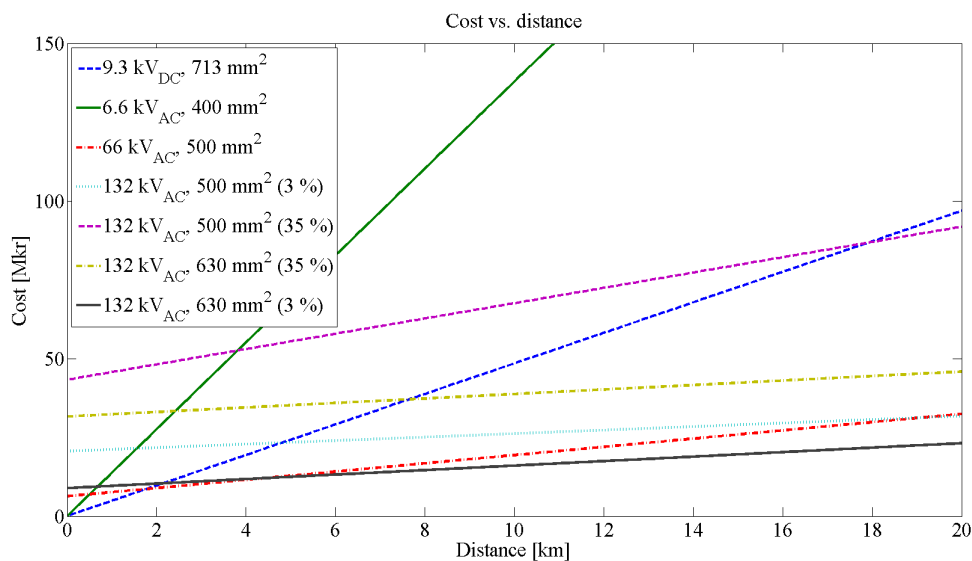


Figure 8.7: Comparison between the system in Table 8.12.

The optimal voltage of the transmission system is dependent on the distance to shore. As can be seen in Fig.8.7, the 9.3 kV<sub>DC</sub> system is the preferred transmission voltage for distances up to 1.8 km. The transmission cables in the case of Gwynt y Môr has a length of 18 km. The optimal voltage at the distance of 18 km is at 66 kV<sub>AC</sub> which is optimal already from 1.8 km. However, since the rental cost of using Gwynt y Môr's components is very uncertain other solutions are possible. If for instance the rental cost is neglected the 132 kV<sub>AC</sub> will become the most favourable option from distances of 13.5 km. Instead the 132 kV<sub>AC</sub> with a 3 % rental cost becomes the most optimal transmission option at 19.3 km. The main reason for the high cost of sharing with Gwynt y Môr comes from the limitation at 700 A. If the cost of 11 701 kkr for lost revenue is neglected, then sharing transmission cable of 500 mm<sup>2</sup> at 132 kV<sub>AC</sub> would be preferable from 3.5 km. At the distance of 18 km the rental cost should not exceed 7.4 %, assuming that the lost of revenue is neglected. As can be seen in Fig.8.7 it is profitable to over dimension the transmission cables to 630 mm<sup>2</sup> when sharing transmission cables with Gwynt y Môr in the 3 % case. This options becomes most cost effective from 4.6 km. At 18 km the 630 mm<sup>2</sup> option is the most cost effective option for rental shares up to 14 %.

In the case when Gwynt y Môr uses 500 mm<sup>2</sup> transmission cables there is a risk of overloading the transmission line. According to calculations in Section 8.4.2 the risk can be up to 5 % of the total time depending on which reference for the maximum current of the transmission cable which is used. These calculations are made with the assumption that there are no losses in the wind and tidal park.

The cost of lost revenue is highly dependent on the specific case. In this case Gwynt y Môr is much larger than the tidal park (576 MW and 50 MW, respectively) and the 500 mm<sup>2</sup> cables are rated at 640 MW. As can be seen, the marginal between the combined park and the transmission cable is good, probably much due to the fact that Gwynt y Môr is much larger than the tidal park. This is probably not the case when a tidal park is connected to a smaller wind park. The size of both parks and the transmission cable are important to study from case to case, since the lost revenue can cost a lot if the transmission cable is too under dimensioned.

The calculations in this study has been performed with data based on the mean power production per day. This is a very simplified case of the reality where the tidal park reaches a high power production four times per day. The power production is exceeding the cables maximum current limitation at many more occasions per day in reality compared to the mean value used. This gives an error in the calculations, especially when calculating the cost of lost revenue when the power production is limited to ensure that the cables are not damaged. However, even if the overloading occasions will increase, the time for each occasion will be rather short. Therefore, the calculated loss of revenue is rather correct since it includes the cost during a whole day, but for fewer days per year.

## 9 Discussion and conclusion

This chapter is a summary of the report, including discussions and conclusions of the most important parts. It is divided in three sections including subsea components, collection grid and transmission to the shore. Future costs in this project, such as cost from losses and cost of lost revenue, are calculated as a present value for a life time of 20 years.

### 9.1 Subsea Components

Subsea components are on its progress, with some components operating today and more are under development. The technology with for example subsea transformers have been used since 1998. There is no differences in the electrical parts between subsea components compared to land based components. The main challenges are to design a construction which can withstand the high pressure from the surrounding water and to isolate the components from water.

Since the business is driven forward by the oil and gas industry, most of the components is developed for deep seas (up to 3000 m) and for high voltages (up to 145 kV). When considering the water depth and voltage level of a tidal/wave park, the subsea components should be able to operate at these conditions without problems. Furthermore, these components could be even cheaper when adapted for the less harsh environment in the tidal/wave systems compared to the oil business. However, even if the technology is known, all the components required for these applications will need to be specially designed for its purpose, which will increase the cost.

One of the most expensive and weakest points of a subsea power system are the connectors. The less expensive connector is the drymate option, however it forces the cable length to increase which increases the cost (both in terms of cable cost and loss cost). For wetmate connectors the price is higher, but with this technology connecting and disconnecting cables under water is possible. It is therefore important to keep the number of connectors down in subsea systems in order to avoid high costs and get a high reliability.

The maintenance of subsea components should be avoided as much as possible due to the severe environment. Firstly, when building a subsea grid it is important to use as few components as possible. Secondly, extra components are usually installed and are used when a fault occur or maintenance is required for an other component. By adapting these principles the need for maintenance can be kept low and with no urgent maintenance required.

## 9.2 Collection grid

This section is a summary of Section 5.7 and Section 7.7, for a deeper discussion please read these sections instead.

The purpose of this project was to design two cost efficient collection grids for a tidal and a wave park, respectively. The installed power for the two parks are 50 MW and 2.5 MW, for the tidal and the wave park, respectively. The main focus has been on the cable dimensioning when concerning cost of cables and lost revenue from the power loss. AC and DC collection grids at the voltages between 0.69-14 kV and with two different infrastructures have been investigated.

There are some major conclusions that can be drawn from the project. Firstly, the star connection is preferable over the radial pattern due to the low number of connectors (which are both expensive and a weak point in the system). Secondly, since a converter is needed, independently of the voltage type used, a DC system will always be cheaper than an AC system as long as the generator can excite high enough voltage for the collection grid. Thirdly, the low voltage of 690 V that is used for wind power generators is too low for a tidal/wave generator. The reason for this is due to the difficulties to transform the voltage close to the kite/buoy compared to a wind power plant (where the voltage is transformed to medium voltage inside the wind tower). The alternative for the tidal/wave case is to place a transformer in each kite/buoy or a subsea transformer next to each kite/buoy. This solution will be costly and a more cost efficient solution is to increase the generator voltage. Fourthly, there are no subsea DC cables manufactured today at the low voltages considered. However, the technology for high voltage subsea DC cables is well known and used. Therefore, lower voltage subsea DC cables should not be of any challenge for the industry to produce. Fifthly, there are no manufactures today of converters at 10 kV for 500 kW, which also will be space demanding and the development of such converter can be costly. Therefore, a collection grid at 10 kV was not an option in the end.

The final collection grid to prefer, for both the tidal and the wave case, is a DC grid in star connection and with 9.3 kV and 1.4 kV, respectively. The tidal system consists of cable dimensions between 30-713 mm<sup>2</sup> with a total cable cost of 7 424 kkr and with a cable loss of 0.16%. For the wave system, the cable dimensions are between 23-488 mm<sup>2</sup> and with a cable cost of 249 kkr and with a cable loss of 0.05%. The large difference in the cable cost of the two systems is mainly due to the difference in cable length and the conductor material. This conclusion is based on the cost associated with the cables while the cost for the rest of the system has not been included. The reason for this is that most of the components need to be specially made for each case since standard components are rare in this business. Furthermore, the cost for the DC cables have been approximated with AC cables with the same conductor volume, due to that there are no DC cables manufactures today at the low voltages concerned. Therefore, if the DC cables will become much more expensive than the AC cables due to special order, the AC system with star connection at 6.6 kV and 3.3 kV, tidal and wave, respectively, is to prefer. The cable cost of those systems (including 100 generating units) reaches 17 718 kkr and 769 kkr, tidal and wave, respectively, and the cable loss of 0.4% and 0.17%, respectively.

When comparing the tidal and wave case at  $3.3 \text{ kV}_{AC}$  and  $4.7 \text{ kV}_{DC}$  there is a main difference in the result. In the tidal case the radial system is cheaper than the star system while in the wave case the result is the opposite. The reason for this is probably mostly due to the approximated cable cost and the large variation in the conductor areas. However, as mentioned earlier, the star connection pattern is to prefer due to the lower number of connection units.

### 9.3 Transmission to shore

The different options that have been compared are: transmission at collection grid voltage, transmission with higher voltage using a transformer and sharing a transmission cable with a large wind power park. More detailed information and results are found in Chapter 8.

The study of the collection grid voltage has been conducted for  $9.3 \text{ kV}_{DC}$  and  $6.6 \text{ kV}_{AC}$ . The total cost of the DC and AC system, respectively, becomes  $4\,840 \text{ kkr/km}$  and  $13\,787 \text{ kkr/km}$  when the cable and loss cost are considered.

The voltages studied at transmission with high voltage are  $45 \text{ kV}_{AC}$ ,  $66 \text{ kV}_{AC}$  and  $132 \text{ kV}_{AC}$ . These calculations have been performed with the respect of cable cost, loss cost and transformer cost. The most cost effective transmission option was  $66 \text{ kV}_{AC}$  for distances over  $1.6 \text{ km}$ . The cost for this system resulted in  $6\,291 \text{ kkr}$  for the transformer and  $1\,306 \text{ kkr/km}$  for the cable and losses.

The option of sharing four  $500 \text{ mm}^2$  transmission cables at  $132 \text{ kV}_{AC}$  with the wind power park Gwynt y Môr (with the installed power of  $576 \text{ MW}$ ) has been conducted. The rated power for the cable is  $640 \text{ MW}$  while the total wind/tidal park has a total installed power of  $626 \text{ MW}$ . The result from the analysis was that the total power output had to be limited six times during one year in order to not over load the cable. To avoid this the maximum size of the tidal park should be  $34 \text{ MW}$  instead of  $50 \text{ MW}$ . The costs for the tidal park is divided into direct costs and rental costs. The direct costs in this case are the additional losses caused by the tidal park, transformers and the cost of lost revenue when the maximum power exceeds. Since the tidal park uses Gwynt y Môr's transformer and transmission cable a rental fee based on the share usage of the components is in order. This share can be calculated in various ways and two ways are presented in this project, resulting in  $35 \%$  and  $3 \%$  share. The total cost when sharing the transmission cable with Gwynt y Môr resulted in  $43\,308 \text{ kkr}$  and  $2\,427 \text{ kkr/km}$  for the  $35 \%$  share and  $20\,598 \text{ kkr}$  and  $557 \text{ kkr/km}$  for the  $3 \%$  share.

A study of sharing four  $630 \text{ mm}^2$  transmission cables at  $132 \text{ kV}_{AC}$  with Gwynt y Môr has been conducted as well. Instead of paying a rental fee for using the cables the tidal park pays for the extra cost for the larger cable. The larger cable reduces the losses to such an extent that the cost will become lower compared to when only the wind park used the transmission cables. Since the tidal park does not contribute to any additional losses this cost is removed. In the case of using  $630 \text{ mm}^2$  cables, the tidal park still have to pay a rental fee depending on the share for using Gwynt y Môr's transformers. The total cost will become  $712 \text{ kkr/km}$  for the cable and the transformers will cost

from 2 129 kkr (3 %) to 31 607 kkr (35 %) depending on the rental share. Since the 630 mm<sup>2</sup> transmission cables are over dimensioned it is possible to increase the tidal park by a factor of four, but if the park is changed so dramatically the best collection grid and transmission option may also differ.

In the case of positioning the tidal park 18 km from shore, which is the distance for Gwynt y Môr, the most cost effective transmission option is to use an own cable at 66 kV<sub>AC</sub>. This is the best options between the distances of 1.8 km to 19.3 km. For distances shorter than 1.8 km the 9.3 kV<sub>DC</sub> option is to prefer if the collection grid uses this voltage. At distances longer than 19.3 km, sharing with Gwynt y Môr became the most cost effective solution when the rental share is equal to 3 %. The study also shows that if the transmission cables would consist of four 630 mm<sup>2</sup> it would become the best option for distances longer than 4.6 km. Even though the cable is more expensive, the advantage of the lower cost of losses and the avoided need of limiting the power makes this options the most cost effective one.

## 10 Future work

This project has the boundary at the shore, before connecting the park to the grid. Depending on which country and grid owner the park under study will be connected to, different requirements from grid owners occurs. Usually there are requirements in electrical quality which needs to be fulfilled before connecting the park to the grid. For example a typical restriction could be that there should be no exchange of reactive power between the grid and the park. An investigation of the requirements should be checked at each specific case.

The mechanical impact on the kite or buoy was not investigated in this study. However, the forces from the water streams and waves can be very large and its impact on the equipment will definitely be required to be studied before the system can be utilised. In the Deep Green case, the cable from the kite to the bottom will be exposed to the strongest mechanical forces in the system and needs to be studied in detail. The offshore systems are exposed to salt sea water and marine biological fouling which can be a problem in the long run for the parks. The impact of the offshore parks on the animal life and nature should be studied as well.

Since there are space limitations inside the kite, the sizes of the components required are of interest. This study has not immerse these limitations in detail. One suggestion to consider is to use a generator with a high supply frequency to keep the size down. The generator frequency can be selected freely since a converter or rectifier is operating next to it, but usually frequencies higher than 400 Hz are not used. One drawback of increasing the generator frequency is that the generator impedance will increase as well. The converter is another space demanding component and by using a DC collection grid only the rectifying part of the converter is placed in the kite. The sizes of the components would however require a more detailed study than this.

When investigating how a collection grid for an offshore tidal or wave power park can be built, the solution of combining each kite/buoy with a wind turbine was discussed. With this solution only the generator is required to be positioned inside the kite/buoy (together with possible control equipment), while the converter and transformer can be placed inside the wind tower. Further positive effects could be a better usage of the cable, shared costs for almost all equipment, less need of subsea components and less space of the sea is used. The solution of combining each kite/buoy with a wind turbine would be interesting to investigate.

During the planning of a park, a study in more specific costs and dimensioning of components need to be performed. This project has assumed worst case scenario and excluded the discount rate. A discount rate, valid for the time of interest, should be taken into account before constructing a collection grid. Since the components used in the high voltage industry usually are specially made for each project, a quotation should be made which will result in an accurate cost. A follow-up is necessary of the subsea component industry, which is in constant development. Also the regular components business is under constant development, and for example power electronics for increasing the DC voltage (so called DC/DC-boost) could be used in the future instead of regular transformers. With this new technology, the solutions for the col-

lection grid will differ in the future. There are also costs related to the installation, maintenance and operation that have not been taken into account in this study. Furthermore, from an economical point of view, the revenue from the electricity as well as potential subsidies should be included in a budget.

The reliability of the park is also interesting to study more in detail. Depending on the final grid connection, breaker positions and fault type the reliability of the park will differ. Also an analysis of the kite/buoy operation reliability itself is interesting to investigate.

In the case of transmitting the power to shore by sharing cables with a wind power park the costs are very dependent on the situation. If the wind power park is already built, an investigation of the cables maximum capacity and the rental cost have to be made. In the case that the cable is under dimensioned, the park's power production can either be limited or a smaller park can be constructed. The choice between these two options is dependent on the correlation between the peaks of the parks which needs to be studied further. The rental cost of using the wind park's components and cables is of great interest and can vary a lot depending on the calculations. If the cost is high it may be of interest to use an own transmission cable instead of sharing it with the wind park.

Depending on which transmission option that is selected the circuit breaker requires to be dimensioned for the system. The fault current will be calculated based on the transformer's impedance in the system. The converters in the collection grid will probably be controlled to turn off when a fault occurs and will therefore not be included for the fault current.

## References

- [1] Center for climate and energy solutions, “The basics,” November 2012. [Online]. Available: <http://www.c2es.org/science-impacts/basics>
- [2] European Commission, “The EU climate and energy package,” November 2012. [Online]. Available: [http://ec.europa.eu/clima/policies/package/index\\_en.htm](http://ec.europa.eu/clima/policies/package/index_en.htm)
- [3] J. F. Chozas *et al.*, “Combined Production of a full-scale Wave Converter and a full-scale Wind Turbine - a Real Case Study.” Dublin: 4th International Conference on Ocean Energy, October 2012, pp. 5–6.
- [4] Guardian Environment Network. (11, October, 2012) Uk tidal power potential estimated at 153 gw. The Guardian. ( Available: February 2013). [Online]. Available: <http://www.guardian.co.uk/environment/2012/oct/11/uk-tidal-power-estimate>
- [5] J. Öjvind Swahn. (February 2013) Tidvatten. Nationalencyklopedin. [Online]. Available: <http://www.ne.se/lang/tidvatten>
- [6] SMHI. (February 2013) Tidvatten. SMHI. [Online]. Available: <http://www.smhi.se/kunskapsbanken/oceanografi/tidvatten-1.321>
- [7] T. Thiringer, J. MacEnri, and M. Reed, “Flicker evaluation of the seagen tidal power plant,” Tech. Rep., 2011.
- [8] World Meteorological Organization, *Guide to wave analysis and forecasting*, 2nd ed., 1998, pp. 1, 35, 44. [Online]. Available: [http://ec.europa.eu/clima/policies/package/index\\_en.htm](http://ec.europa.eu/clima/policies/package/index_en.htm)
- [9] Anthoni, Dr J. F. (2000) Oceanography: waves theory and principles of waves, how they work and what causes them. Seafriends. (Available: January 2013). [Online]. Available: <http://www.seafriends.org.nz/oceano/waves.htm#environment>
- [10] Seabased AB. (2009) About wave energy. Seabased AB. (Available: January 2013). [Online]. Available: [http://www.seabased.com/index.php?Itemid=72&id=73&option=com\\_content&view=article](http://www.seabased.com/index.php?Itemid=72&id=73&option=com_content&view=article)
- [11] National Geographic. (21, January, 2013) Tidal energy. National Geographic Education. [Online]. Available: [http://education.nationalgeographic.com/education/encyclopedia/tidal-energy/?ar\\_a=1](http://education.nationalgeographic.com/education/encyclopedia/tidal-energy/?ar_a=1)
- [12] Picture SeaGen, 2013-01-15. [Online]. Available: <http://www.evwind.es/2012/08/22/wind-energy-update-major-european-utility-commits-to-tidal-energy-meeting/22051/>
- [13] Picture OpenHydro, 2013-01-15. [Online]. Available: <http://whataboutenergy.blogspot.se/2010/04/ten-sites-named-in-4bn-uk-marine-energy.html>
- [14] Picture DeepGreen, 2013-01-15. [Online]. Available: <https://www.dropbox.com/sh/ifzbtgcyersu8hy/0gvHB-J0Zm#f:Deep%20Green.jpg>

- [15] Picture Pelamis, 2013-01-15. [Online]. Available: <http://www.pelamiswave.com/image-library>
- [16] Picture Wavedragon, 2013-01-15. [Online]. Available: [http://www.wavedragon.net/index.php?option=com\\_content&task=view&id=6&Itemid=5](http://www.wavedragon.net/index.php?option=com_content&task=view&id=6&Itemid=5)
- [17] Picture Seabased, 2013-01-15. [Online]. Available: [http://seabased.se/index.php?option=com\\_content&view=article&id=67&Itemid=80](http://seabased.se/index.php?option=com_content&view=article&id=67&Itemid=80)
- [18] Minesto, 2013. [Online]. Available: <http://www.minesto.com/Resources/Minesto-DG-12.pdf?1365759397634>
- [19] A. Hulth. (2012) Dags att testa vågkraften i stor skala. Uppsala Univeristy. (Available: February 2013). [Online]. Available: <http://www.uu.se/nyheter/nyhet-visning/?id=2051&area=5,16&typ=artikel&na=&lang=sv>
- [20] Picture Seabased, 2013-01-15. [Online]. Available: <http://seabased.se/index.php?Itemid=78>
- [21] *IEC 60287-1-1 ed.1.2*, International Electrotechnical Commission, IEC Std., 12 2006.
- [22] ABB, “Performance under pressure,” Press release, September 2012. [Online]. Available: <http://www.abb.se/cawp/seitp202/2a247737ec6f567cc1257a7000716080.aspx>
- [23] A. O. Systems, “Subsea power transfer - what is the challenge,” February 2003. [Online]. Available: <http://www.spe.no/oslo/html/workshopfiles/papers/Subsea%20Power.pdf>
- [24] H. Gedde *et al.*, “Ormen Lange Long Step-Out Power Supply,” no. OTC 20042. Houston, Texas, USA: Offshore Technology Conference, May 2009.
- [25] VetcoGray, “VetcoGray Subsea Power Transformer,” Mars 2013. [Online]. Available: [http://www.ge-energy.com/products\\_and\\_services/products/subsea-power\\_and\\_processing\\_systems/vetcogray\\_subsea\\_power\\_transformer.jsp](http://www.ge-energy.com/products_and_services/products/subsea-power_and_processing_systems/vetcogray_subsea_power_transformer.jsp)
- [26] A. Akdag and E. Virtanen, “Power below the waves,” *ABB review Special Report Transformers*, pp. 33–36, November 2012. [Online]. Available: [http://www05.abb.com/global/scot/scot271.nsf/veritydisplay/c3791bac5b25bd10c1257ab80037553b/\\$file/ABB%20SR%20Transformers-121031.pdf](http://www05.abb.com/global/scot/scot271.nsf/veritydisplay/c3791bac5b25bd10c1257ab80037553b/$file/ABB%20SR%20Transformers-121031.pdf)
- [27] E. Enger and S. Rock, “Emerging Technologies, Subsea Power Systems,” September 2006, (Available: Mars 2013). [Online]. Available: [http://www.demo2000.no/filearchive/pdf/4\\_enger\\_vetco\\_subsea\\_power.pdf](http://www.demo2000.no/filearchive/pdf/4_enger_vetco_subsea_power.pdf)
- [28] C. A. Godinho *et al.*, “The development of a subsea power transmission system for deep water boosting applications,” no. OTC 8061. Houston, Texas, USA: Offshore Technology Conference, May 1996.
- [29] B. E. Brath, “Subsea Power Grid,” Presentation at OTC 2010 X-pert Center, 2010. [Online]. Available: [http://www.energy.siemens.com/br/pool/hq/energy-topics/tradeshows/2010otc/downloads/Subsea%20Power%20Grid\\_b.pdf](http://www.energy.siemens.com/br/pool/hq/energy-topics/tradeshows/2010otc/downloads/Subsea%20Power%20Grid_b.pdf)

- [30] Siemens oil and gas solutions offshore, “Enabling large-scale subsea processing - Subsea solutions from Siemens.” Brochure, 2010. [Online]. Available: [http://www.energy.siemens.com/co/pool/hq/energy-topics/tradeshows/2010otc/downloads/OG\\_26975\\_B\\_Subsea\\_final7A.pdf](http://www.energy.siemens.com/co/pool/hq/energy-topics/tradeshows/2010otc/downloads/OG_26975_B_Subsea_final7A.pdf)
- [31] VetcoGray, “VetcoGray Subsea Switchgear,” Mars 2013. [Online]. Available: [http://www.ge-energy.com/products\\_and\\_services/products/subsea\\_power\\_and\\_processing\\_systems/vetcogray\\_switchgear.jsp](http://www.ge-energy.com/products_and_services/products/subsea_power_and_processing_systems/vetcogray_switchgear.jsp)
- [32] T. Hazel, “Impact of subsea processing power distribution: Subsea switchgear module a key enabling component in subsea installations,” Schneider Electric, July 2011, 998-4670\_GMA.
- [33] Siemens Subsea department, “SpecTRON Evolution,” Mars 2013, (Brochure for SpecTRON connectors). [Online]. Available: [http://www.energy.siemens.com/hq/pool/hq/industries-utilities/oil-gas/applications/subsea/downloads/SpecTRON\\_brochure.pdf](http://www.energy.siemens.com/hq/pool/hq/industries-utilities/oil-gas/applications/subsea/downloads/SpecTRON_brochure.pdf)
- [34] VetcoGray oil and gas, “VetcoGray MECON WM 36/500,” Mars 2013, (Brochure for VetcoGray MECON WM 36/500). [Online]. Available: [http://www.ge-energy.com/content/multimedia/\\_files/downloads/VetcoGray%20MECON%20WM%2036500.pdf](http://www.ge-energy.com/content/multimedia/_files/downloads/VetcoGray%20MECON%20WM%2036500.pdf)
- [35] VetcoGray, “VetcoGray MECON Wet Mate Connector,” Mars 2013. [Online]. Available: [http://www.ge-energy.com/products\\_and\\_services/products/subsea\\_power\\_and\\_processing\\_systems/vetcogray\\_mecon\\_wet\\_mate\\_connector.jsp](http://www.ge-energy.com/products_and_services/products/subsea_power_and_processing_systems/vetcogray_mecon_wet_mate_connector.jsp)
- [36] O. Svensson, “Experimental results from the lysekil wave power research site,” Div. for Electricity, Uppsala University, Tech. Rep., 2012, ISBN: 978-91-554-8433-0 and ISSN: 1651-6214.
- [37] M. Rahm *et al.*, “Offshore underwater substation for wave energy converter arrays,” *IET Renewable Power Generation*, vol. 4, no. 6, pp. 602–612, 2010.
- [38] Boström, C and others, “Design proposal of electrical system for linear generator wave power plants,” Div. for Electricity, Uppsala University, Box 534, 751 21 Uppsala, Sweden, Tech. Rep., 2009.
- [39] Normann, Truls. First Chief Engineer, Head of Power Products & Technology, Aker Solutions. Email. March 20, 2013.
- [40] P. Weiss *et al.*, “Novel wet-mate connectors for high voltage and power transmissions of ocean renewable energy systems,” COMEX S.A., 36 Bvd des Océans, 13009 Marseille, France, Tech. Rep., 2012.
- [41] Wida, Roland. Product Manager medium voltage converters, ABB. Email. Västerås. March 6, 2013.
- [42] Sonerud, Björn. Ph.D., R&D Engineer Submarine High Voltage Cables (SHV), Nexans Norway AS. Email. Halden. February 8, 2013.

- [43] “Kostnadskatalog 2012, Lokalnät 0,4-24 kV samt optonät,” Elbyggnadsrationaliseringen, EBR, Planeringskatalog P1, Arbetskod: G150 Sjökabelförläggning. [Online]. Available: <http://www.svenskenergi.se/Vi-erbjuder/Webbshop/EBR-Ekonomi/Kostnadskataloger/>
- [44] Forex, Mars 2013. [Online]. Available: <http://www.forex.se/Valuta/Valutagrafer/>
- [45] APX Power UK, “Reference Price Data HH 2H 4HB 2012.xls,” Mars 2013. [Online]. Available: <ftp://ftp.apxgroup.com/2012/>
- [46] H. Saadat, *Power System Analysis*, 1st ed. MCGraw-Hill Companies, 1999, attached CD to the book.
- [47] U. M. Office., Met Office Integrated Data Archive System (MIDAS) Land and Marine Surface Stations Data, NCAS British Atmospheric Data Centre, 2012. [Online]. Available: [http://badc.nerc.ac.uk/view/badc.nerc.ac.uk\\_\\_ATOM\\_\\_dataent\\_ukmo-midas](http://badc.nerc.ac.uk/view/badc.nerc.ac.uk__ATOM__dataent_ukmo-midas)
- [48] “EBR-e Kostnadskatalog 2012, Regionnät 36-145 kV,” Elbyggnadsrationaliseringen, EBR, Projekteringskatalog P2, Arbetskod: 14 Transformatorarbeten and Arbetskod: 13 Kabelarbeten t o m 145 kV. [Online]. Available: <http://www.svenskenergi.se/Vi-erbjuder/Webbshop/EBR-Ekonomi/Kostnadskataloger/>
- [49] 4C offshore, “Gwynt y Mor 1 Substation,” April 2013. [Online]. Available: <http://www.4coffshore.com/windfarms/substation-gwynt-y-mor-1-substation-sid31.html>
- [50] Seabased, “Pressbilder - Vgkraftpark,” April 2013.
- [51] Ludvig Lindström, “Evaluating impact on ampacity according to IEC-60287 regarding thermally unfavourable placement of power cables,” Master’s thesis, Kungliga Tekniska Högskolan, 2011.
- [52] *IEC 60287-2-1 ed.1.2*, International Electrotechnical Commission, IEC Std., 5 2006.
- [53] H. Saadat, “Power flow analysis,” in *Power System Analysis*, 1st ed. MCGraw-Hill Companies, 1999, ch. 6, pp. 189–238.
- [54] E. Eriksson, “Wind farm layout - a reliability and investment analysis,” Master thesis, Uppsala University, 2008.
- [55] Chalmers, course material ENM050 - Power system Analysis: Lecture 13: Power Flow: Newton-Raphson.
- [56] King Saud University, course material EE342 - Electrical Power Lab: Load Flow Analysis.
- [57] Nexans, “Submarine Power Cables,” April 2013. [Online]. Available: [http://www.nexans.com/Germany/group/doc/en/NEX\\_Submarine\\_neu.pdf](http://www.nexans.com/Germany/group/doc/en/NEX_Submarine_neu.pdf)

- [58] Caledonian cables / Addison cables, “Caledonian Medium Voltage Cables Three Core Cables to IEC 60502,” April 2013. [Online]. Available: <http://www.caledonian-cables.com/download/Three%20Core%20Cables%20To%20IEC%2060502.pdf>
- [59] LORC, 2013. [Online]. Available: [http://www.lorc.dk/offshore-wind-farms-map/gwynt-y-m%c3%b4r?os\\_tmdl=Siemens+SWT-3.6-107](http://www.lorc.dk/offshore-wind-farms-map/gwynt-y-m%c3%b4r?os_tmdl=Siemens+SWT-3.6-107)
- [60] “XLPE Submarine Cable Systems - Attachment to XLPE Land Cable Systems - Users Guide,” ABB, 2013. [Online]. Available: [http://www05.abb.com/global/scot/scot245.nsf/veritydisplay/2fb0094306e48975c125777c00334767/\\$file/xlpe%20submarine%20cable%20systems%202gm5007%20rev%205.pdf](http://www05.abb.com/global/scot/scot245.nsf/veritydisplay/2fb0094306e48975c125777c00334767/$file/xlpe%20submarine%20cable%20systems%202gm5007%20rev%205.pdf)
- [61] Ericsson, “AKKJ 1 kV - Product Information,” April 2013. [Online]. Available: <http://archive.ericsson.net/service/internet/picov/get?DocNo=16/28701-FGC101680&Lang=EN&HighestFree=Y>
- [62] Ericsson AB, Cables&Interconnect , “Kraftkabelhandboken,” 2003.
- [63] NDT Resource Center. (26, March, 2013) The international annealed copper standard. NDT Resource Center. [Online]. Available: <http://www.ndt-ed.org/GeneralResources/IACS/IACS.htm>

# Appendices

## A Description of IEC 60287

This appendix will describe in detail how to calculate the cable temperature using (A.1) from IEC 60287. There are many different cable options to select between in the IEC 60287 in order to get a correct value. In this appendix, only the equations corresponding to a single-core cable will be described. This since the three phase cable, used throughout in this report, is of SL type and will therefore use the same equations as the single-core cable according to IEC. The equation (A.1) and the parameter descriptions are a citation from [51] which in its turn is a summary of IEC 60287.

$$\Delta\theta = (I^2R + \frac{1}{2}W_d)T_1 + [I^2R(1 + \lambda_1) + W_d]nT_2 + [I^2R(1 + \lambda_1 + \lambda_2) + W_d]n(T_3 + T_4) \quad (\text{A.1})$$

where

- I is the current flowing in one conductor [A]
- $\Delta\theta$  is the conductor temperature rise above the ambient temperature [K]  
NOTE The ambient temperature is the temperature of the surrounding medium or are to be installed, including the effect of any local source of heat, but not the increase of temperature in the immediate neighbourhood of the cables due to heat arising therefrom.
- R is the alternating current resistance per unit length of the conductor at maximum operating temperature [ $\Omega/\text{m}$ ]
- $W_d$  is the dielectric loss per unit length for the insulation surrounding the conductor [W/m]
- $T_1$  is the thermal resistance per unit length between one conductor and the sheath [Km/W]
- $T_2$  is the thermal resistance per unit length of the bedding between sheath and armour [Km/W]
- $T_3$  is the thermal resistance per unit length of the external serving of the cable [Km/W]
- $T_4$  is the thermal resistance per unit length between the cable surface and the surrounding medium [Km/W]
- n is the number of load-carrying conductors in the cable (conductors of equal size and carrying the same load)
- $\lambda_1$  is the ratio of losses in the metal sheath to total losses in all conductors in that cable
- $\lambda_2$  is the ratio of losses in the armouring to total losses in all conductors in that cable

The dielectric loss per unit length in each phase is given by:

$$W_d = \omega CU_0^2 \tan\delta \quad [\text{W}/\text{m}] \quad (\text{A.2})$$

where

- $\omega = 2\pi f$
- C is the capacitance per unit length [F/m]
- $U_0$  is the voltage to earth [V].

The power loss in the sheath or screen ( $\lambda_1$ ) consists of losses caused by circulating currents ( $\lambda'_1$ ) and eddy currents ( $\lambda''_1$ ), thus:

$$\lambda_1 = \lambda'_1 + \lambda''_1 \quad (\text{A.3})$$

The formula given in this section express the loss in terms of the total power loss in the conductor(s).

$$R_s = R_{s0}[1 + \alpha_{20}(\theta_{SC} - 20)] \quad [\Omega/m] \quad (\text{A.4})$$

where

- $R_{S0}$  is the resistance of the cable sheath or screen at 20°C [ $\Omega/m$ ].
- $\alpha_{20}$  is the constant mass temperature coefficient for copper at 20 °C per Kelvin
- $\theta_{SC}$  is the maximum operating temperature in °C

$$\lambda'_1 = \frac{R_s}{R} \frac{1}{1 + \left(\frac{R_s}{X}\right)^2} \quad (\text{A.5})$$

where

- $R_s$  is the resistance of sheath or screen per unit length of cable at its maximum operating temperature [ $\Omega/m$ ]
- X is the reactance per unit length of sheath or screen per unit length of cable =  $2\omega 10^{-7} \ln\left(\frac{2s}{d}\right)$
- s is the distance between conductor axes in the electrical section being considered [mm]
- d is the mean diameter of the sheath [mm]
- $\lambda''_1 = 0$ . The eddy-current loss is ignored according to IEC 60287-1-1 section 2.3.1 [1].

**To calculate the  $\lambda_2$  (the ratio of losses in the armouring to total losses in all conductors) the equations is taken from [21] word by word.**

#### 2.4.2.3 Three-core cables steel wire armour

##### 2.4.2.3.1 Round conductor cable

$$\lambda_2 = 1,23 \frac{R_A}{R} \left(\frac{2c}{d_A}\right)^2 \frac{1}{\left(\frac{2,77R_A 10^6}{\omega}\right)^2 + 1} \quad (\text{A.6})$$

where

- $R_A$  is the a.c. resistance of armour at maximum armour temperature [ $\Omega/m$ ]
- $d_A$  is the mean diameter of armour [mm]
- $c$  is the distance between the axis of a conductor and the cable centre [mm]

**To calculate the different thermal resistances wished, the equations is taken directly from [52].**

### 2.1.1 Thermal resistance between one conductor and sheath T1

2.1.1.1 Single-core cables The thermal resistance between one conductor and the sheath T1 is given by:

$$T_1 = \frac{\rho_T}{2\pi} \ln \left[ 1 + \frac{2t_1}{d_c} \right] \quad (\text{A.7})$$

where

- $\rho_T$  is the thermal resistivity of insulation [Km/W]
- $d_c$  is the diameter of conductor [mm]
- $t_1$  is the thickness of insulation between conductor and sheath [mm]

### 2.1.2.2 SL and SA type cables

The thermal resistance of fillers and bedding under the armour is given by:

$$T_2 = \frac{\rho_t \bar{G}}{6\pi} \quad (\text{A.8})$$

where G is the geometric factor given in figure 6, i.e. Fig. A.1.

### 2.1.3 Thermal resistance of outer covering (serving) T3

The external servings are generally in the form of concentric layers and the thermal resistance T3 is given by:

$$T_3 = \frac{1}{2\pi} \rho_T \ln \left( 1 + \frac{2t_3}{D'_a} \right) \quad (\text{A.9})$$

where

- $t_3$  is the thickness of serving [mm]
- $D'_a$  is the external diameter of the armour [mm]

### 2.2.2 Single isolated buried cable

$$T_4 = \frac{1}{2\pi} \rho_T \ln(u + \sqrt{u^2 - 1}) \quad (\text{A.10})$$

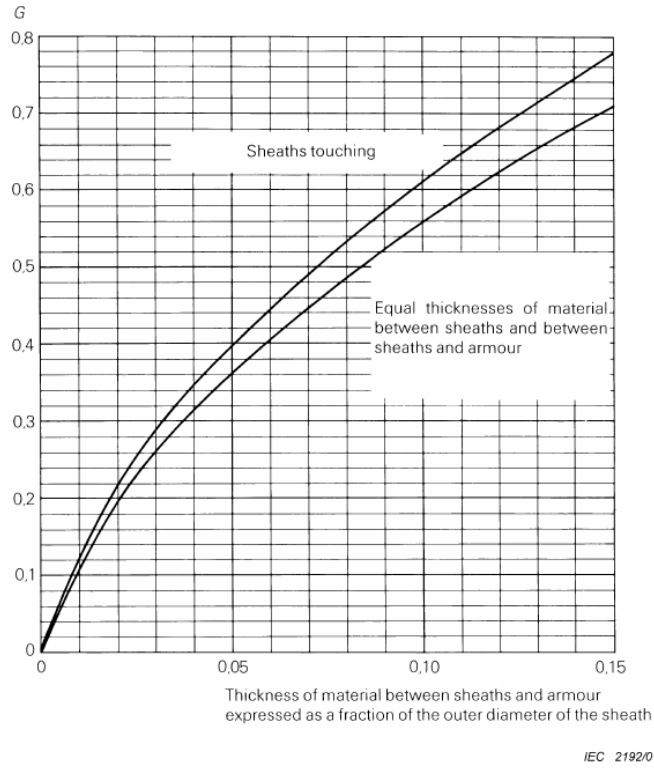


Figure 6 – Geometric factor  $\bar{G}$  for obtaining the thermal resistances of the filling material between the sheaths and armour of SL and SA type cables (see 2.1.2.2)

Figure A.1: Geometric factor to calculate  $T_2$ .

where

$\rho_T$  is the thermal resistivity of the soil [Km/W]

$$u = \frac{2L}{D_e}$$

$L$  is the distance from the surface of the ground to the cable axis [mm]

$D_e$  is the external diameter of the cable [mm] for corrugated sheaths

$$D_e = D_{oc} + 2 t_3$$

## B An example of a Newton-Raphson power flow analysis

This appendix is inspired by [53–56] to explain how a Newton-Raphson power flow analysis is done. The first step in a power flow analysis is to set up an admittance matrix over the system. To explain the procedure an example will be used. The example is a downscaled system of the system analysed in this project. As can be seen in Fig.B.1 the example consists of two generator buses, one load bus and one slack bus. The slack bus represents the main grid which can be modelled as an infinite grid with constant voltage.

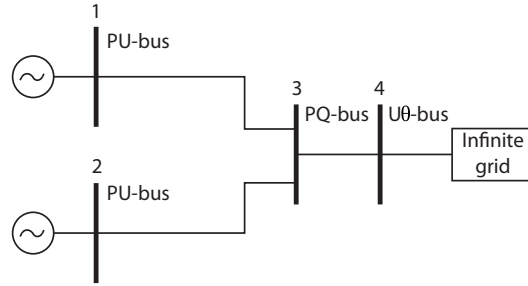


Figure B.1: The system which is calculated in the example where bus one and two are PU-buses, bus 3 is a PQ-bus and bus 4 is a U-bus.

Kirchhoff's current law is used at all buses according to (B.1) to (B.4) with the systems admittances expressed in per unit.

$$I_1 = Y_{13}(U_1 - U_3) = Y_{13} * U_1 + 0 * U_2 - Y_{13} * U_3 + 0 * U_4 \quad (\text{B.1})$$

$$I_2 = Y_{23}(U_2 - U_3) = 0 * U_1 + Y_{23} * U_2 - Y_{23} * U_3 + 0 * U_4 \quad (\text{B.2})$$

$$0 = Y_{13}(U_3 - U_1) + Y_{23}(U_3 - U_2) + Y_{34}(U_3 - U_4) = -Y_{13} * U_1 - Y_{23} * U_2 + (Y_{13} + Y_{23} + Y_{34}) * U_3 - Y_{34} * U_4 \quad (\text{B.3})$$

$$0 = Y_{34}(U_4 - U_3) = 0 * U_1 + 0 * U_2 - Y_{34} * U_3 + Y_{34} * U_4 \quad (\text{B.4})$$

The equations are written as a matrix in the form  $I = Y * U$  where Y is the admittance

matrix as can be seen in (B.5).

$$\begin{bmatrix} I_1 \\ I_2 \\ 0 \\ 0 \end{bmatrix} = \begin{bmatrix} Y_{13} & 0 & -Y_{13} & 0 \\ 0 & U_{23} & -Y_{23} & 0 \\ -Y_{13} & -Y_{23} & Y_{13} + Y_{23} + Y_{34} & -Y_{34} \\ 0 & 0 & -Y_{34} & Y_{34} \end{bmatrix} * \begin{bmatrix} U_1 \\ U_2 \\ U_3 \\ U_4 \end{bmatrix} \quad (\text{B.5})$$

The admittance matrix is used in ohms model to express the current in each bus as in (B.6). Equation (B.6) can be rewritten into polar form as in (B.7).

$$I_i = \sum_{j=1}^n Y_{ij} U_j \quad (\text{B.6})$$

$$I_i = \sum_{j=1}^n |Y_{ij}| |U_j| \angle(\Psi_{ij} + \delta_j) \quad (\text{B.7})$$

The power flow in the system can be expressed according to (B.8) which can be rewritten into (B.9) and (B.10) using the expression for the current.

$$P_i - jQ_i = U_i * I_i^* \quad (\text{B.8})$$

$$\begin{aligned} P_i &= |U_i| \angle -\delta_i * \sum_{j=1}^n |U_j| |Y_{ij}| \angle(\Psi_{ij} + \delta_j) = \\ &\sum_{j=1}^n |U_i| |U_j| |Y_{ij}| \cos(\Psi_{ij} - \delta_i + \delta_j) \end{aligned} \quad (\text{B.9})$$

$$\begin{aligned} Q_i &= |U_i| \angle -\delta_i * \sum_{j=1}^n |U_j| |Y_{ij}| \angle(\Psi_{ij} + \delta_j) = \\ &\sum_{j=1}^n |U_i| |U_j| |Y_{ij}| \sin(\Psi_{ij} - \delta_i + \delta_j) \end{aligned} \quad (\text{B.10})$$

Equation (B.9) and (B.10) are two non-linear functions which can be expressed in a matrix form, using a Taylor's series where all higher order terms are neglected, as in

(B.11).

$$\begin{bmatrix} \Delta P_1 \\ \Delta P_2 \\ \Delta P_3 \\ \Delta P_4 \\ \Delta Q_1 \\ \Delta Q_2 \\ \Delta Q_3 \\ \Delta Q_4 \end{bmatrix} = \begin{bmatrix} \frac{\delta P_1}{\delta \Psi_1} & \frac{\delta P_1}{\delta \Psi_2} & \frac{\delta P_1}{\delta \Psi_3} & \frac{\delta P_1}{\delta \Psi_4} & \frac{\delta P_1}{\delta |U_1|} & \frac{\delta P_1}{\delta |U_2|} & \frac{\delta P_1}{\delta |U_3|} & \frac{\delta P_1}{\delta |U_4|} \\ \frac{\delta P_2}{\delta \Psi_1} & \frac{\delta P_2}{\delta \Psi_2} & \frac{\delta P_2}{\delta \Psi_3} & \frac{\delta P_2}{\delta \Psi_4} & \frac{\delta P_2}{\delta |U_1|} & \frac{\delta P_2}{\delta |U_2|} & \frac{\delta P_2}{\delta |U_3|} & \frac{\delta P_2}{\delta |U_4|} \\ \frac{\delta P_3}{\delta \Psi_1} & \frac{\delta P_3}{\delta \Psi_2} & \frac{\delta P_3}{\delta \Psi_3} & \frac{\delta P_3}{\delta \Psi_4} & \frac{\delta P_3}{\delta |U_1|} & \frac{\delta P_3}{\delta |U_2|} & \frac{\delta P_3}{\delta |U_3|} & \frac{\delta P_3}{\delta |U_4|} \\ \frac{\delta P_4}{\delta \Psi_1} & \frac{\delta P_4}{\delta \Psi_2} & \frac{\delta P_4}{\delta \Psi_3} & \frac{\delta P_4}{\delta \Psi_4} & \frac{\delta P_4}{\delta |U_1|} & \frac{\delta P_4}{\delta |U_2|} & \frac{\delta P_4}{\delta |U_3|} & \frac{\delta P_4}{\delta |U_4|} \\ \frac{\delta Q_1}{\delta \Psi_1} & \frac{\delta Q_1}{\delta \Psi_2} & \frac{\delta Q_1}{\delta \Psi_3} & \frac{\delta Q_1}{\delta \Psi_4} & \frac{\delta Q_1}{\delta |U_1|} & \frac{\delta Q_1}{\delta |U_2|} & \frac{\delta Q_1}{\delta |U_3|} & \frac{\delta Q_1}{\delta |U_4|} \\ \frac{\delta Q_2}{\delta \Psi_1} & \frac{\delta Q_2}{\delta \Psi_2} & \frac{\delta Q_2}{\delta \Psi_3} & \frac{\delta Q_2}{\delta \Psi_4} & \frac{\delta Q_2}{\delta |U_1|} & \frac{\delta Q_2}{\delta |U_2|} & \frac{\delta Q_2}{\delta |U_3|} & \frac{\delta Q_2}{\delta |U_4|} \\ \frac{\delta Q_3}{\delta \Psi_1} & \frac{\delta Q_3}{\delta \Psi_2} & \frac{\delta Q_3}{\delta \Psi_3} & \frac{\delta Q_3}{\delta \Psi_4} & \frac{\delta Q_3}{\delta |U_1|} & \frac{\delta Q_3}{\delta |U_2|} & \frac{\delta Q_3}{\delta |U_3|} & \frac{\delta Q_3}{\delta |U_4|} \\ \frac{\delta Q_4}{\delta \Psi_1} & \frac{\delta Q_4}{\delta \Psi_2} & \frac{\delta Q_4}{\delta \Psi_3} & \frac{\delta Q_4}{\delta \Psi_4} & \frac{\delta Q_4}{\delta |U_1|} & \frac{\delta Q_4}{\delta |U_2|} & \frac{\delta Q_4}{\delta |U_3|} & \frac{\delta Q_4}{\delta |U_4|} \end{bmatrix} * \begin{bmatrix} \Delta \Psi_1 \\ \Delta \Psi_2 \\ \Delta \Psi_3 \\ \Delta \Psi_4 \\ \Delta |U_1| \\ \Delta |U_2| \\ \Delta |U_3| \\ \Delta |U_4| \end{bmatrix} \quad (\text{B.11})$$

A few simplifications of (B.11) can be made using the slack bus and the generator buses. Since the voltage magnitude,  $\Delta|U_4|$ , and the angle,  $\Delta\Psi_4$ , at the slack bus are known, the columns containing these variables can be removed. Also all the rows containing the power,  $\Delta P_4$  and  $\Delta Q_4$ , can be removed since these can be calculated later when all the voltage magnitudes and angles are known using (B.9) and (B.10). The columns containing the voltage magnitude of the generator buses,  $\Delta|U_1|$  and  $\Delta|U_2|$ , can be removed since they are also known as well as the rows containing the reactive power of the generator buses,  $\Delta Q_1$  and  $\Delta Q_2$  which can be calculated later. The simplification of (B.11) is presented in (B.12).

$$\begin{bmatrix} \Delta P_1 \\ \Delta P_2 \\ \Delta P_3 \\ \Delta Q_3 \end{bmatrix} = \begin{bmatrix} \frac{\delta P_1}{\delta \Psi_1} & \frac{\delta P_1}{\delta \Psi_2} & \frac{\delta P_1}{\delta \Psi_3} & \frac{\delta P_1}{\delta |U_3|} \\ \frac{\delta P_2}{\delta \Psi_1} & \frac{\delta P_2}{\delta \Psi_2} & \frac{\delta P_2}{\delta \Psi_3} & \frac{\delta P_2}{\delta |U_3|} \\ \frac{\delta P_3}{\delta \Psi_1} & \frac{\delta P_3}{\delta \Psi_2} & \frac{\delta P_3}{\delta \Psi_3} & \frac{\delta P_3}{\delta |U_3|} \\ \frac{\delta Q_3}{\delta \Psi_1} & \frac{\delta Q_3}{\delta \Psi_2} & \frac{\delta Q_3}{\delta \Psi_3} & \frac{\delta Q_3}{\delta |U_3|} \end{bmatrix} * \begin{bmatrix} \Delta \Psi_1 \\ \Delta \Psi_2 \\ \Delta \Psi_3 \\ \Delta |U_3| \end{bmatrix} \quad (\text{B.12})$$

$$[\text{Power mismatches}] = [\text{Jacobian matrix}] * [\text{Errors in } |U| \text{ and } \Psi]$$

The power mismatch matrix in (B.12) represents the difference between the given and the calculated power at the buses. The Jacobian matrix contains the derivatives of the power flow equations (B.9) and (B.10). The last matrix contains the errors of the voltage magnitudes and angles.

The next step is to calculate the unknowns in the matrix which are  $\Delta\Psi_1$ ,  $\Delta\Psi_2$ ,  $\Delta\Psi_3$ ,  $\Delta|U_3|$ . These variables need a first estimation to be able to perform the calculations and the estimates are usually put to the same value as the slack bus. In Table B.1 all the known and estimated variables are presented for this example.

The first element in all the matrices in (B.12) will be derived to show the process of the calculations. The power mismatch is calculated in (B.13) using (B.9) and (B.10).

Table B.1: Known and estimated parameters

	Bus 1	Bus 2	Bus 3	Bus 4
Known:	$P_1$	$P_2$	$P_3$	$\Psi_4$
	$\Delta U_1 $	$\Delta U_2 $	$Q_3$	$\Delta U_4 $
Estimated:	$\Psi_1 = 0$	$\Psi_2 = 0$	$\Psi_4 = 0$	-
	-	-	$ U_3  = 1$	-

$$\begin{aligned}
\Delta P_1 &= P_{1(given)} - P_{1(calculated)}^0 \\
&= P_{1(given)} - \sum_{j=1}^4 |U_1||U_j||Y_{1j}|\cos(\Psi_{1j} - \delta_1 + \delta_j) \\
&= P_{1(given)} - |U_1|^2|Y_{11}|\cos(\Psi_{11} - \delta_1 + \delta_1) \\
&\quad - |U_1||U_2||Y_{12}|\cos(\Psi_{12} - \delta_1 + \delta_2) \\
&\quad - |U_1||U_3||Y_{13}|\cos(\Psi_{13} - \delta_1 + \delta_3) \\
&\quad - |U_1||U_4||Y_{14}|\cos(\Psi_{14} - \delta_1 + \delta_4)
\end{aligned} \tag{B.13}$$

The Jacobian matrix is calculated by derivation of (B.9) and (B.10) and first element is derived in (B.14).

$$\begin{aligned}
&\frac{\delta P_1}{\delta \Psi_1} \left( P_{1,calculated}^0 \right) \\
&+ |U_1||U_2||Y_{12}|\cos(\Psi_{12} - \delta_1 + \delta_2) \\
&+ |U_1||U_3||Y_{13}|\cos(\Psi_{13} - \delta_1 + \delta_3) \\
&+ |U_1||U_4||Y_{14}|\cos(\Psi_{14} - \delta_1 + \delta_4) \\
&= |U_1||U_2||Y_{12}|\sin(\Psi_{12} - \delta_1 + \delta_2) \\
&+ |U_1||U_3||Y_{13}|\sin(\Psi_{13} - \delta_1 + \delta_3) \\
&+ |U_1||U_4||Y_{14}|\sin(\Psi_{14} - \delta_1 + \delta_4)
\end{aligned} \tag{B.14}$$

With the power mismatch and Jacobian matrix a first estimated error of the voltage magnitude and angle can be calculated using (B.15).

$$\begin{bmatrix} \Delta \Psi_1 \\ \Delta \Psi_2 \\ \Delta \Psi_3 \\ \Delta |U_3| \end{bmatrix} = \begin{bmatrix} \frac{\delta P_1}{\delta \Psi_1} & \frac{\delta P_1}{\delta \Psi_2} & \frac{\delta P_1}{\delta \Psi_3} & \frac{\delta P_1}{\delta |U_3|} \\ \frac{\delta P_2}{\delta \Psi_1} & \frac{\delta P_2}{\delta \Psi_2} & \frac{\delta P_2}{\delta \Psi_3} & \frac{\delta P_2}{\delta |U_3|} \\ \frac{\delta P_3}{\delta \Psi_1} & \frac{\delta P_3}{\delta \Psi_2} & \frac{\delta P_3}{\delta \Psi_3} & \frac{\delta P_3}{\delta |U_3|} \\ \frac{\delta Q_3}{\delta \Psi_1} & \frac{\delta Q_3}{\delta \Psi_2} & \frac{\delta Q_3}{\delta \Psi_3} & \frac{\delta Q_3}{\delta |U_3|} \end{bmatrix}^{-1} * \begin{bmatrix} \Delta P_1 \\ \Delta P_2 \\ \Delta P_3 \\ \Delta Q_3 \end{bmatrix} \tag{B.15}$$

A new estimate of the voltage magnitudes and angles,  $\Delta\Psi_1, \Delta\Psi_2, \Delta\Psi_3, \Delta|U_3|$ , are calculated using (B.16).

$$\begin{bmatrix} \Psi_1^1 \\ \Psi_2^1 \\ \Psi_3^1 \\ |U_3|^1 \end{bmatrix} = \begin{bmatrix} \Psi_1^0 \\ \Psi_2^0 \\ \Psi_3^0 \\ |U_3|^0 \end{bmatrix} * \begin{bmatrix} \Delta\Psi_1^0 \\ \Delta\Psi_2^0 \\ \Delta\Psi_3^0 \\ \Delta|U_3|^0 \end{bmatrix} \quad (\text{B.16})$$

The next step is to calculate new power mismatch and a Jacobian matrix using the new estimates,  $\Psi_1^1, \Psi_2^1, \Psi_3^1, |U_3|^1$ , in (B.13) and (B.14). The iterations are repeated until a satisfied level of error in the estimates are reached. Finally the variables which were neglected from (B.11) can be calculated with (B.9) and (B.10).

## C Enlargement of the 25 Deep Green star circuit

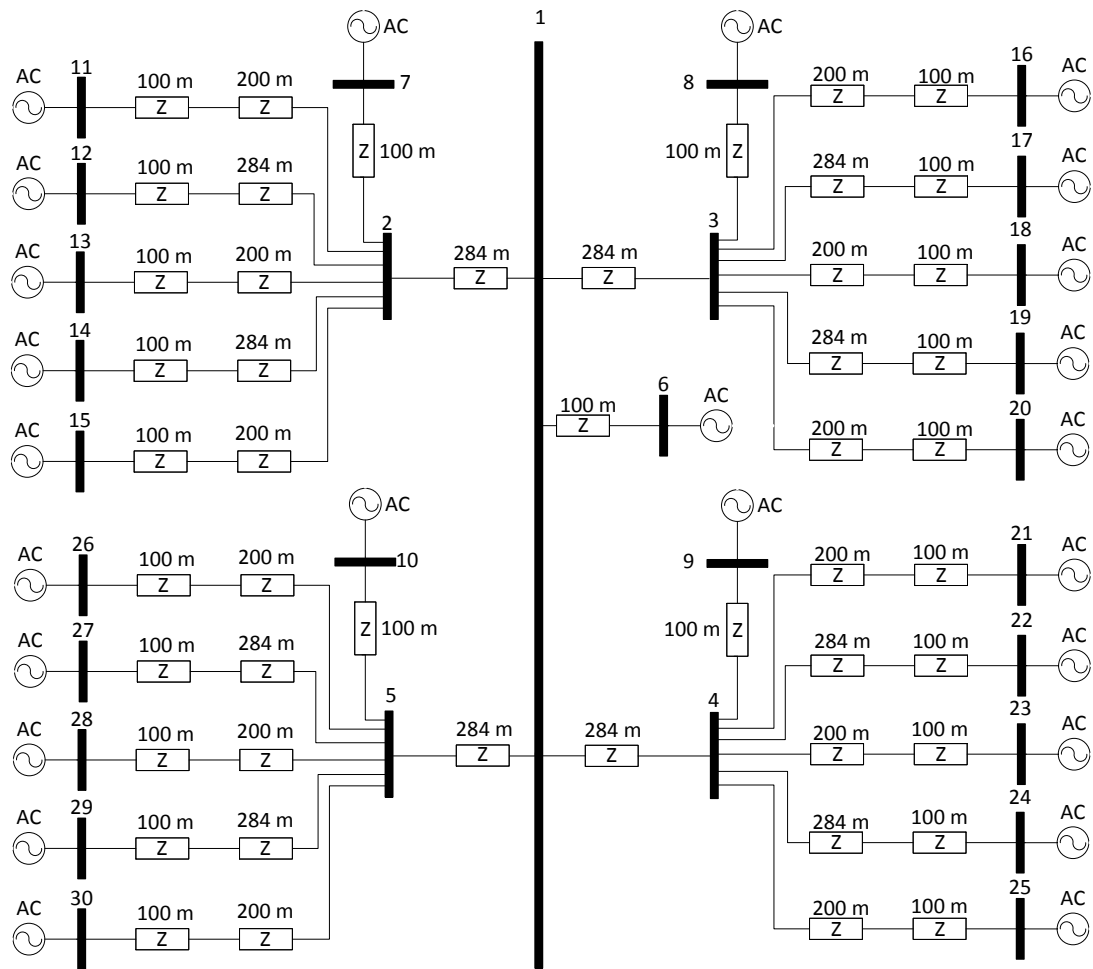


Figure C.1: Circuit of 25 Deep Green generating units in the selected star connection.

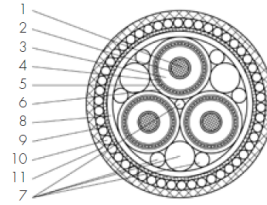
# D Cable data sheets

## Cable Data XLPE

These constructional and electrical data are values of typical submarine cables up to 36 kV (Standard IEC), with radial and longitudinal water barrier.

- 1 Conductor
- 2 Conductor screening
- 3 XLPE insulation

- 4 Insulation screening
- 5 Metal screen and sealing
- 6 Laminated core sheath
- 7 Fillers, FO cables
- 8 Binder tapes
- 9 Bedding
- 10 Armour
- 11 Serving



### Legend for tables

#### Constructional Data

- 1, 2, 3, 4, 5, 6, 7, 8 – Nominal values
- 9, 10, 11 – Approx. values

#### Electrical Data

- 1 – Nominal value
- 2 – Max. value to IEC 60228
- 3, 4, 5, 6, 9 – Approx. values
- 7 – Calculated in accordance to IEC publications 60287 and the following assumptions
  - Max. conductor temperature at continuous load 90°C
  - Frequency 50 Hz
  - Max. ambient temperature 20°C
  - Screens bonded at both ends and connected to earth
  - burial depth of cables 1.0 m
  - Thermal resistivity of surroundings 1.0 K·m/W
  - at current acc. to 7
- 8

### Constructional Data, Electrical Data

#### 2XS2YRAA 6/10(12) kV

#### Constructional Data

1	2	3	4	6		7	8	9	10	11
Nominal cross sectional area of conductor	Conductor copper round stranded diameter over conductor	Insulation XLPE wall thickness	Screen copper wires and counter helix cross sectional area	Core sheath PE black wall thickness	Core sheath PE black diameter	Bedding wall thickness	Armour steel wires round galvanized diameter	Serving bitumen fib. material and lime wash wall thickness	Outer diameter of cable	Cable weight
(mm <sup>2</sup> )	(mm)	(mm)	(mm <sup>2</sup> )	(mm)	(mm)	(mm)	(mm)	(mm)	(mm)	(t/km)
35	7.0	3.4	16	2.5	22	2	3.15	3.5	65	6.3
50	8.2	3.4	16	2.5	23	2	3.15	3.5	68	7.0
70	9.9	3.4	16	2.5	25	2	4.0	3.5	72	8.8
95	11.5	3.4	16	2.5	26	2	4.0	3.5	76	10.0
120	13.0	3.4	16	2.5	28	2	4.0	3.5	79	11.2
150	14.5	3.4	25	2.5	29	2	4.0	3.5	82	12.3
185	16.1	3.4	25	2.5	31	2	5.0	4.0	89	15.5
240	18.6	3.4	25	2.5	33	2	5.0	4.0	94	17.8

#### 2XS2YRAA 6/10(12) kV

#### Electrical Data

1		2	3	4	5	6	7	8	9	
Nominal cross sectional area		Conductor resistance DC 20°C	Conductor resistance AC 90°C	Screen resistance 20°C	Capacitance	Inductance	Current rating	Losses	1s short circuit current after full load at 90°C conductor temperature	
conductor (mm <sup>2</sup> )	screen (mm <sup>2</sup> )	(Ω/km)	(Ω/km)	(Ω/km)	(μF/km)	(mH/km)	(A)	(W/m)	conductor (kA)	screen (kA)
35	16	0.524	0.67	1.15	0.23	0.41	166	56	5.0	0.72
50	16	0.387	0.49	1.15	0.26	0.39	196	58	7.1	0.72
70	16	0.268	0.34	1.15	0.29	0.37	240	61	10.0	0.98
95	16	0.193	0.25	1.15	0.32	0.35	287	63	13.6	0.98
120	16	0.153	0.20	1.15	0.35	0.34	325	65	17.1	0.98
150	25	0.124	0.16	0.73	0.38	0.33	364	66	21.4	1.1
185	25	0.0991	0.13	0.73	0.42	0.32	408	68	26.5	1.1
240	25	0.0754	0.10	0.73	0.47	0.30	471	72	34.3	1.1

Figure D.1: Electrical and physical data for a 10 kV submarine cable from Nexans [57].

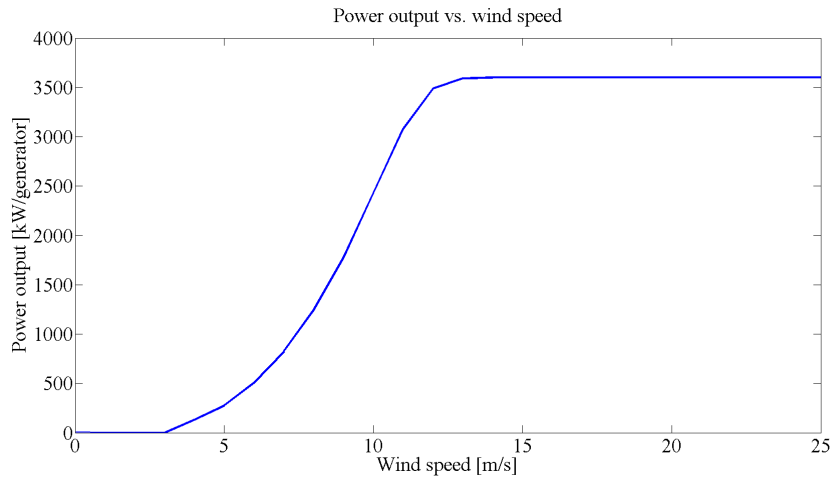


Figure D.2: Power curve for Siemens SWT-3.6-107 used in Gwynt y Môr [59]

**Table 1.** Insulation Thickness of XLPE or EPR/HEPR insulation

Nom. Cross Section Area mm <sup>2</sup>	Insulation Thickness at Nom. Voltage									
	1.8/3KV (Um=3.6)KV	3.6/6KV (Um=7.2)KV			6/10KV (Um=12KV)	8.7/15KV (Um=17KV)	12/20KV (Um=24KV)	18/30KV (Um=36KV)	21/35KV (Um=42KV)	26/35KV (Um=42KV)
	mm	mm		mm	mm	mm	mm	mm	mm	mm
	XLPE/EPR	XLPE	EPR		XLPE/EPR	XLPE/EPR	XLPE/EPR	XLPE/EPR	XLPE/EPR	XLPE/EPR
			Unscreened	Screened						
10	2.0	2.5	3.0	2.5	-	-	-	-	-	-
16	2.0	2.5	3.0	2.5	3.4	-	-	-	-	-
25	2.0	2.5	3.0	2.5	3.4	4.5	-	-	-	-
35	2.0	2.5	3.0	2.5	3.4	4.5	5.5	-	-	-
50 – 185	2.0	2.5	3.0	2.5	3.4	4.5	5.5	8.0	9.3	10.5
240	2.0	2.6	3.0	2.6	3.4	4.5	5.5	8.0	9.3	10.5
300	2.0	2.8	3.0	2.8	3.4	4.5	5.5	8.0	9.3	10.5
400	2.0	3.0	3.0	3.0	3.4	4.5	5.5	8.0	9.3	10.5
500 - 1600	2.2-2.8	3.2	3.2	3.2	3.4	4.5	5.5	8.0	9.3	10.5

Figure D.3: Isolation thickness for different voltages from Caledonian [58].

Three Core 1.8/3KV (Um=3.6KV)  
Dimensional Data

Nom. Cross-Section Area	Nom. Insulation Thickness	Copper Tape Thickness	Copper Wire Screen Area*	Unarmoured Cables				Steel Round-Wire Armoured Cables					
				Nom. Sheath Thickness	Approx. Overall Diameter	Approx. Weight		Nom. Bedding Thickness	Armour Wire Size	Nom. Sheath Thickness	Approx. Overall Diameter	Approx. Weight	
						CU	AL					kg/km	CU
mm <sup>2</sup>	mm	mm	mm <sup>2</sup>	mm	mm	kg/km		mm	mm	mm	mm	kg/km	
10	2.0	0.1	16	1.8	23	650	460	1.2	1.6	1.8	28	1480	1290
16	2.0	0.1	16	1.8	24	840	540	1.2	1.6	1.9	29	1720	1410
25	2.0	0.1	16	1.8	26	1160	680	1.2	1.6	1.9	32	2130	1650
35	2.0	0.1	16	1.8	29	1490	820	1.2	2.0	2.1	36	2810	2140
50	2.0	0.1	16	1.9	32	1900	1000	1.2	2.0	2.2	39	3340	2450
70	2.0	0.1	16	2.0	36	2580	1290	1.2	2.0	2.3	42	4200	2910
95	2.0	0.1	16	2.2	40	3440	1640	1.3	2.5	2.4	47	5620	3820
120	2.0	0.1	16	2.3	43	4220	1950	1.3	2.5	2.5	51	6580	4310
150	2.0	0.1	25	2.4	46	5090	2290	1.4	2.5	2.7	54	7680	4870
185	2.0	0.1	25	2.5	50	6240	2730	1.5	2.5	2.8	58	9060	5560
240	2.0	0.1	25	2.7	56	8030	3430	1.6	2.5	3.0	64	11200	6600
300	2.0	0.1	25	2.8	60	9890	4100	1.6	2.5	3.1	69	13590	7500
400	2.0	0.1	35	3.1	68	12530	5150	1.8	3.15	3.4	78	17260	9880
500	2.2	0.1	35	3.3	75.7	16680	7510	1.8	3.15	3.5	84.3	21780	13025
630	2.4	0.1	35	3.5	84.9	21770	10040	1.8	3.15	3.8	94.6	27400	16050

\*Optional wire screen can be provided in combination of copper tapes. Nominal screen area, as stated in the table, can be supplied as standard.

Electrical Data

Nom. Cross-Section Area	D C Resistance CU / AL	A C Resistance CU / AL	Short Circuit Rating of Conductor CU / AL 1 sec	Capacitance	Charging Current	Short Circuit Rating of Copper Wire Screen Per Core 1 sec	Short Circuit Rating of Copper Tape Screen Per Core 1 sec	Reactance	Inductance
mm <sup>2</sup>	μΩ/m	μΩ/m	kA	pF/m	mA/m	kA	kA	μΩ/m	nH/m
10	1830/3080	2330/3920	1.4/0.9	160	0.25	2.6	0.4	101	390
16	1150/1910	1460/2420	2.2/1.4	180	0.27	2.6	0.4	98	370
25	727/1200	929/1538	3.6/2.3	220	0.29	2.6	0.4	95	350
35	524/868	668/1113	5.0/3.2	250	0.31	2.6	0.5	92	330
50	387/641	494/822	6.8/4.4	270	0.33	2.6	0.5	88	310
70	268/443	343/568	9.8/6.3	310	0.35	2.6	0.6	84	290
95	193/320	248/410	13.3/8.5	350	0.38	2.6	0.6	81	270
120	153/253	196/325	17.2/11.0	380	0.46	2.6	0.7	79	250
150	124/206	159/265	21.2/13.5	420	0.50	2.6	0.7	77	260
185	99.1/164	128/211	26.6/17.0	460	0.56	2.6	0.8	76	250
240	75.4/125	98/161	34.9/22.3	510	0.61	4.3	0.9	74	240
300	60.1/100	80/130	43.8/28.0	570	0.68	4.3	1.0	73	250
400	47.0/77.8	64/102	57.3/36.6	590	0.70	5.8	1.1	71	240
500	36.6/60.5	57/81	72.3/46.2	610	0.72	5.8	1.2	69	230
630	28.3/46.9	42/64	91.2/58.3	630	0.74	5.8	1.3	67	220

Figure D.4: Electrical and physical data for a 3 kV submarine cable from Caledonian [58].

Three Core 3.8/6.6KV (Um=7.2KV)  
Dimensional Data

Nom. Cross-Section Area	Nom. Insulation Thickness	Copper Tape Thickness	Copper Wire Screen Area*	Unarmoured Cables				Steel Round-Wire Armoured Cables					
				Nom. Sheath Thickness	Approx. Overall Diameter	Approx. Weight		Nom. Bedding Thickness	Armour Wire Size	Nom. Sheath Thickness	Approx. Overall Diameter	Approx. Weight	
						CU	AL					CU	AL
mm <sup>2</sup>	mm	mm	mm <sup>2</sup>	mm	mm	kg/km		mm	mm	mm	mm	kg/km	
10	2.5	0.1	16	2.0	30	980	790	1.2	2.0	2.1	36	2310	1210
16	2.5	0.1	16	2.0	31	1190	890	1.2	2.0	2.2	38	2600	2290
25	2.5	0.1	16	2.1	34	1560	1080	1.2	2.0	2.3	41	3080	2600
35	2.5	0.1	16	2.2	37	1930	1270	1.3	2.5	2.4	45	3950	3280
50	2.5	0.1	16	2.3	40	2370	1480	1.3	2.5	2.5	47	4530	3630
70	2.5	0.1	16	2.4	43	3110	1820	1.4	2.5	2.6	51	5510	4210
95	2.5	0.1	16	2.5	47	4000	2200	1.5	2.5	2.8	55	6660	4860
120	2.5	0.1	16	2.6	50	4820	2550	1.5	2.5	2.9	59	7630	5360
150	2.5	0.1	25	2.8	54	5770	2970	1.6	2.5	3.0	62	8800	6000
185	2.5	0.1	25	2.9	58	6960	3460	1.6	2.5	3.1	66	10180	6670
240	2.6	0.1	25	3.1	65	8940	4340	1.8	3.15	3.4	75	13480	8870
300	2.8	0.1	25	3.3	70	10980	5190	1.9	3.15	3.6	81	15920	10130
400	3.0	0.1	35	3.5	79	13820	6440	2.0	3.5	3.9	90	19980	12590
500	3.2	0.1	35	3.7	87	19100	10755	2.1	3.5	4.1	98	24160	14820
630	3.2	0.1	35	4.0	95	30470	13150	2.2	3.5	4.4	107	29650	17710

\*Optional wire screen can be provided in combination of copper tapes. Nominal screen area, as stated in the table, can be supplied as standard.

Electrical Data

Nom. Cross-Section Area	D C Resistance CU / AL	A C Resistance CU / AL	Short Circuit Rating of Conductor CU / AL 1 sec	Capacitance	Charging Current	Short Circuit Rating of Copper Wire Screen Per Core 1 sec	Short Circuit Rating of Copper Tape Screen Per Core 1 sec	Reactance	Inductance
mm <sup>2</sup>	μΩ/m	μΩ/m	kA	pF/m	mA/m	kA	kA	μΩ/m	nH/m
10	1830/3080	2330/3920	1.4/0.9	212	0.27	2.6	0.4	132	410
16	1150/1910	1470/2420	2.2/1.4	242	0.30	2.6	0.4	124	390
25	727/1200	927/1538	3.6/2.3	272	0.33	2.6	0.4	116	370
35	524/868	668/1113	5.0/3.2	301	0.36	2.6	0.5	108	350
50	387/641	494/822	6.8/4.4	332	0.40	2.6	0.5	102	330
70	268/443	343/568	9.8/6.3	383	0.46	2.6	0.6	97	310
95	193/320	248/410	13.3/8.5	432	0.52	2.6	0.6	92	290
120	153/253	196/325	17.2/11.0	474	0.57	2.6	0.7	89	280
150	124/206	159/265	21.2/13.5	511	0.61	4.3	0.7	87	280
185	99.1/164	128/211	26.6/17.0	562	0.67	4.3	0.8	86	270
240	75.4/125	98/161	34.9/22.3	602	0.72	4.3	0.9	83	260
300	60.1/100	80/130	43.8/28.0	622	0.75	4.3	1.0	82	260
400	47.0/77.8	64/102	57.3/36.6	648	0.78	5.8	1.1	80	250
500	36.6/60.5	51/81	72.3/46.2	668	0.82	5.8	1.2	78	250
630	28.3/46.9	42/64	91.2/58.3	758	0.92	5.8	1.3	76	240

Figure D.5: Electrical and physical data for a 6.6 kV submarine cable from Caledonian [58].

# TECHNICAL DATA FOR XLPE SUBMARINE CABLE SYSTEMS

## Three-core cables with lead sheath

Cross-section of conductor	Diameter of conductor	Insulation thickness	Diameter over insulation	Lead sheath thickness	Outer diameter of cable	Cable weight (Aluminium)	Cable weight (Copper)	Capacitance	Charging current per phase at 50 Hz	Inductance
mm <sup>2</sup>	mm	mm	mm	mm	mm	kg/m	kg/m	μF/km	A/km	mH/km

Table 44

Three-core cables, nominal voltage 45 kV (Um = 52 kV)										
95	11.2	8.0	29.6	1.3	109.0	19.1	20.8	0.18	1.5	0.43
120	12.6	8.0	31.0	1.3	112.0	20.0	22.3	0.19	1.6	0.42
150	14.2	8.0	32.6	1.4	116.0	21.6	24.4	0.21	1.6	0.40
185	15.8	8.0	34.2	1.4	119.0	22.7	26.2	0.22	1.8	0.39
240	18.1	8.0	36.5	1.5	124.0	25.0	29.5	0.24	2.0	0.37
300	20.4	8.0	38.8	1.6	130.0	27.3	32.9	0.26	2.2	0.36
400	23.2	8.0	41.6	1.7	136.0	30.4	37.9	0.29	2.3	0.35
500	26.2	8.0	45.0	1.8	144.0	33.8	43.2	0.32	2.6	0.33
630	29.8	8.0	48.6	1.9	152.0	37.8	49.7	0.35	2.9	0.32
800	33.7	8.0	52.5	2.1	162.0	43.5	58.6	0.38	3.1	0.31
1000	37.9	8.0	57.3	2.2	173.0	49.3	68.1	0.42	3.5	0.30

Table 45

Three-core cables, nominal voltage 66 kV (Um = 72.5 kV)										
95	11.2	9.0	31.6	1.3	113.0	19.8	21.6	0.17	2.0	0.44
120	12.6	9.0	33.0	1.4	116.0	21.6	23.8	0.18	2.1	0.43
150	14.2	9.0	34.6	1.4	120.0	22.9	25.7	0.19	2.3	0.41
185	15.8	9.0	36.2	1.4	124.0	24.5	28.0	0.20	2.4	0.40
240	18.1	9.0	38.5	1.6	129.0	26.8	31.3	0.22	2.6	0.38
300	20.4	9.0	40.8	1.6	134.0	28.7	34.3	0.24	2.8	0.37
400	23.2	9.0	43.6	1.7	141.0	31.7	39.2	0.26	3.1	0.35
500	26.2	9.0	47.0	1.9	149.0	36.0	45.4	0.29	3.5	0.34
630	29.8	9.0	50.6	2.0	157.0	40.1	52.0	0.32	3.7	0.33
800	33.7	9.0	54.5	2.1	167.0	45.1	60.1	0.35	4.1	0.32
1000	37.9	9.0	59.3	2.3	178.0	51.8	70.7	0.38	4.6	0.31

Table 46

Three-core cables, nominal voltage 110 kV (Um = 123 kV)										
185	15.8	16.0	50.2	2.0	156.0	37.4	40.9	0.14	2.8	0.46
240	18.1	15.0	50.5	2.0	157.0	38.0	42.5	0.15	3.0	0.43
300	20.4	14.0	50.8	2.0	157.0	38.5	44.1	0.17	3.5	0.41
400	23.2	13.0	51.6	2.0	159.0	39.7	47.2	0.20	3.9	0.38
500	26.2	13.0	55.0	2.1	167.0	43.6	53.0	0.22	4.3	0.37
630	29.8	13.0	58.6	2.3	176.0	48.8	60.7	0.24	4.7	0.36
800	33.7	13.0	62.5	2.4	185.0	54.4	69.5	0.26	5.2	0.34
1000	37.9	13.0	67.3	2.6	197.0	61.6	80.5	0.28	5.6	0.33

Figure D.6: High voltage cable from ABB used for calculations for transmission cables [60]

Technical data								
AKKJ 1kV								
Conductors x size (mm <sup>2</sup> )	Diameter, nominal (mm)			Weight/100m (kg)	Minimum bending radius (mm)	Maximum pulling force (kN)	Resistance (ohm/km)	
	Conductor	Insulation	Sheath				Conductor	Screen
3 x 50/15	7,8	10,7	29	105	232	4,2	0,641	1,200
3 x 70/21			30	135	240	4,5	0,443	0,868
3 x 95/29			35	180	280	6,1	0,320	0,641
3 x 120/41			38	220	204	7,2	0,253	0,443
3 x 150/41			42	265	336	8,8	0,206	0,443
3 x 185/57			47	320	376	11,0	0,164	0,320
3 x 240/72			51	420	408	13,0	0,125	0,253

Figure D.7: Specifications for the 1 kV cable from Ericsson [61]. Observe that the cable used is the three conductor cable.

**Tabell 39. Induktans och driftskapacitans för 1 kV 3- och 4-ledarkabel.**

	Ledararea mm <sup>2</sup>													
	2,5	4	6	10	16	25	35	50	70	95	120	150	185	240
Induktans mH/km	0,32	0,32	0,30	0,29	0,27	0,25	0,24	0,24	0,24	0,24	0,23	0,22	0,22	0,22
Driftskapacitans µF/km	0,24	0,27	0,29	0,32	0,36	0,41	0,45	0,50	0,54	0,56	0,57	0,58	0,59	0,60

Figure D.8: Inductance and capacitance for Ericsson cable 1 kV [62]

## E Calculation of cable temperature using IEC 60287

This appendix will go through all the calculations and assumptions that have been made to be able to calculate the cable temperature by using (A.1) from IEC 60287. The cable type that have been studied is a 10 kV cable from Nexans with conductor area between 35-240 mm<sup>2</sup>. Detailed cable information is found in appendix D in Fig.D.1. The following calculations is done for the cable of size 240 mm<sup>2</sup>, with all needed data taken from Fig.D.1, the same approach have been used for all the different cable sizes.

The dielectric loss per unit length in each phase is given by:

$$W_d = \omega C U_0^2 \tan \delta = 2\pi 50 \cdot 0.47 \cdot 10^{-9} \cdot \left( \frac{10000}{\sqrt{3}} \right)^2 \cdot 2 \cdot 10^{-4} = 9.84 \cdot 10^{-4} \quad [W/m] \quad (\text{E.1})$$

where

$$\begin{aligned} \omega &= 2\pi f \\ C &\text{ is the capacitance per unit length [F/m]} \\ U_0 &\text{ is the voltage to earth [V].} \end{aligned}$$

The total power loss in the conductor is given by

$$R_s = R_{s0} [1 + \alpha_{20} (\theta_{SC} - 20)] = 0.73 \cdot 10^{-3} [1 + 3.93 \cdot 10^{-3} (90 - 20)] = 9.31 \cdot 10^{-4} \quad [\Omega/m] \quad (\text{E.2})$$

where

$$\begin{aligned} R_{s0} &\text{ is the resistance of the cable sheath or screen at } 20 \text{ }^\circ\text{C} [\Omega/m]. \\ \alpha_{20} &\text{ is the constant mass temperature coefficient for copper at } 20 \text{ }^\circ\text{C per Kelvin} \\ \theta_{SC} &\text{ is the maximum operating temperature in } ^\circ\text{C} \end{aligned}$$

The constant mass temperature for copper is taken from [63].

The power loss in the sheath ( $\lambda_1$ ) consists of losses caused by circulating currents ( $\lambda_1'$ ) and eddy currents ( $\lambda_1''$ ), where the eddy currents are neglected according to

IEC 60287.

$$\lambda_1 = \lambda'_1 + \lambda''_1 = \lambda'_1 = \frac{R_s}{R} \frac{1}{1 + \left(\frac{R_s}{X}\right)^2} = \frac{9.31 \cdot 10^{-4}}{0.1 \cdot 10^{-3}} \frac{1}{1 + \left(\frac{9.31 \cdot 10^{-4}}{2\pi 50 \cdot 10^{-7} \ln\left(\frac{2 \cdot 18.6}{35 - 2.5}\right)}\right)^2} = 0.0051 \quad (\text{E.3})$$

where

- $R_s$  is the resistance of sheath or screen per unit length of cable at its maximum operating temperature [ $\Omega/m$ ]
- $X$  is the reactance per unit length of sheath or screen per unit length of cable =  $2\omega 10^{-7} \ln\left(\frac{2s}{d}\right)$
- $s$  is the distance between conductor axes in the electrical section being considered [mm]
- $d$  is the mean diameter of the sheath [mm]

The distance between the conductor axis,  $s$ , have been assumed to be equal to the core sheath diameter, which seems reasonable according to the cable sketch in Fig.D.1. The mean diameter of the sheath,  $d$ , is calculated by the core sheath diameter minus the thickness of the sheath.

The armour is assumed to be made of steel with a resistivity at 300 K at  $16 \cdot 10^{-8} \Omega m$  and rise at a maximum temperature of 300 K. The total armouring resistance is calculated by

$$R_A = \frac{\rho_{steel}}{A_{armour}} = \frac{16 \cdot 10^{-8}}{\left(\frac{99-8}{2}\right)^2 \pi - \left(\frac{99-8-5.2}{2}\right)^2 \pi} = 1.18 \cdot 10^{-10} \quad [\Omega/m] \quad (\text{E.4})$$

where

- $A_{armour}$  is the area of the armour [ $mm^2$ ]

The armour area is calculated by subtracting two areas around the armour; the first area has the diameter of the cable diameter subtracted with twice the thickness of the serving and the second area is in addition subtracting twice the armour thickness.

The ratio of losses in the armouring to the total losses in all conductors,  $\lambda_2$ , is

calculated by

$$\begin{aligned}
\lambda_2 &= 1.23 \frac{R_A}{R} \left( \frac{2c}{d_A} \right)^2 \frac{1}{\left( \frac{2.77 R_A 10^6}{\omega} \right)^2 + 1} \\
&= 1.23 \frac{1.18 \cdot 10^{-10}}{0.1 \cdot 10^{-3}} \left( \frac{2 \cdot 20}{5} \right)^2 \frac{1}{\left( \frac{2.77 \cdot 1.18 \cdot 10^{-10} \cdot 10^6}{2\pi 50} \right)^2 + 1} \\
&= 9.32 \cdot 10^{-5}
\end{aligned} \tag{E.5}$$

where

- $R_A$  is the a.c. resistance of armour at maximum armour temperature  
[ $\Omega/m$ ]
- $d_A$  is the mean diameter of armour [mm]
- $c$  is the distance between the axis of a conductor and the cable  
centre [mm]

The distance between the axis of a conductor and the cable centre,  $c$ , is assumed to be some millimetres bigger than half of the sheath's diameter, as can be seen in Fig.D.1.

The thermal resistance between one conductor and the sheath  $T_1$  is given by

$$T_1 = \frac{\rho_{Ti}}{2\pi} \ln \left[ 1 + \frac{2t_1}{d_c} \right] = \frac{3.5}{2\pi} \ln \left[ 1 + \frac{2 \cdot 3.4}{18.6} \right] = 0.2142 \text{ [Km/W]} \tag{E.6}$$

where

- $\rho_{Ti}$  is the thermal resistivity of insulation [Km/W]
- $d_c$  is the diameter of conductor [mm]
- $t_1$  is the thickness of insulation between conductor and sheath [mm]

The cable insulation consists of XLPE which have a thermal resistivity of 3.5 Km/W.

The thermal resistance of fillers and bedding under the armour is given by

$$T_2 = \frac{\rho_{Tf}}{6\pi} \overline{G} = \frac{6}{6\pi} \cdot 0.44 = 0.1401 \quad [Km/W] \quad (E.7)$$

where

$\rho_{Tf}$  is the thermal resistivity of fillers and bedding [Km/W]  
 $\overline{G}$  is the geometric factor given in Fig. A.1.

The thermal resistivity of fillers and bedding is taken from [52], where a table is showing common thermal resistances for different filling materials; the highest thermal resistance have been chosen as a worst case. The geometric factor is set to 0.44, by following the upper curve (sheaths touching) in Fig.A.1, and by calculating the ratio between the distance from the sheath to the armour (2 mm) and the outer diameter of the sheath (35 mm).

The thermal resistance of external servings,  $T_3$ , is given by

$$T_3 = \frac{1}{2\pi} \rho_{Te} \ln \left( 1 + \frac{2t_3}{D'_a} \right) = \frac{1}{2\pi} 6 \left( 1 + \frac{2 \cdot 4}{99 - 8} \right) = 0.0805 \quad [Km/W] \quad (E.8)$$

where

$\rho_{Te}$  is the thermal resistivity of external serving [Km/W]  
 $t_3$  is the thickness of serving [mm]  
 $D'_a$  is the external diameter of the armour [mm]

The thermal resistivity of serving is taken from [52], where a table is showing common thermal resistances for different serving materials; the highest thermal resistance have been chosen as a worst case. The external diameter of the armour,  $D'_a$ , is calculated by subtracting twice the serving thickness from the cable diameter.

The thermal resistance of external surrounding,  $T_4$ , is given by

$$\begin{aligned}
 T_4 &= \frac{1}{2\pi} \rho_{Ts} \ln(u + \sqrt{u^2 - 1}) \\
 &= \frac{1}{2\pi} 1 \cdot \ln \left( \frac{2 \cdot 1000}{99} + \sqrt{\left( \frac{2 \cdot 1000}{99} \right)^2 - 1} \right) \\
 &= 0.5886 \quad [Km/W]
 \end{aligned}
 \tag{E.9}$$

where

- $\rho_{Ts}$  is the thermal resistivity of soil [Km/W]
- $u = \frac{2L}{D_e}$
- $L$  is the distance from the surface of the ground to the cable axis [mm]
- $D_e$  is the external diameter of the cable [mm]

A summary of all used parameters is shown in Table E.1.

Table E.1: Summary of all parameters used for the temperature calculation.

	Cable, 240 mm <sup>2</sup>	Unit
$W_d$	$9.84 \cdot 10^{-4}$	[W/m]
$\lambda_1$	0.0051	
$\lambda_2$	$9.32 \cdot 10^{-5}$	
$T_1$	0.2142	[Km/W]
$T_2$	0.1401	[Km/W]
$T_3$	0.0805	[Km/W]
$T_4$	0.5886	[Km/W]